

# ***Ex Vivo* Expansion and Differentiation of Primary Human B Lymphocytes in Suspension and Encapsulated Cultures for Novel Culturing Approaches**

Der Fakultät für Ingenieurwissenschaften  
der Universität Bayreuth  
zur Erlangung der Würde  
**Doktor-Ingenieur (Dr.-Ing.)**  
genehmigte Dissertation

von

M. Sc. Moritz Richard Helm

aus

Bad Neustadt a.d. Saale

Erstgutachterin: Prof. Dr. Ruth Freitag

Zweitgutachter: Prof. Dr. Klaus Ersfeld

Tag der mündlichen Prüfung: 15.06.2023

Lehrstuhl Bioprozesstechnik

Universität Bayreuth

2023

# Content

Abstract .....	1
Kurzfassung.....	3
1 Introduction.....	5
2 Fundamentals.....	7
2.1 B Cells.....	7
2.2 B Cell Maturation .....	10
2.3 <i>In Vivo</i> B Cell Activation .....	11
2.3.1 Unspecific Activation of B Cells .....	12
2.3.2 Pokeweed Mitogen .....	12
2.3.3 Specific Activation of B Cells .....	13
2.3.4 Primary Follicles .....	14
2.3.5 Secondary Follicles .....	14
2.3.6 Germinal Centers .....	14
2.4 B Cell Signaling Molecules.....	15
2.4.1 CD40 Ligand .....	15
2.4.2 IL-4 .....	16
2.4.3 IL-21 .....	16
2.4.4 BAFF .....	17
2.5 Phenotyping and Genotyping of B Cell Subclasses .....	17
2.5.1 Cluster of Differentiation (CD) Antigen expression on B Cells.....	17
2.5.2 Gene Expression in B Cells.....	18
2.6 State-of-the-Art <i>In Vitro</i> Culturing Systems for B Cells.....	20
2.6.1 Suspension Cell Cultures .....	20
2.6.2 Micro-Cell-Encapsulation and SCS-PDADMAC Capsules .....	21
2.6.3 Organoids for Controlled <i>Ex Vivo</i> Germinal Center Reactions .....	23

<b>3 Material &amp; Methods</b> .....	<b>24</b>
3.1 Isolation of Human B Cells from Buffy Coats .....	24
3.2 Isolation of Human B Cells from Tonsillar Tissue.....	24
3.3 Freezing and Thawing of B Cells .....	26
3.4 B Cell Cultivation and Stimulation .....	27
3.5 Determination of Cell Number and Viability.....	28
3.6 Cellular Proliferation Assay .....	28
3.7 FC-Analysis of Lymphocytes.....	29
3.8 Purification of Total RNA from B Cells .....	30
3.9 Reverse Transcription (RT) of Purified RNA .....	30
3.10 qPCR of cDNA .....	31
3.11 Calculation of Reference Gene Stability.....	32
3.12 Calculating Gene Expression via $\Delta\Delta\text{Ct}$ Method .....	33
3.13 Agarose Gel Electrophoresis of cDNA .....	34
3.14 ELISA.....	34
3.15 3D Printing of Microencapsulation Unit .....	35
3.16 Alginate Encapsulation.....	35
3.17 Cell Encapsulation in SCS-PDADMAC .....	35
3.18 Cell Release from SCS-PDADMAC Capsules .....	36
3.19 Capsule Microscopy and Image-Based Size Determination .....	37
3.20 Diffusion Assay with Vitamin B <sub>12</sub> and Resorufin.....	37
3.21 Statistical Analysis .....	37
<b>4 Results and Discussion</b> .....	<b>38</b>
4.1 Unspecific Stimulation with PWM.....	38
4.1.1 Primary Human B Cells from Blood and Tonsils.....	38
4.1.2 Tracking Cellular Division via CFSE Intensity Reduction.....	39
4.1.2 Proliferative Response to PWM in Primary Human B Cells.....	40

4.1.3 Effect of T Cell Impurities in PWM-Stimulated B Cell Cultures .....	42
4.1.4 Effect of PWM on B Cell Differentiation .....	44
4.2 Specific Stimulation with Soluble CD40L in Suspension .....	47
4.2.1 Primer Specificity and Reference Gene Selection for RT-qPCR .....	47
4.2.2 CSA and Human AB Serum in B Cell Cultures.....	49
4.2.3 Optimizing Seeding Densities and Soluble CD40L Utilization .....	51
4.2.4 Memory and ASC Expansion Medium in Batch Cultures.....	53
4.2.5 B Cell Expansion with Medium Change and Memory Pre-Culture .....	62
4.2.6 ASC and Memory Pre-Culture with Blood-Derived B Cells.....	73
4.2.7 Conclusion of Specific Stimulation with Soluble CD40L in Suspension....	77
4.3 Encapsulated B Cell Cultures Stimulated with Soluble CD40L .....	80
4.3.1 Microencapsulation Unit and Alginate Encapsulation .....	81
4.3.2 Molecular Weight Cut-Off (MWCO) and Size of SCS-PDADMAC Capsules .....	83
4.3.3 FC Analyses of B Cells in Suspension and SCS-PDADMAC Capsules ...	84
4.3.4 Suspension Culture of B Cells Compared to Encapsulated Culture .....	86
4.3.5 SCS-PDADMAC Encapsulation with or without Human AB Serum Inside	88
4.3.6 Capsules Cultured in Base Medium with or Without Human AB Serum ...	93
4.3.7 SCS-PDADMAC Encapsulation with Different Quantities of CD40L.....	94
4.3.8 SCS-PDADMAC Encapsulation with or without Pre-Culture .....	95
4.3.9 Conclusion of Subclass Development in SCS-PDADMAC Capsules .....	98
<b>5 Outlook .....</b>	<b>99</b>
<b>6 List of Figures .....</b>	<b>101</b>
<b>7 List of Tables .....</b>	<b>106</b>
<b>8 List of Abbreviations .....</b>	<b>107</b>
<b>9. Materials, Devices and Software .....</b>	<b>111</b>
9.1 Buffers and Solutions .....	111

9.2 Cell Culture Supplements .....	112
9.3 Chemicals, Reagents and Kits .....	113
9.4 Accessories.....	116
9.5 Devices and Equipment .....	117
9.6 Software.....	119
10 References .....	120
11 Appendix.....	128



## Abstract

The propagation of human B cells in the laboratory holds potential as basis for novel therapies for the treatment of currently incurable diseases. In the first part of this work, we applied B cell expansion protocols via pokeweed mitogen (PWM) stimulation. Furthermore, we improved the state-of-the-art suspension culturing approaches via soluble CD40L protein with defined cytokine cocktails and used this knowledge to establish a novel tissue engineering-like culturing platform for B cells in sodium cellulose sulfate (SCS) poly-diallyl-dimethyl-ammonium chloride (PDADMAC) capsules.

We used human primary tonsillar B cells and blood derived B cells to demonstrate the mitogenic potential of PWM for cheap and easy expansion of B cells of both sources. We were able to show, for the first time, that the proliferative response to PWM was lower in younger donors. PWM stimulated the proliferation of specific subpopulations and induced Antibody secreting cell (ASC) development, indicated by CD20 reduction. This showed the functionality of our B cell isolation protocols and describes a simple essay to evaluate B cell responsiveness utilizing PWM.

We developed two culturing media with different properties to stimulate specific B cell proliferation and differentiation via CD40L. Using a memory expansion medium without IL-21 maintained high memory cell content, led to comparably low expansion, showed upregulation of Activation-induced deaminase (AID) and caused immunoglobulin (Ig) class switch recombination (CSR) in B cells. ASC expansion medium with IL-21 caused plasmablast (PB) and plasma cell (PC) development and led to higher B cell expansion. A pre-culture with memory expansion medium and later transition to ASC expansion medium led to boosted B cell expansion exceeding pure ASC culture after 11 days. AID upregulation additionally indicated CSR and somatic hypermutation (SHM) in memory pre-culture. Contrary to PWM stimulation, the proliferative response to a memory pre-culture was higher in younger donors. PC development was more pronounced in adult-derived B cells, indicating a still developing immune system in children and confirming age-dependent differences.

For a closer mimicking of *in vivo* B cell development, we applied the newly generated knowledge regarding B cell suspension cultures, stimulated with soluble CD40L, and developed a novel culturing platform. Microcapsules made of SCS-PDADMAC were

shown to possess features similar to the tissue environment inside the human body. We showed that this system can facilitate human primary tonsillar B cell cultures, as previously demonstrated for primary human T cells. Proliferation and subclass development were tracked during encapsulated culture in comparison to suspension culture. The differentiation of initially mainly memory B cells into various subtypes, particularly PC, was altered significantly compared to suspension cultures. The development of germinal center (GC)-like phenotype and PC survival are major features of this novel culturing platform. We additionally describe possible adjustments to guide B cells in encapsulated culture toward PC or GC phenotype. Variation of these parameters during encapsulation offers a novel tool for finetuning the B cell response. Hence, this platform may pave the way for developing *ex vivo* human immune organoids.



## Kurzfassung

Die Vermehrung menschlicher B Zellen im Labor kann die Entwicklung neuartiger Therapien für die Behandlung bisher unheilbarer Krankheiten ermöglichen. Im ersten Teil dieser Arbeit wurde die Expansion von B Zellen mit Hilfe von Pokeweed Mitogen (PWM) stimuliert. Weiterhin konnten wir den aktuellen Stand der Technik mit löslichem CD40L und definierten Zytokinen verbessern und das dabei erlangte Wissen anwenden, um eine neuartige Kultivierungsplattform, nach dem Vorbild des Tissue Engineerings, in Sodium Cellulose Sulfate (SCS) Poly-Diallyl-Dimethyl-Ammoniumchlorid (PDADMAC) kapseln zu schaffen.

Humane primäre B Zellen wurden aus Blut und Mandeln isoliert und das mitogene Potenzial von PWM als B Zell Stimulanz demonstriert. Es konnte hierbei zum ersten Mal gezeigt werden, dass die proliferative Antwort im Vergleich bei jüngeren Spendern geringer als bei älteren ausfiel. PWM stimulierte die Proliferation bestimmter Subpopulationen und induzierte die Entwicklung von Antikörper produzierenden Zellen (ASC), was durch die Reduktion von CD20 nachgewiesen werden konnte. So konnte die Funktionalität des B Zell Isolationsprotokolls mit Hilfe eines einfachen Essays für die Analyse von B Zell Aktivität gezeigt werden.

Für eine spezifische B Zell Stimulation und -differenzierung wurden zwei Kulturmedien mit unterschiedlichen Eigenschaften entwickelt. Ein Memory Expansionsmedium ohne IL-21 konnte hohe Memory Zellzahlen aufrechterhalten, führte jedoch zu einer vergleichsweise geringen Zellexpansion. Die Hochregulierung von aktivierungsinduzierter Cytidin-Desaminase (AID) führte dabei zu einem Immunglobulin (Ig) Klassenwechsel der B Zellen. Das ASC Expansionsmedium mit IL-21 führte zur Entwicklung von Plasmablasten (PB) und Plasma Zellen (PC) und erhöhte die Zellexpansion. Eine Vorkultur in dem Memory Expansionsmedium mit einem späteren Übergang zu ASC Expansionsmedium konnte die endgültige Zellexpansion merklich verbessern und die reine ASC Kultur nach 11 Tagen übertreffen. Die Hochregulierung von AID in der Memory Vorkultur lies eine Immunadaption durch Immunglobulin Klassenwechsel und somatische Hypermutation (SHM) vermuten. Im Gegensatz zur PWM-Stimulation konnte bei CD40L stimulierten Kulturen eine höhere Expansion bei jüngeren Spendern beobachtet werden. Bei B Zellen die von erwachsenen Spendern gewonnen wurden war außerdem die Entwicklung zu PC stärker ausgeprägt, was auf unterschiedliche Entwicklungsstadien

des Immunsystems zwischen Erwachsenen und Kindern hindeutet. Diese Beobachtung bestätigte altersbedingte Unterschiede bei der Stimulation von B Zellen erneut.

Für eine bessere Imitation der *in vivo* B Zell Entwicklung haben wir die Erkenntnisse aus den B Zell Suspensionskulturen übertragen und eine neue Kultivierungsplattform entwickelt. Wir konnten zeigen, dass Mikrokapseln aus SCS-PDADMAC Eigenschaften besitzen, die der Umgebung im Gewebe ähnlich sind. Die Kultivierung von B Zellen in diesem System war grundsätzlich möglich, was zuvor schon für T Zellen gezeigt werden konnte. Die Proliferation und Subklassenentwicklung wurden während der Verkapselung- im Vergleich zur Suspensionskultur beobachtet. Im Vergleich zur Suspensionskultur wurde die Differenzierung von ursprünglichen Memory Zellen in unterschiedliche Subtypen und speziell PC merklich verändert. Die Entwicklung von Keimzentrums (GC)-ähnlichem Phänotyp und das Überleben von PC sind die Haupteigenschaften dieser neuartigen Kultivierungsplattform. Wir konnten zusätzlich mögliche Anpassungen aufzeigen, um die verkapselten B Zellen zu einem PC- oder GC-Phänotyp zu lenken. Eine Änderung dieser Parameter während der Verkapselung stellt ein neues Instrument dar, mit dessen Hilfe die B Zell-Entwicklung optimiert werden kann. Die von uns entwickelte Plattform kann den Weg für die Entwicklung von *ex vivo* immun Organoiden ebnen.

# 1 Introduction

To date, there is still no adequate method for the directed *ex vivo* expansion and activation of B cells on a large scale. Investigation over the last decades led to the identification of several important signaling factors for the proliferation and differentiation of B cells. B cell development starts in the bone marrow, progresses in the blood and ends with affinity maturation in the GCs before the cells re-enter the vascular system. Most of the signaling takes place in a packed tissue environment with close cell-to-cell contacts. These insights into B cell development can be applied and transferred to state-of-the-art technologies to create new processes closely mimicking the *in vivo* situation. Advances in bioprocess engineering lead to frequent invention of new technologies and improvement of old technologies, which can be applied to solve these problems. Advancing technologies like flow cytometry (FC) helped to further understand influences of several cytokines and the central signaling role of CD40L via cell-cell-interaction of B and T cells. In this research, I will combine this knowledge to find new and better processes for the directed *ex vivo* expansion and differentiation of human B cells.

All currently generated *in vitro* human therapeutic antibodies, are based on monoclonal antibodies, issued from genetic engineering or single-cell antibody technologies. *In vitro* expansion and activation of B cells for the development of specialized antibodies outside the human body holds potential for production of polyclonal antibodies, *ex vivo* immunization therapies or *in vitro* generation of highly specific antibodies for therapies. Polyclonal preparations of therapeutic immunoglobulins are essential in the treatment of immunodeficiency and are increasingly used for the treatment of autoimmune and inflammatory diseases. Currently, patients' accessibility depends exclusively upon volunteer blood donations followed by the fractionation of pooled human plasma obtained from thousands of individuals. Presently, there are no *in vitro* cell culture procedures allowing the preparation of human polyclonal antibodies (Néron et al. 2012).

Numerous diseases are preventable by routine vaccination, but for some illnesses or sensitive patients, a regular vaccination by injecting the antigen into the body is not possible. Human immunodeficiency virus (HIV) is one of the most prominent and persistent examples. It is widely agreed, that the most effective method to slow the Acquired Immunodeficiency Syndrome (AIDS) epidemic is a vaccine (Kwong et al.

2011; Letvin 2006). However, human efficacy trials of vaccine candidates designed to elicit antibody- or T cell-based immunity have failed (Pitisuttithum et al. 2006; Watkins et al. 2008). The body's B lymphocytes are dedicated producers of antibodies, so if they could be programmed *ex vivo* to make a protective antibody, this might prove a valuable asset in preventing the spread of AIDS. Such a method might also be valuable for delivering other proteins of therapeutic importance. Successful and sufficient *ex vivo* expansion of naïve B lymphocytes, that did not encounter antigens yet, could open the possibility for *ex vivo*-immunization. Subsequently, the cells could be returned into the patient's body to provide immunity (Luo et al. 2009; Giese et al. 2010). *Ex vivo* memory B cell expansion has been recently used to identify an extremely potent HIV-1 broadly neutralizing antibody named N6, encouraging the existence of such cures (Huang et al. 2016).

Reports like this bring research closer toward life-saving drugs and will help us solve disease problems and form the basis for new therapies. Therefore, further understanding of the mechanics leading to the development of highly specific immune cells need to be generated. This work aims to develop B cell expansion protocols in a controlled microenvironment and reaches out to create a novel form of B cell cultures.

## 2 Fundamentals

### 2.1 B Cells

Specialized lymphocytes, known as B cells, can secrete large quantities of antibodies, also called immunoglobulins, found in bodily fluids such as the blood serum and lymphatics. They are the only cells able to produce antibodies. The role of antibodies within the immune system is to recognize and bind to foreign proteins derived from microorganisms or pathogens themselves. Any molecule bound by an antibody is known as an antigen. The interaction between an antibody and an antigen is a key principle in immunology. The binding of an antibody to an antigen has several downstream consequences, including the neutralization and clearance of the antigen and the activation of the effector functions of numerous immune cells (Williams and Hussell 2012).

The Ig class (or isotype), shown in Figure 1, ultimately defines how the immune system is activated. Each antibody consists of two heavy chains and two light chains joined to form a "Y" shaped molecule that can form dimers (IgA) and multimers (IgM). The amino acid sequence in the tips of the "Y" varies greatly among different antibodies. This variable region (V) gives the antibody its specificity for binding antigens. The variable region includes the ends of the light and heavy chains (yellow and blue).

The constant (C) region determines the antibody isotype and mechanism used to destroy the antigen. Each antibody isotype leads to distinct immunological functions. Immunoglobulin M (IgM) and IgD are the first-line defense mechanism. IgM accounts for 5 – 10 % of the immunoglobulin pool and is the predominant antibody in the primary immune response. IgD accounts for less than 1 % of the total plasma immunoglobulin but is present in large quantities on the membrane of B cells. IgA is secreted in mucosal tissues to prevent pathogen colonization. IgA represents approximately 5 – 15 % of the antibody pool and either exists as a monomer or a dimer. IgE binds to allergens and parasitic worms. It is very rare in the serum but is found on the basophils and mast cells of all individuals. IgG provides the bulk of antibody-based immunity to pathogens. IgG is the most abundant antibody in normal human serum, accounting for 70 – 85 % of the total immunoglobulin pool (Duarte 2016).

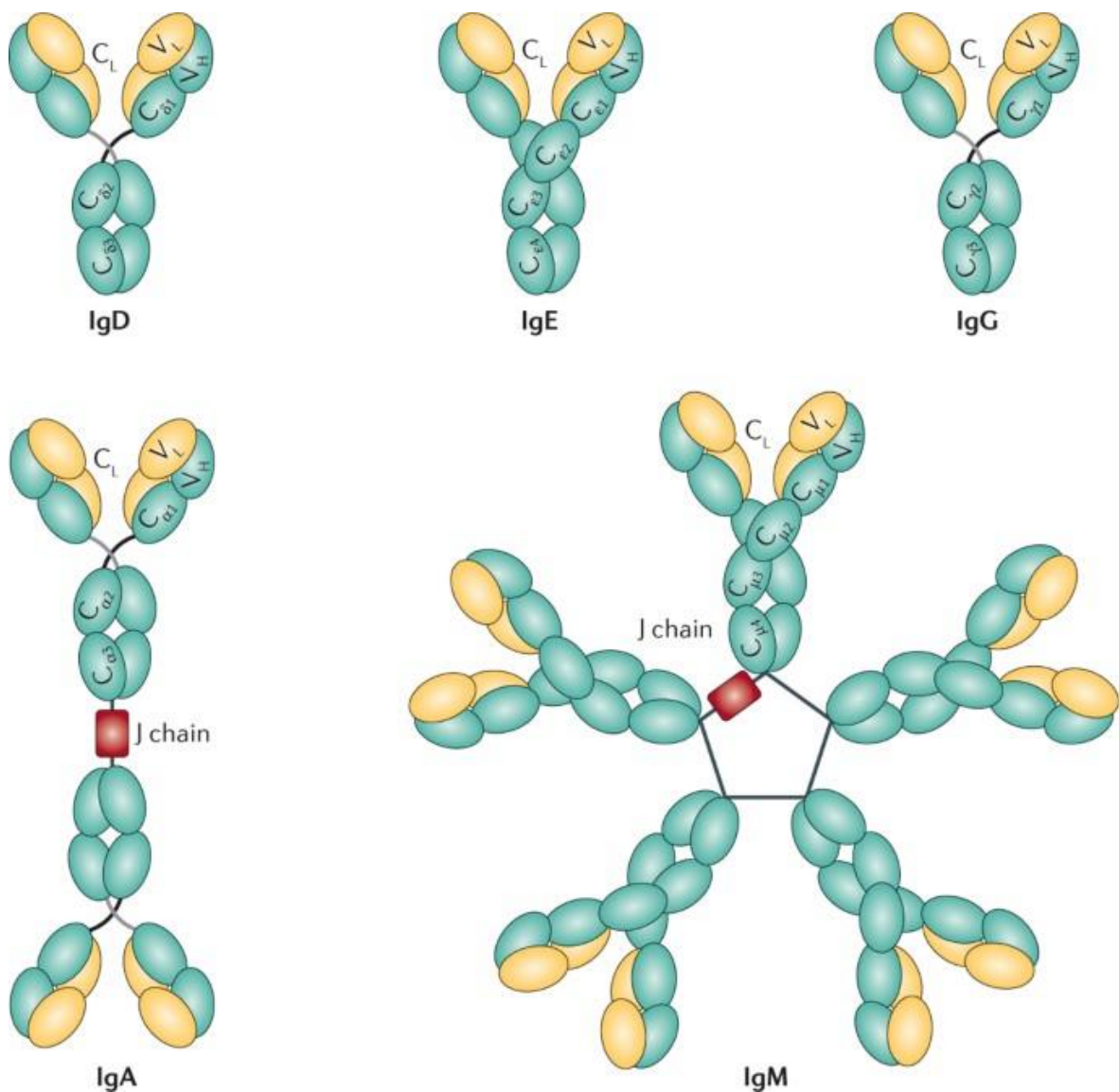


**Figure 1: Schematic representation of the five immunoglobulin classes or isotypes in mammals. Each antibody consists of four polypeptides. Two heavy chains (green) and two light chains (yellow) joined to form a "Y" shaped molecule. Monomeric IgD, IgE, IgG, and the dimeric and pentameric forms of IgA and IgM are shown. This figure is adopted from Duarte (2016).**

Immune responses generated as a result of antibody and antigen interactions are commonly referred to as antibody-mediated immunity, which can be considered to be part of the humoral or adaptive immune response (Williams and Hussell 2012).

A secondary immune response occurs when an individual encounters the same pathogen for a second time and principally involves B and T cells of the adaptive immune system. It is much quicker in establishing itself than a primary immune response, because the antigens derived from the pathogen have been encountered before. The magnitude of a secondary immune response is also higher, meaning that more cells participate in the reaction, which results in a much more effective response as seen in Figure 2.

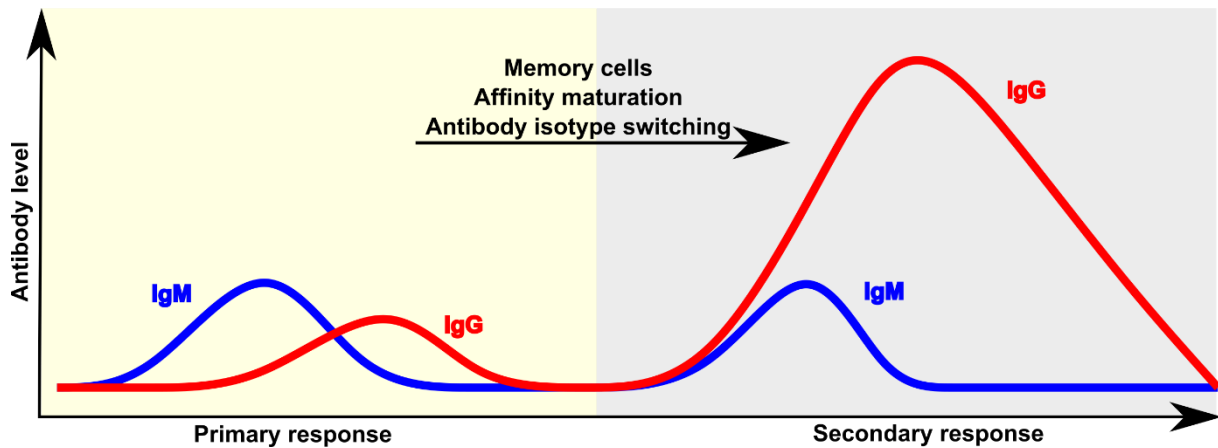


Figure 2: Antibody production in primary and secondary immune responses. Primary antibody responses are initially dominated by IgM, while secondary responses are dominated by elevated IgG. This figure is derived from Williams and Hussell (2012).

There is a rapid elevation in antibody levels within the bloodstream, which remains elevated for a longer period. This heightened response involves the activation of memory B cells, which can directly differentiate into antibody secreting PC, without having to undergo the various stages of B cell development that a naive B cell must undergo. A secondary immune response is also dominated by the production of highly specific antibodies for a particular antigen. The antibodies produced during a secondary immune response are much more specific than those produced during a primary response. This is due to a process known as affinity maturation and antibody isotype switching, which involves a switch in IgM production to IgG production and changes in antibody affinity. Likewise, memory T cells are much more readily activated and they too have a heightening effector response, which is capable of responding more rapidly and with a greater magnitude than during a primary response. The effectiveness of a secondary immune response relies on the generation of memory B cells and memory T cells, which develop following the initiation of a primary immune response. These memory cells reside in various lymphoid tissues throughout the body and contribute to what is known as immunological memory. The term immunity was first used to describe the ability of the immune system to provide protection against infectious diseases and relies on the activation of memory B and T cells. Importantly, vaccination relies on the ability of the immune system to respond more effectively to a secondary encounter with an antigen. Many infectious diseases can be prevented by immunization, through the generation of antigen-specific memory cells that become activated in response to a challenge from the real pathogen (Williams and Hussell 2012).

## 2.2 B Cell Maturation

In the maturation, hematopoietic stem cells (HSC) divide and eventually generate mature naïve B cells through a process tightly controlled by cytokines but independent of foreign antigens. Mature naïve B cells then take residence in the secondary lymphoid tissues in the body's periphery, waiting for activation (Shahaf et al. 2016) (Figure 3).

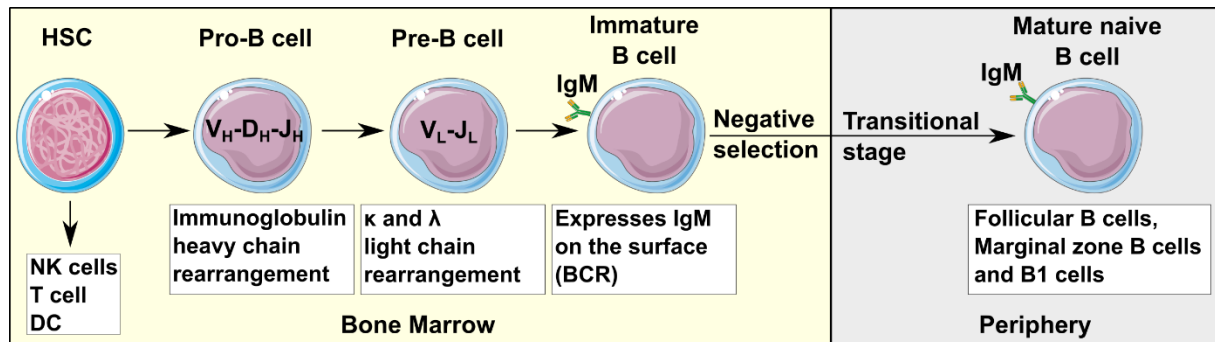


Figure 3: Development of HSC toward mature B cells is defined by Ig rearrangements and negative selection of autoreactive B cells. After the transition from bone marrow to the periphery, mature naïve B cells migrate through the spleen into secondary lymphoid tissues. Some elements in the image have been obtained from Smart Servier Medical Art.

Pro-B cells are the first hematopoietic cells clearly recognizable as being of the B lineage. These cells are identified by their expression of specific B lineage markers and by the fact that all their Ig genes are still in germline configuration or unmutated configuration of the V genes (Hardy et al. 1991). As the next maturation step, Pre-B cells that complete V(D)J rearrangement of the heavy chain can be detected. The pre-B cell receptor (BCR) is expressed transiently on the pre-B cell membrane to test the functionality of the particular  $V_H D_H J_H$  combination. A pre-BCR is not a true immune globulin (Ig) and cannot respond to antigens. It is thought to bind to ligands on bone marrow stromal cells leading to intracellular signal delivery, telling the cell that a functional H chain has been successfully synthesized. The presence of the complete BCR complex on the B cell surface delivers an intracellular signal that terminates all Ig locus rearrangements and marks the next step in B cell maturation (Hardy et al. 1991; Edry and Melamed 2004). Immature B cells in the bone marrow are screened for central tolerance. B cells that recognize self-antigens are removed. Bone marrow stromal cells express housekeeping molecules that are produced by all body cells. B cells with a BCR binding to one of these molecules with high affinity are potentially autoreactive. The release of such a B cell from the bone marrow into the periphery could lead to autoreactive antibodies (Rolink et al. 2001). Immature B cells remain in



the bone marrow before commencing the expression of new adhesion molecules and homing receptors that allow them to leave the bone marrow and travel via the blood to the secondary lymphoid tissues as transitional B cells. Transitional B cells start to colonize the B cell-rich areas of the spleen and acquire the ability to emigrate to other secondary lymphoid tissues, like the lymph nodes, thymus or the tonsils. Once transitional B cells establish themselves in the lymphoid follicles and splenic marginal zone, they are considered to be mature naïve B cells in the periphery (Carsetti et al. 1995; Osmond 1991).

### 2.3 *In Vivo* B Cell Activation

For the activation of mature naïve B cells, two different modes of action can occur, dependent on the antigen binding to the cell (Figure 4). B cells can be activated without T cell help, leading to a quick response with rapid cell division and secretion of IgM antibodies. This is a quick response and part of the innate immune system. Alternatively, B cells can be activated in a T-dependent (Td) manner, leading to a slower response, including multiple steps. The response leads to affinity maturation, Ig CSR and memory cells, therefore being part of the adaptive immune response.

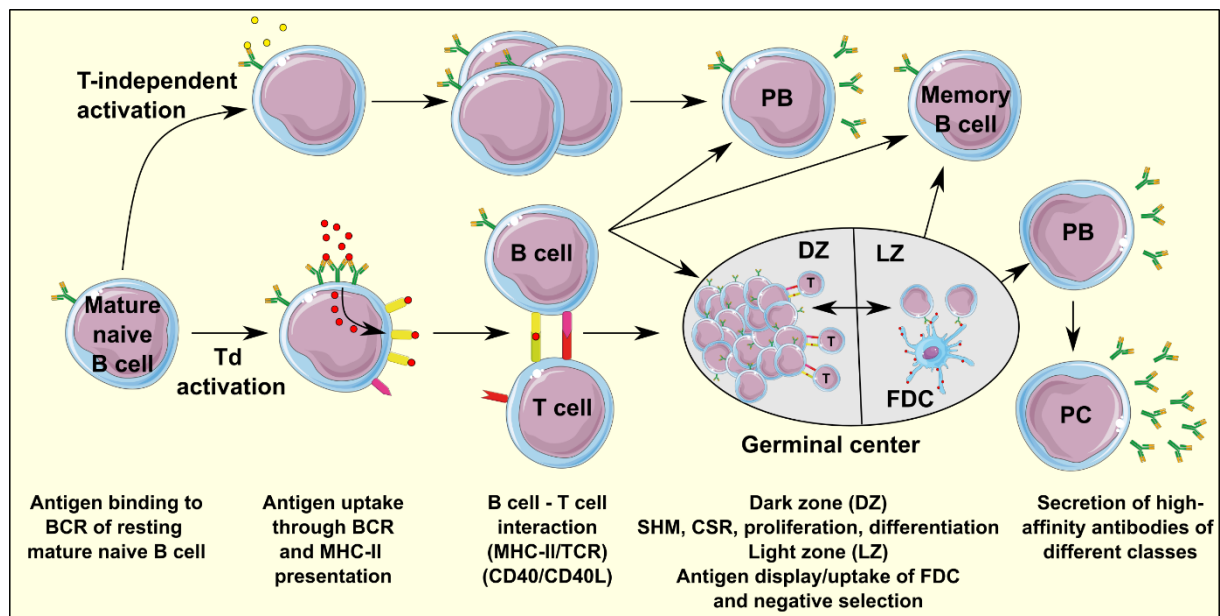


Figure 4: The differentiation of mature naïve B cells upon antigen encounter. B cells can undergo unspecific (T-independent) or specific (T-dependent) activation. Unspecific activation leads to proliferation, PB differentiation and IgM secretion but is restricted to IgM and no affinity maturation occurs. Specific activation leads to the formation of GC, enabling affinity maturation and Ig class switch. B cells also differentiate into memory cells, PB and PC, enabling adaptive immunity. Some elements in the image have been obtained from Smart Servier Medical Art.

### **2.3.1 Unspecific Activation of B Cells**

Microorganisms such as bacteria and viruses produce a multitude of proteins, carbohydrates and glycolipids, which can all be recognized by cellular receptors expressed on the surface of immune cells. The most widely studied family of microbial recognition receptors are known as pattern recognition receptors (PRRs), because they recognize evolutionary conserved molecular patterns produced by microorganisms. The recognition of microbial products, which are known as pathogen associated molecular patterns (PAMPs), is one of the first steps in the activation of an immune response. Numerous cells of the immune system, and also tissue cells such as epithelial cells, express these PRRs. The most ubiquitous family of PRRs are known as the toll-like receptor (TLR) family, which are responsible for the recognition of a host of PAMPs (Williams and Hussell 2012). TLRs play a significant role in innate immune defense by recognizing evolutionarily conserved microbial structures and providing downstream signals for cell activation. Homologues were discovered in mammals, of which there are a total of 13 that have so far been identified, 10 recognized in humans and 12 in mice, of which TLR1-9 are conserved between the two species. Each TLR recognizes explicitly one type of microbial component, or PAMP, such as lipopolysaccharide (only in mice), lipopeptides, RNA or DNA (Hartmann and Krieg 2000; Krieg et al. 1995). These antigens have epitopes that bind multiple B cell receptors and activate the B cell directly to secrete IgM antibodies (Figure 4). However, as there is no germinal center formation, no affinity maturation takes place, and there is no class switching or generation of memory. Therefore T cell-independent responses are IgM limited, of poor specificity, and short-lived (Mond et al. 1995).

### **2.3.2 Pokeweed Mitogen**

Lectins are carbohydrate-binding proteins that are highly specific for sugar groups that are part of other molecules, thus cause agglutination of particular cells or precipitation of glycoconjugates and polysaccharides. Lectins have a role in recognition at the cellular and molecular level and play numerous roles in biological recognition phenomena involving cells, carbohydrates, and proteins (Goldstein and Hayes 1978). They are isolated from a wide variety of natural sources, including seeds, plant roots and bark, fungi, bacteria, seaweed and sponges, mollusks, fish eggs, body fluids of invertebrates and lower vertebrates, and from mammalian cell membranes. The precise physiological role of lectins in nature is still unknown, but they have proved to induce mitogenic stimulation of lymphocytes (Hivrale and Ingale 2013; Maciel et al.

2004). PWM is a lectin derived from the plant *Phytolacca Americana* (pokeweed), with a molecular weight of 32 kDa (Reisfeld et al. 1967). Due to their potent immunostimulatory properties, pokeweed extracts are used in patients with infections and cancer. Furthermore, the purified PWM is commonly used for B cell assays *in vitro* (Bekeredjian-Ding et al. 2012). Based on previous studies, PWM potently stimulates B cell proliferation and immunoglobulin production (Crotty et al. 2004; Farnes et al. 1964). However, the TLR, responsible for B cell stimulation is still debated to this date (Bekeredjian-Ding et al. 2012). To improve *in vitro* cultures of B cells, stimulated with mitogens, resveratrol (3,5,4'-trihydroxy-trans-stilbene), a plant antibiotic, can be utilized. Resveratrol inhibits the enzyme cyclooxygenase-2, which is induced by mitogens, cytokines and bacterial lipopolysaccharides and plays a key role in inflammatory processes (Aggarwal et al. 2004; O'Leary et al. 2004). This provides a synergistic effect on the Proliferative Response and Apoptosis in Human Activated B cells *in vitro* (Zunino and Storms 2009).

### **2.3.3 Specific Activation of B Cells**

T-dependent (Td) B cell activation is regulated by lymphokines binding to their receptors and the interaction of cellular adhesion receptors with their ligands (Eales 2003)(Figure 4). First, the specific antigen molecule binds to the BCR (Pape et al. 2007). The antigen molecule is processed internally and presented to T cells via major histocompatibility complex-II (MHC-II). As a consequence of the antigen recognition, T helper (Th) effector cell contacts are established, leading to CD40/CD40L stimulation (Elgueta et al. 2009; Banchereau et al. 1994; Mackey et al. 1998). Lastly, the cells are activated by binding of secreted cytokines to the B cell surface (Howard et al. 1982; Parrish-Novak et al. 2000). CD40L gives a signal to the Th cell and induces the expression of interleukin 4 (IL-4). CD40 signaling results in the activation of resting B cells and acts in conjunction with IL-4 signaling to cause B cells to undergo proliferation, immunoglobulin class switching, antibody synthesis and formation of memory B cells (Spriggs et al. 1992; Castigli et al. 1994; Xu et al. 1994; van Kooten and Banchereau 2000). Without CD40/CD40L interactions, B cells are unable to proliferate and cannot produce Td antibodies. The interaction between Th cells and antigen-specific B cells usually occurs in secondary lymphoid structures such as lymph nodes and specialized mucosal sites, including Peyer's patches in the intestine and the tonsils (Williams and Hussell 2012).

### **2.3.4 Primary Follicles**

Prior to a B cell encounter with antigen, the follicles within secondary lymphoid structures are known as primary follicles. A primary follicle is filled with resting naïve B cells and a collection of follicular dendritic cells (FDCs) that can trap whole antigens on their surfaces (Mandel et al. 1980). Upon the arrival of the antigen specific for the BCR of a naïve B cell, several downstream consequences lead to the migration of T cells to the primary follicles (Nieuwenhuis and Ford 1976). On the edge of the follicle, the receptive B cell meets a Th effector cell specific for the same antigen. It forms the B–T conjugate necessary for the delivery of CD40 and cytokine stimulation (Okada et al. 2005). In some cases, the B cells on the edge of the follicle immediately proliferate and terminally differentiate into a population of PB without carrying out isotype switching or SHM. The majority of the progeny of this B cell will become PC, while the remainder will become memory B cells (Chan et al. 2009).

### **2.3.5 Secondary Follicles**

An activated B cell destined to produce PC and memory B cells undergoes rapid clonal expansion within the primary follicle that converts it into a secondary follicle. This expansion requires the presence of antigen, displayed on the surfaces of FDCs (Suzuki et al. 2009), continued engagement of CD40 by the CD40L of an activated antigen-specific Th effector cell, and stimulatory cytokines secreted by the Th effector (Pape et al. 2007; Banchereau et al. 1994; Howard et al. 1982). Six days after antigen contact, the uninvolved naïve B cells that filled the primary follicle are displaced by the proliferating B cell clone and are compressed at the edges of the follicle to form the follicular mantle (MacLennan 1994).

### **2.3.6 Germinal Centers**

Eight days after antigen contact, the secondary follicle polarizes into two distinct areas, a dark zone and a light zone (Röhlich 1930; Kerfoot et al. 2011), and becomes a GC (Figure 4). This process of polarization is called the germinal center reaction. Activated B cells are found first in the dark zone, where they continue to proliferate rapidly and become centroblasts. It is within the centroblasts population that the antibody repertoire undergoes its final diversification by somatic hypermutation. As centroblasts mature and differentiate further, they migrate into the light zone, where they become centrocytes. Centrocytes bearing the newly generated somatic mutation, interact with antigens on the FDCs in the light zone and are selected, based on their antigen affinity (Bannard et al. 2013; MacLennan 1994). Negative selection in the GC induces B cells

that no longer recognize the antigen to undergo apoptosis. Positive selection ensures the survival of B cells that continue to recognize the FDC-displayed antigen with the same or increased affinity (Chan et al. 2009). At the end of all these processes, the surviving centrocytes either return to the beginning of the GC cycle for further expansion, diversification and selection or continue their differentiation into PC or memory B cells that exit the GC and enter the circulation and tissues (Okada et al. 2005). The proliferation and differentiation in GCs can persist 21-28 days post antigen encounter, after which fresh assault by antigen is required for further GC reaction (Reimer et al. 2020).

## **2.4 B Cell Signaling Molecules**

B cell behavior is initiated and controlled, to a large degree, via signaling through the BCR. The initial antibodies produced by the B cells are not secreted to the circulation but are inserted into the cell membrane to serve as BCR. The binding of a specific antigen causes the activation of the B cell receptor. This initiates a cascade of intracellular signaling, which leads to the internalization of the antigen-bound BCR for processing and presenting the antigen to T cells, which in turn stimulate B cells via surface interaction (e.g., CD40L) or secreted cytokines (e.g., IL-4, IL-21, B cell activating factor (BAFF)) (Kwak et al. 2019).

### **2.4.1 CD40 Ligand**

B cells can be activated by a variety of stimuli to acquire immunostimulatory capacity, including BCR binding to antigen and TLR-mediated signals. However, signals transmitted via CD40 have consistently been found to be the most potent inducer of many features of antigen-presenting B cells (van Belle et al. 2016). Several strategies have been investigated to exploit CD40-CD40L interaction for the generation of antigen-presenting B cells (Néron et al. 2011a). These include the usage of recombinant soluble CD40L proteins (Fournel et al. 2005; Garcia-Marquez et al. 2014; Jourdan et al. 2017; Naito et al. 2013), triggering CD40 with agonistic monoclonal CD40 antibodies (Carpenter et al. 2009; Tu et al. 2008), and CD40L-expressing feeder cells (Ivanov et al. 2005; Yoon et al. 2005). Several factors affect the extent of B cell activation by CD40-mediated signals. For instance, the effect of anti-CD40 antibodies on B cell activation is determined by the exact location of their binding to CD40 (Barr and Heath 2001). Another factor that crucially determines the extent of B cell activation is the degree of CD40 crosslinking. It has long been established that optimal bioactivity

is only observed when using a multimerized form of the CD40L homotrimer, thus allowing clustering on the cell surface (Fanslow et al. 1994a; Haswell et al. 2001; Morris et al. 1999). Furthermore, it was observed that amount and activity of CD40L on the surface of recombinant feeder cells, expressing the ligand, was influencing the fate of B cells. Therefore, the amount of CD40L present on surfaces, in contact with B cells, influences whether the cells proliferate or produce antibodies (Fanslow et al. 1994b; Gordon and Pound 2000; Néron et al. 2005).

#### **2.4.2 IL-4**

IL-4 was first discovered in 1982, when its capacity to enhance the proliferative responses of B cells to anti-immunoglobulin antibodies was investigated (Howard et al. 1982). Later the ability of IL-4 to function as B cell growth factor was proposed to be associated with enhanced autocrine growth of activated B cells (Tadmori et al. 1989). It was also found that IL-4 had to be present continuously during the culture period of B cells to exert an optimal growth-promoting effect on B cell blasts (Defrance et al. 1987). Most B cell growth media nowadays contain IL-4 as a growth factor (GF) (Su et al. 2016; Luo et al. 2009; Bryant et al. 2007; Ettinger et al. 2005; Fluckiger et al. 1993).

#### **2.4.3 IL-21**

IL-21 is predominantly produced by activated CD4<sup>+</sup> T cells and natural killer T cells (Harada et al. 2006; Spolski and Leonard 2008). The importance of IL-21 in regulating B cell responsiveness was first reported in 2000. It was shown that IL-21 costimulates the proliferation of human B cells activated with anti-CD40 (Parrish-Novak et al. 2000). To address the impact of IL-21 on B cell responsiveness in more detail, experiments were carried out in which human B cells were isolated and stimulated with recombinant human IL-21 in combination with either antibodies that engage CD40 (to mimic T cell interaction) and/or the BCR (to mimic antigen cross-linking). Notably, IL-21 was found to be the most potent T cell-derived cytokine to induce the proliferation of human B cells derived from peripheral blood, spleen, and tonsil after stimulation through CD40 (Ettinger et al. 2005; Ettinger et al. 2007; Good et al. 2006). Importantly, IL-2, IL-4, IL-10, and IL-13, which are other cytokines for human B cell response, had minor effects on B cell proliferation compared to IL-21 (Ettinger et al. 2005; Good et al. 2006). IL-21, in combination with anti-CD40, and more so with anti-CD40 and anti-IgM, is a potent inducer of PC differentiation of B cells isolated from peripheral blood, spleen and tonsil. In addition to expansion and differentiation, IL-21 also influences B cell

survival. In contrast to its ability to synergize with anti-CD40 to induce B cell proliferation and differentiation, IL-21 triggers cell death when BCR is ligated. This induction of cell death is preceded by activation and several rounds of proliferation, suggesting that IL-21 is inducing an activation-induced type of cell death which can be reversed by the addition of either anti-CD40 or IL-4. Moreover, the interplay of IL-21 and IL-4 may exert an essential function in determining the outcome of the human humoral immune response (Ettinger et al. 2005; Ettinger et al. 2008).

#### **2.4.4 BAFF**

The interest in survival proteins in the immune system led to the discovery of BAFF of the tumor necrosis factor (TNF) family by several research groups (Gross et al. 2000; Moore et al. 1999; Mukhopadhyay et al. 1999; Schneider et al. 1999; Shu et al. 1999). The proliferative signal mediated by BAFF is a consequence of more cells surviving to enter the cell cycle, rather than the actual co-stimulation of B cells. Likewise, the cooperation between BAFF and CD40 signaling seems to be related to increased cell survival, which allows more cells to respond to CD40L (Do et al. 2000; Avery et al. 2003). It is important to note that increased levels of BAFF have been associated with autoimmune diseases (Pers et al. 2005; Kindler and Zubler 1997).

### **2.5 Phenotyping and Genotyping of B Cell Subclasses**

Immunophenotyping focuses on the expression of specific surface markers on B cells. During the different developmental states, B cells change the composition of their surface markers allowing the identification of subclasses via flow cytometry (Figure 5). Additionally, the development of immature B cells toward terminally differentiated PC is a complex process tightly regulated by transcription factors (Figure 6). Therefore, gene expression analyses via Real Time Quantitative Polymerase chain reaction (RT-qPCR) can give additional insight into the developmental state of B cells.

#### **2.5.1 Cluster of Differentiation (CD) Antigen expression on B Cells**

CD antigens are cell surface markers that can be used to identify different stages of B cell development or activation, based on their expression level (Kjeldsen et al. 2011). Most major parental populations of human peripheral B cells can be identified using a relatively small number of surface phenotypic markers, including CD19, CD20, CD27 and CD38 (Kaminski et al. 2012)(Figure 5).

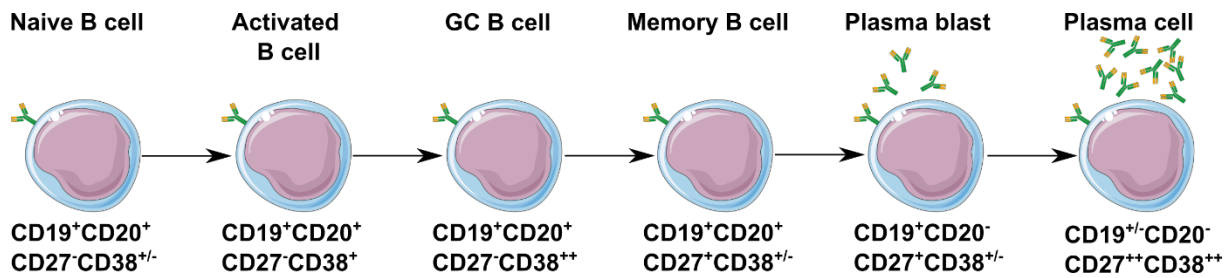


Figure 5: Surface receptor expression pattern for different developmental states of B cells from naïve B cells to PC. Some elements in the image have been obtained from Smart Servier Medical Art.

With the exception of PB and PC, the expression of CD19 and CD20 is a good marker for B cells in general (Kjeldsen et al. 2011). CD20 is expressed from naïve B cells throughout the following states. It is reduced when cells develop toward PB and PC, therefore being slightly earlier reduced than CD19, which is only downregulated in some PC (Kjeldsen et al. 2011). Generally, these markers are used in conjunction with non-B cell lineage markers (exclusion channel) for positive identification of members of the B cell lineage and exclusion of non-B cells from the analysis.

In turn, while the absence of CD20 is a valuable indicator of PB and PC, identification of all ASC can also be achieved through the combination of CD27 and CD38 upregulation (Sanz et al. 2019). CD27 is only upregulated in B cells that received stimulation and carry somatically mutated variable regions (Klein et al. 1998). CD27 can therefore be assumed as a marker for antigen-experienced cells (Seifert and Küppers 2016). CD38 is sequentially upregulated upon activation, with GC cells being the only cells with upregulated CD20 and CD38 in parallel. CD38 is downregulated when cells exit the GC reaction as memory B cells, while CD38 upregulation marks commitment toward antibody secreting PB and PC (Kanutte Huse et al. 2019; Rebecca Caeser et al. 2021).

### 2.5.2 Gene Expression in B Cells

Various genes, coding for proteins, are expressed in different quantities inside B cells. Their expression level can give further insight into cellular behavior and differentiation (Figure 6). B cell activation and differentiation are controlled by a network of transcription factors, which maintain the B cell program (e.g., paired box protein 5 (Pax5), promote class-switch recombination (e.g., interferon regulatory factor 4 (IRF4) and AID), or facilitate PC differentiation (e.g., B-lymphocyte induced maturation protein 1 (Blimp-1) and IRF4) (Nutt et al. 2011).



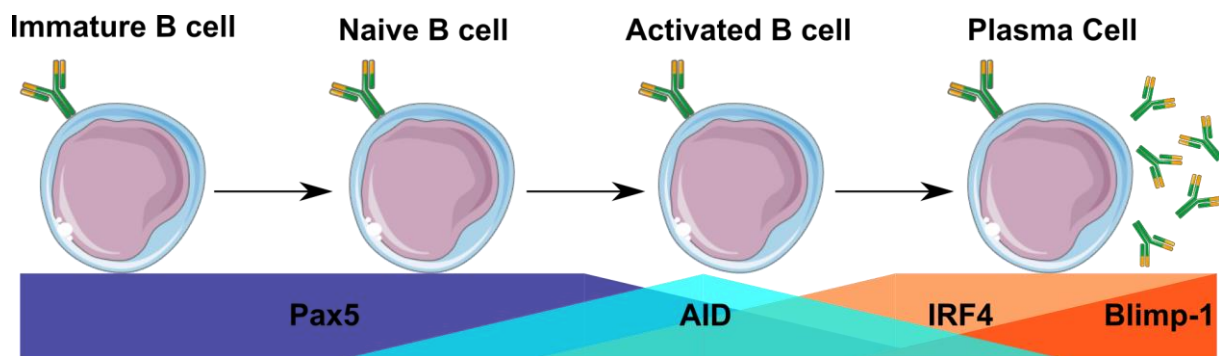


**Figure 6: The expression levels of major transcription factors during B cell differentiation. The height of the colored fields marks the expression level of Pax5 (green), AID (blue), IRF4 (orange) and Blimp-1 (red) over the different B cell stages. Some elements in the image have been obtained from Smart Servier Medical Art.**

Pax5 has an instructive role in early B cell development. It promotes B cell commitment by repressing lineage-inappropriate gene expression and reinforcing B cell-specific gene expression (Nutt and Kee 2007; Medvedovic et al. 2011). Pax5 is expressed throughout B cell development from the pro-B to the mature B cell stage and is subsequently repressed during terminal PC differentiation (Fuxa and Busslinger 2007). Decreased expression of Pax5 can therefore serve as an indicator of B cell activation.

IRF4 has been validated as a master regulator of fate choices in B cells, driving affinity maturation and terminal differentiation of PC (Shinnakasu and Kurosaki 2017). It is one of the key transcription factors to foster PC differentiation within GCs. Transgenic mice with conditional deletion of IRF4 in germinal center B cells lacked post-germinal center PCs and were unable to differentiate memory B cells into PCs. Plasma cell differentiation required IRF4 as well as Blimp-1 as a transcriptional repressor. Blimp-1 is also necessary for the development of immunoglobulin-secreting cells and the maintenance of long-lived PC (Turner et al. 1994; Kallies et al. 2004). No Blimp-1 expression has been observed in memory B cells, making it a suitable marker for B cell differentiation (Kuo et al. 2007).

During GC reaction, Centroblasts in the dark zone of GCs express AID (Muramatsu et al. 2000), which deaminates cytidine residues in the V(D)J and switch regions of the Ig gene, leading to SHM and CSR (Pavri and Nussenzweig 2011). SHM can lead to higher specificity of antibodies to the epitope, which is called affinity maturation. The Ig class switch changes the effector function of the antibody by switching from IgM and IgD expression to IgG, IgE or IgA expression. This improves its ability to eliminate the pathogen that induced the response (Pavri and Nussenzweig 2011). AID can therefore serve as an indicator of immune adaption, when T cell help in the form of CD40L is received. (Bergwelt-Baildon et al. 2002; Kanutte Huse et al. 2019)

## 2.6 State-of-the-Art *In Vitro* Culturing Systems for B Cells

### 2.6.1 Suspension Cell Cultures

Besides adherent cell culture, suspension culture is the most used form of cultivation for animal cells. In suspension cultures, cells are allowed to float or sediment freely as single cells or small aggregates of cells to function, multiply and differentiate in suspension. In these suspension *in vitro culturing systems*, differentiation and proliferation of B cells can be stimulated via CD40L in many variations, paired with defined cytokine composition, to orchestrate the desired outcome, as summarized in (Néron et al. 2011a). Soluble CD40L in monomeric or trimeric form and anti-CD40 antibodies are the most readily available options (Fanslow et al. 1994a; Haswell et al. 2001; Morris et al. 1999; Garcia-Marquez et al. 2014; Naito et al. 2013; Néron et al. 2011a). Using these soluble forms provides the advantage of tightly controllable molecular concentration in suspension culture. Soluble CD40L molecules were however shown to be transferred to and endocytosed by B cells via trogocytosis after CD40/CD40L interaction (Gardell and Parker 2017; Reed et al. 2021). Consumption of soluble CD40L in B cell cultures demands that concentration and cell numbers should always be in constant proportion, to obtain comparable results.

Immobilized CD40L can also be used to mimic membrane-bound presentation found on T cells *in vivo*. Membrane extracts, anti-CD40 Abs, immobilized on cells or magnetosomes with membrane-bound CD40L have been developed (Mickoleit et al. 2020; Néron et al. 2011a).

Lastly, feeder cells or T cells, expressing CD40L and secreting other cytokines are used to stimulate B cells in co-culture. Feeder cell lines are often cultured to a certain extent, at which they are irradiated or treated with chemicals to stop cellular proliferation and overgrowth (Luo et al. 2009; Armitage et al. 1993; Su et al. 2016; Fluckiger et al. 1993; Ivanov et al. 2005; Yoon et al. 2005; Néron et al. 2011a). CD40L-expression and IL-secretion are still active at this point, even though alterations could occur, caused by growth-arresting procedures. Exact concentrations of secreted or expressed stimuli are fairly unknown in such systems. Culturing B cells on feeder cells also bares the risk of possible alterations in cell density, CD40L-expression and IL-secretion levels, making this system unpredictable to a certain extent. These variations can be caused by natural causes or differences in irradiation procedure or chemicals for growth arrest of feeder cells (Roy et al. 2001). In general, suspension cultures lack

the tightly packed environment and extracellular matrix (ECM), which is their natural environment in lymphoid tissue.

### **2.6.2 Micro-Cell-Encapsulation and SCS-PDADMAC Capsules**

Cell encapsulation aims for the immobilization of cells in favorable growth conditions, which enables them to produce bioactive molecules with synergistic intercellular interactions without being washed out or damaged due to the surrounding shear forces. Cell immobilization techniques have been achieved using natural and synthetic biomaterials, which isolates and protects cells from the extracellular environment while allowing diffusion of nutrients (Uludag et al. 2000). It also provides some degree of organization to cells through intercellular interactions creating a natural cellular niche. Cell immobilization has also been shown as a result of spontaneous cell-to-cell interaction, which allows the formation of cell colonies or cell aggregates even under dynamic cell suspension conditions (Goetghebeur and Hu 1991; Tolbert et al. 1980).

Microcapsules are spherical structures with a diameter greater than 1  $\mu\text{m}$  but less than 2000  $\mu\text{m}$ . The material surrounding or encasing the cells is referred to as the core material, while the biomaterial encapsulating this core is referred to as coating, membrane, outer layer, shell or wall material. This membrane is semipermeable and protects the cells from interaction with local inflammatory cells, when used as an implant, while still allowing the bidirectional diffusion of nutrients and oxygen and also secretion of therapeutic products from cells (Orive et al. 2004; Uludag et al. 2000)(Figure 7). This is also the case when capsules are utilized for *in vitro* culturing systems. The small size of these platforms allows a large surface area per volume ratio, which is considered advantageous for efficient mass transport (Lanza et al. 1996; Vos and Marchetti 2002).

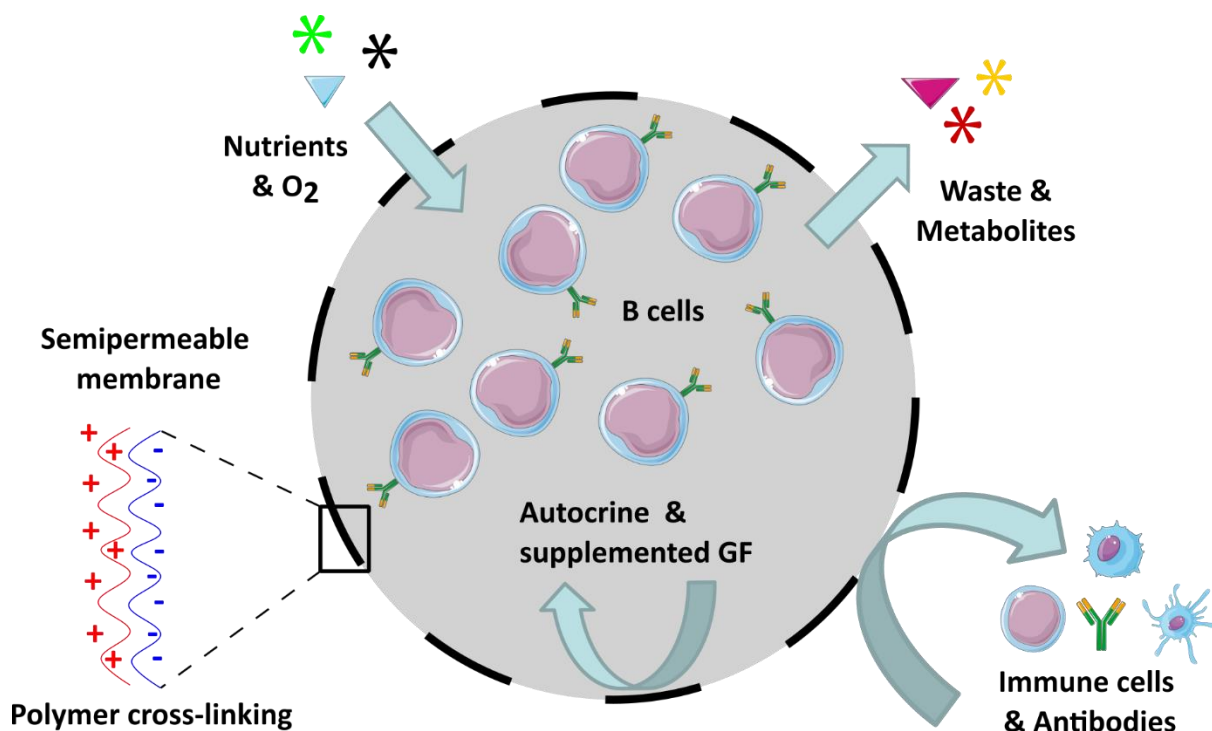


Figure 7: Schematic representation of a microcapsule, produced by polyelectrolyte complexation (PEC). Nutrients, oxygen, waste and metabolites cross the semipermeable membrane freely. Immune cells and antibodies are excluded, while autocrine and supplemented GF are entrapped. For semipermeable membrane formation, negative charges of anion polymer interact with positive charges of cation polymer, forming a PEC reaction. Some elements in the image have been obtained from Smart Servier Medical Art.

Several microencapsulation techniques have been developed in independent laboratories. All of them differ in the mechanism of cell entrapment, the core and wall material, the distribution of cells within the capsule and capsule fabrication methods. The general process of microcapsule fabrication includes a mechanism to generate a controlled-size droplet followed by a forming reaction (e.g., ionotropic gelation, PEC), which results in the formation of a stable capsule (Uludag et al. 2000; Hernández et al. 2010). There are different techniques to generate a controlled-size microcapsule, including physical (e.g., air-suspension coating, spray-drying, vibration nozzle), physico-chemical (e.g., complex coacervation also called phase separation) or chemical (e.g., in situ polymerization and interfacial polymerization) methods. All of them yield capsules with different chemical, mechanical and size properties.

### 2.6.3 Organoids for Controlled *Ex Vivo* Germinal Center Reactions

An organoid is a miniaturized and simplified version of an organ produced *in vitro* in three dimensions that shows realistic micro-anatomy. They are derived from pluripotent stem cells or isolated organ progenitors that differentiate to form an organlike tissue exhibiting multiple cell types that self-organize to create a structure, not unlike the organ *in vivo*. The technique for growing organoids has rapidly gained interest in recent years. Organoid technologies are used by scientists to study diseases and treatments in a laboratory (Lancaster and Knoblich 2014).

GC B cell organoids have been mentioned as such by Purwada et al. (2015). An Arg-Gly-Asp- (RGD)-presenting hydrogel scaffold reinforced with silicate nanoparticles (SiNP) was engineered as base of an immune organoid. Primary naïve mouse splenic B cells were then co-cultured with stromal cells that simultaneously presented Th-specific CD40L and BAFF in the presence of IL-4 (Purwada et al. 2015; Purwada and Singh 2017). This system was already close to the *in vivo* situation and recapitulated close functions of the GC reaction, showcasing clear advantages over 2D cultures.

Most recently, a human tonsil organoid system producing germinal center reaction was published by Wagar et al. (2021). The functional organotypic system recapitulated key germinal center features *in vitro*, including the production of antigen-specific antibodies, SHM, affinity maturation, PB differentiation and CSR. For an organoid generation, single-cell suspensions from tonsil tissues were plated at high density along with the antigen of interest. Influenza vaccines and viruses were used as model antigens to stimulate GC formation *in vitro*. This was the first report of an *in vitro* system supporting antigen-specific SHM, affinity maturation and class switching of human B cells. Reports like this bring research closer toward imitating the *in vivo* situation and will eventually help us to solve problems in diseases and form the basis for new therapies.

For the development of fully functional organoids with immune adaptive properties, the co-culture of multiple cell types (e.g., T cells, B cells, FDC) needs to be orchestrated. Development of such platforms, with tissue-like properties, is still in its infancy.

### 3 Material & Methods

This chapter provides the reader with detailed methods and some materials of special importance. For precise material information, the reader is referred to chapter 9.

Written consent for utilizing primary cells was obtained from the donor, after verbal and written information about research goals, as approved by the ethical review committee from the University of Bayreuth, Germany (written approval #O 1305/1-GB, 2021).

#### 3.1 Isolation of Human B Cells from Buffy Coats

Human peripheral B cells were isolated from buffy coats of anonymous, healthy, adult donors. B cells were isolated from the buffy coats by magnetically assisted cell sorting using the MACSxpress Whole Blood B Cell Isolation Kit Human (Miltenyi Biotec, Bergisch Gladbach, Germany) according to the supplier's instructions. The kit is based on a negative isolation strategy removing all blood cells except the B cells. The remaining erythrocytes, still contaminating the B cell population after magnetic sorting, were lysed by 5 min incubation in **erylysis buffer** (155 mM NH<sub>4</sub>Cl, 10 mM KHCO<sub>3</sub>, 0.1 mM EDTA) followed by centrifugation (300 g, 10 min) and subsequent resuspension of the cell pellet in phosphate-buffered saline (PBS). The List of blood donors with information on gender, age and sample type is given in Table 1.

Table 1: Donor list for blood derived B cells.

Donor	Gender	Age [years]	Type of sample
B1	Male	62	Buffy Coat
B2	Male	50	Buffy Coat
B3	Female	39	Buffy Coat
B4	Female	52	Buffy Coat
B5	Male	51	Buffy Coat
B6	Male	44	Buffy Coat

#### 3.2 Isolation of Human B Cells from Tonsillar Tissue

After removal by surgery, tonsillar tissue was immediately transferred into ice-cold **buffer 1** (HBSS containing 100 U/mL penicillin, 100 µg/mL streptomycin, 2.5 µg/mL amphotericin B, 2mM EDTA and 0.5 % (w/v) Bovine serum albumin (BSA)) and placed on ice for the transport. Figure 8 shows a schematic depiction of the B cell isolation procedure from tonsillar tissue.

Upon arrival in the laboratory, the tonsillar tissue was placed in RPMI1640 culture medium and cut into small pieces. For mechanical cell release, tissue samples were cut into small pieces, transferred into a 70 µm cell strainer, and placed on a 50 mL centrifuge tube. The material was pushed through the mesh with the help of a syringe piston. Yields were improved by three consecutive washes of the strainer with 3 mL buffer 1 for each wash. The remaining erythrocytes were lysed by incubation in erylisis buffer for 5 min. Cell debris and any remaining red cells were removed by Ficoll density gradient centrifugation (FDG) (Ficoll LSM 1077; PAA Laboratories GmbH, Pasching, Austria) according to the suppliers' instructions. Mononuclear cells at the interphase (FDG fraction) were collected and resuspended in HBSS containing 10 % (v/v) heat-inactivated fetal calf serum (FCS) (**buffer 2**).

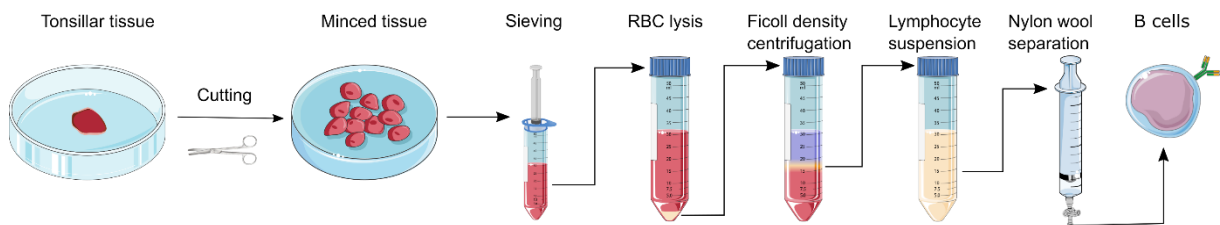


**Figure 8: Overview of the isolation procedure for B cells from tonsils. Tonsillar tissue was minced and sieved to receive single cells for red blood cell lysis. After lysis, cells were separated via Ficoll density centrifugation to obtain a lymphocyte suspension containing T and B cells. Finally, B cells were purified via nylon wool column (Helm et al. 2021).**

As prescribed by the supplier of the nylon wool, Polysciences Inc (Hirschberg an der Bergstrasse, Germany), a maximum of  $4 \times 10^8$  cells in 4 mL buffer 2 (FDG fraction) were applied to a sterilized 20 mL syringe column (B. Braun, Melsungen, Germany) packed with 1 g sterile nylon wool and incubated upright for 1 h in the cell culture incubator (37 °C, 5 % CO<sub>2</sub>, 95 % humidity). If necessary, several columns were used to process all cells released from the available tonsillar material. After incubation, the T cells were eluted by gently rinsing the wool twice with one column volume of buffer 2 (**NW-T** fraction). After that, B cells were collected (**NW-B** fraction) by filling the column with fresh buffer 2, followed by mechanical agitation to detach the cells. For this purpose, the wool was first loosened in buffer 2 with a sterilized laboratory spatula and cells were further detached by tapping the column with a metal rod. Subsequently, the wool was squeezed by pushing down the syringe piston to flush out the B cells. This step was repeated twice. NW-T and NW-B cell fractions were pooled separately in 50 mL centrifuge tubes. NW-B cells were centrifuged and resuspended in culturing medium for some cultivation, while the rest was cryopreserved before further use. The

List of tonsil donors with information on gender, age and sample type is given in Table 2 & Table 3.

**Table 2: Donor list for child-derived tonsillar B cells.**

<b>Donor</b>	<b>Gender</b>	<b>Age [years]</b>	<b>Type of surgery</b>
<b>C1</b>	Female	4	Tonsillotomy
<b>C2</b>	Male	4	Tonsillotomy
<b>C3</b>	Male	4	Tonsillotomy
<b>C4</b>	Male	3	Tonsillotomy

**Table 3: Donor list for adult-derived tonsillar B cells.**

<b>Donor</b>	<b>Gender</b>	<b>Age [years]</b>	<b>Type of surgery</b>
<b>A1</b>	Female	20	Tonsillectomy
<b>A2</b>	Female	28	Tonsillectomy
<b>A3</b>	Female	22	Tonsillectomy
<b>A4</b>	Male	34	Tonsillectomy
<b>A5</b>	Female	21	Tonsillotomy
<b>A6</b>	Female	38	Tonsillectomy
<b>A7</b>	Female	N/A	Tonsillotomy

### **3.3 Freezing and Thawing of B Cells**

B cells were recovered by centrifugation (300 g, 5 min) and resuspended in cryomedium (90 % FCS, 10 % DMSO) prior to cryopreservation. Subsequently, the cells were placed in a Mr. Frosty™ (ThermoFisher, Waltham, Massachusetts, USA) and pre-cooled in a freezer at -80 °C for 24 h. For long-term storage, the cryovials were transferred to a cryogenic storage tank (Cryo200; ThermoFisher, Waltham, Massachusetts, USA) and stored at -195 °C.

For thawing, the cryovial was placed in a water bath at 37 °C and left there until the ice began to melt, but there was still ice left in the tube. The vial was then poured into 9 mL of PBS and the cells were recovered by centrifugation (400 g, 10 min). The supernatant was discarded, and mechanical agitation was used to dislocate the cell pellet. Subsequently, the cells were subjected to the indicated culture by resuspension in medium and transfer to cell culture dishes or well-plates.



### 3.4 B Cell Cultivation and Stimulation

B cells were always cultivated in IMDM containing 10 % (v/v) human AB serum, 2 mM UltraGlutamine, ITS-G (1X), 100 U/mL penicillin and 100 µg/mL streptomycin, referred to as **base medium 1**. This base medium was supplemented with 10 µmol/mL resveratrol and 5 µg/mL PWM to obtain **unspecific growth medium** (Table 4).

**Table 4: Composition of media for unspecific B cell stimulation with PWM**

IMDM	88 % (v/v)	Base medium 1	Unspecific expansion medium
human AB serum	10 % (v/v)		
UltraGlutamine	2 mM		
Penicillin	100 U/mL		
Streptomycin	100 µg/mL		
Insulin	10 µg/mL		
Transferrin	5.5 µg/mL		
Sodium Selenite	6.7 ng/mL		
Resveratrol	10 µmol/mL		
PWM	5 µg/mL		

For specific stimulation with CD40L, cyclosporin A (CSA) was added to the base medium 1 to prevent T cell activation and obtain **base medium 2**. A mixture of GF, namely, 4 ng/mL BAFF, 10 ng/mL IL-4, 20 ng/mL IL-21 and 0.4 µg/mL CD40L, to generate the specific **expansion media** (Table 5).

**Table 5: Composition of media for specific B cell stimulation with CD40L**

IMDM	88 % (v/v)	Base medium 2	Memory expansion medium	ASC expansion medium
human AB serum	10 % (v/v)			
UltraGlutamine	2 mM			
Penicillin	100 U/mL			
Streptomycin	100 µg/mL			
Cyclosporin A	1 µg/mL			
Insulin	10 µg/mL			
Transferrin	5.5 µg/mL			
Sodium Selenite	6.7 ng/mL			
IL-4	10 ng/mL			
BAFF	4 ng/mL			
CD40L	4 µg/mL			
IL-21	20 ng/mL			

For standard cultivation, the B cells were seeded at a cell density of  $0.1 \times 10^6$  cells/mL if not indicated otherwise. Cultures were carried out in 24-well tissue culture plates with 1 mL medium per well or in 10 cm cell culture dishes with 10 mL (preculture for encapsulation). For medium change, B cells were recovered via centrifugation (400 g, 5 min) and resuspended in fresh medium at a cell density of  $0.1 \times 10^6$  cells/mL. Encapsulated cells (3 mg of capsules) were cultured in 10 mL **base medium 2** in 10 cm tissue culture plates if not indicated otherwise. All cultures were performed in a cell culture incubator (37 °C, 95 % humidity, 5 % CO<sub>2</sub>).

### **3.5 Determination of Cell Number and Viability**

A LUNA-FL™ Dual Fluorescence Cell Counter (Logos Biosystems, Gyeonggi-do, South Korea) was used to determine the number and viability of the cells. For this purpose, cells were stained with an Acridine Orange/Propidium Iodide solution (Logos Biosystems, Gyeonggi-do, South Korea) for live/dead staining according to the supplier's instructions. Cell expansion was calculated as the total amount of living cells measured on a given day divided by the number of living cells on starting day of culture or encapsulation.

### **3.6 Cellular Proliferation Assay**

For tracking of cellular proliferation, a carboxyfluorescein succinimidyl ester (CFSE) dilution assay was performed based on a previously described protocol with some modifications (Parish et al. 2009; Quah and Parish 2010). The cells were washed twice with PBS and their number was adjusted to  $5 \times 10^6$  cells/mL in PBS. Afterward, the same volume of a CFSE solution prepared from the 5 μM stock solution in PBS was added to reach a final concentration of 2.5 μM CFSE and  $2.5 \times 10^6$  cells/mL. After 5 min incubation at room temperature in the dark, the labeling was quenched by adding one volume of FCS. The cells were washed once with PBS (300 g, 5 min) and resuspended in 4 mL IMDM without supplements. Finally, the cells were recovered by centrifugation (300 g, 5 min) and resuspended in fresh base medium 1 at a density of  $0.4 \times 10^6$  cells/mL in a 24-well plate with 1 mL per well. CFSE-stained cells were left in the incubator overnight before inducing cellular proliferation with PWM and resveratrol (unspecific expansion medium).

### 3.7 FC-Analysis of Lymphocytes

For phenotyping, characteristic cell surface markers for B cell subsets, CD19, CD20, CD27 and CD38 were assessed by flow cytometry (Cytomics FC500; dual laser (488 nm, 635 nm); Beckman Coulter, Krefeld, Germany) after staining the cells with CD-specific murine antibodies (anti-CD19-APC, #302212; anti-CD20-PE, #302306; anti-CD27-PE-Cy7, #356412; anti-CD38-FITC, #356610; all from BioLegend, San Diego, California, USA) according to the manufacturer's instructions. Briefly,  $0.5 \times 10^6$  cells were washed twice in 1 mL PBS (400 g, 5 min) and resuspended in 100  $\mu$ L PBS before incubation with the antibodies on ice for 30 min. Subsequently, cells were washed twice with 1 mL PBS (400 g, 5 min) and resuspended in 500  $\mu$ L PBS prior to analysis. Flow cytometric measurements were set to 80,000 events in total. Control cells (cells subjected to mock-immunostaining) were used to set the measurement parameters. Forward scatter (FSC), side scatter (SSC) and fluorescence intensity (FITC emission 525 nm, PE emission 575 nm, APC emission 655 nm, PE-Cy7 emission 750 nm) were recorded. For each antibody, spillover compensation was acquired by single stains of OneComp eBeads (ThermoFisher, Waltham, Massachusetts, USA).

For analysis, the population was gated to identify single, viable, non-apoptotic cells using scattering properties (FSC/SSC) (Gate: Lymphocytes). Dead cells (low FSC and high SSC) and cell aggregates (high FSC) were excluded from the analysis. The lymphocyte population was further analyzed for the presence of surface markers. Within the Lymphocyte population, the B cell gate (B cells) was defined as containing the CD19<sup>+</sup> fraction. T cells were defined as the CD3<sup>+</sup> fraction. The cells in the B cell gate were further analyzed for CD20, CD27 and CD38 expression. Cells stimulated with PWM were analyzed for each surface receptor separately.

Cells in suspension were assigned to subsets as follows:

Memory cells: CD19<sup>+</sup>/CD20<sup>+</sup>/CD27<sup>+</sup>/CD38<sup>-</sup>; GC cells: CD19<sup>+</sup>/CD20<sup>+</sup>/CD27<sup>+</sup>/CD38<sup>+</sup>; PB: CD19<sup>+</sup>/CD20<sup>-</sup>/CD27<sup>++</sup>/CD38<sup>-</sup>; PC: CD19<sup>+</sup>/CD20<sup>-</sup>/CD27<sup>++</sup>/CD38<sup>++</sup>. After B cells were released from capsules, CD27 expression analysis was not possible, as shown in Figure 36. For encapsulated cells, we, therefore, used the gating strategy shown in Figure 37. Flow cytometry data were evaluated using FlowJo software v10.7.1 (Tree Star, Stanford University, Stanford, CA, USA, 2016).

### **3.8 Purification of Total RNA from B Cells**

To isolate the total RNA of B cells, we used the RNeasy mini Kit (Qiagen, Hilden, Germany). The ideal number of cells for purification was  $3 \times 10^6$  B cells. Fewer cells were possible as well but yielded less concentrated RNA. B cells were recovered by centrifugation (400 g, 10 min) and resuspended in 350  $\mu$ L RLT-buffer for lysis. Cells were then lysed by 15-times passing through a 21-gauge (0.8 mm) needle attached to a sterile 1 mL plastic syringe (B. Braun, Melsungen, Germany). The lysate was filled with one surplus volume (350  $\mu$ L) of 70 % ethanol and mixed by pipetting to resuspend precipitates as completely as possible.

The whole sample, including precipitate, was transferred to an RNeasy Mini spin column and placed on a 2 mL collection tube for RNA binding. The lid was closed and the column, including the collection tube, was centrifuged (8000 g, 15 s) and the flow-through was discarded. For a first wash, 700  $\mu$ L of buffer RW1 was added, passed by centrifugation (8000 g, 15 s) and the flow-through was discarded. For the second wash, 500  $\mu$ L of buffer RPE was added, passed by centrifugation (8000 g, 15 s) and the flow through was discarded. For the third wash, 500  $\mu$ L of buffer RPE was added, passed by centrifugation (8000 g, 2 min) and the flow through was discarded.

For RNA-release, the column was transferred to a new 1.5 mL collection tube. Dependent on the input number of cells, 30 – 50  $\mu$ L RNA-free water was added directly to the spin column membrane (50  $\mu$ L were used when the input cell number reached  $3 \times 10^6$ ). The lid of the spin column was closed and RNA was recovered as flow-through by centrifugation (8000 g, 1 min). Finally, the RNA concentration and purity were measured via a spectrophotometer (NanoDrop™, ThermoFisher, Waltham, Massachusetts, USA). The sample was either stored in a freezer (-20 °C) or directly subjected to reverse transcription.

### **3.9 Reverse Transcription (RT) of Purified RNA**

For reverse transcription, we used QuantiTect Reverse Transcription Kit (Qiagen, Hilden, Germany). The minimal RNA concentration in water was 83 ng/ $\mu$ L to reach an input RNA of 1000 ng in 12  $\mu$ L per reaction. Before RT, the sample was thawed on ice, gDNA Wipeout Buffer, Quantiscript® Reverse Transcriptase, Quantiscript RT Buffer, RT Primer Mix and RNase-free water were thawed at room temperature. Each solution

was flicked and centrifuged briefly to collect residual liquid from the sides of the tubes and always kept on ice.

1000 ng of template RNA was prepared in 12  $\mu\text{L}$ , if necessary, diluted with RNase-free water and 2  $\mu\text{L}$  of gDNA wipeout buffer was added for gDNA wipeout. The mixture was incubated for 2 min at 42 °C and placed on ice immediately.

Reverse-transcription master mix was prepared by mixing 4  $\mu\text{L}$  Quantiscript RT Buffer, 1  $\mu\text{L}$  Quantiscript Reverse Transcriptase and 1  $\mu\text{L}$  RT Primer Mix. 14  $\mu\text{L}$  of template RNA without gDNA was added, mixed and stored on ice. For reverse transcription, the mixture was incubated for 15 min at 42 °C. For inactivation of RT, the sample was subsequently incubated for 3 min at 95 °C. Yielded cDNA (20  $\mu\text{L}$ ) was split to 5 x 4  $\mu\text{L}$  and stored at -20 °C. Before use for qPCR, 16  $\mu\text{L}$  PCR-water was added to 4  $\mu\text{L}$  of cDNA-solution.

### **3.10 qPCR of cDNA**

For analyses of 8 genes in triplicate, 280  $\mu\text{L}$  of master-mix was prepared. 20  $\mu\text{L}$  of cDNA input was brought to 98  $\mu\text{L}$  by adding PCR-water. Then 175  $\mu\text{L}$  SYBR FAST Universal and 7  $\mu\text{L}$  KSF-ROX-Low (SuperMix, # 733-1250, VWR, Radnor, Pennsylvania, USA) were added.

Forward and reverse primer (4  $\mu\text{L}$  each at 10  $\mu\text{M}$ ) (Table 6) was added to a micro reaction tube and 32  $\mu\text{L}$  of the master mix was added. The reaction mixture was split to 3 x 10  $\mu\text{L}$  per well in a 96-well PCR plate and closed with qPCR caps for plate set up in triplicates. Before qPCR, the well-plate was centrifuged (300 g, 5 min) to remove bubbles from reaction mixtures. For qPCR, the well plate was placed in the qPCR cycler (MX3005P, Stratagene) and cycled once for 10 min at 95 °C, followed by 45 cycles at 95 °C for 15 s, 56 °C for 15 s and 72 °C for 20 s. Data were assessed via MxPro QPCR software (Agilent) and exported to Excel (Microsoft, Redmond, Washington, USA). The threshold for Ct acquisition was always set to 0.15, to be above the noise but as low as possible.

**Table 6: Sequences of used primer for RT-qPCR. Primers were stored at -20 °C at 100 µM and diluted with PCR water to 10 µM before use.**

Gene	Sequence (5'-3')	
	Forward	Reverse
<b>AID</b>	AGAGGCGTGACAGTGCTACA	TGTAGCGGAGGAAGAGCAAT
<b>Blimp-1</b>	GAAAGGCTTCACTACCCTTATCC	CAGAGTTCATTTTTCTCAGTGCTC
<b>IRF4</b>	CTACACCATGACAACGCCTTACC	GGCTGATCCGGGACGTAGT
<b>Pax5</b>	GCGCAAGAGAGACGAAGGT	CTGCTGCTGTGTGAACAAGTC
<b>HPRT</b>	GCCCTGGCGTCGTGATTAGT	CGAGCAAGACGTTTCAGTCCTGTC
<b>β<sub>2</sub>microglobulin</b>	CAAACCTCCATGATGCTGCTTAC	CCCACTGAAAAAGATGAGTATGCC
<b>GAPDH</b>	TGACTCCGACCTTCACCTCC	TTCGCTCTCTGCTCCTCCTGT
<b>βactin</b>	TCACCTTACCGTTCAGTTTT	AACAAGATGAGATTGGCATGGC

### 3.11 Calculation of Reference Gene Stability

To determine the most stable reference gene for the  $\Delta\Delta C_t$  Method, we utilized the GeNorm algorithm, the details of which are described in Vandesompele's study (Vandesompele et al. 2002). The most stable reference gene has to be selected to ultimately calculate the correct gene regulation and transcript levels of target genes.

For the calculation of reference gene stability, the ratio of the target genes  $C_t$  to all other potential reference genes and the reciprocal values were calculated. Next, the variation across samples (days/donors) was calculated. The arithmetic mean of the ratios variation across samples provided the M value (Formula 1)

$$\text{arithmetic mean} \left[ \text{variation} \left( \frac{C_t(G1)}{C_t(G2; 3; 4)} \right)_{\text{day/donor}} ; \text{variation} \left( \frac{C_t(G2; 3; 4)}{C_t(G1)} \right)_{\text{day/donor}} \right]$$

**Formula 1: Calculation of the M value with four available genes. The ratio of a pair of reference genes and all pairwise variations is calculated across all samples. The M value is the arithmetic mean of all pairwise variations.**

The reference gene stability was the natural logarithm of the reciprocal M value.

$$\text{reference gene stability} = \ln \left( \frac{1}{(M \text{ value})} \right)$$

**Formula 2: Calculation of the reference gene stability. Stability is the natural logarithm of the reciprocal M value.**

A tabular example for the calculation of the gene stability of HPRT in comparison to 3 other genes and 4 other donors is given in Appendix 4.

### 3.12 Calculating Gene Expression via $\Delta\Delta\text{Ct}$ Method

Mean Ct values and standard deviations were used for all  $\Delta\Delta\text{Ct}$  calculations. Based on our results for reference gene stability, we always used  $\beta$ -actin as endogenous control. First, the  $\Delta\text{Ct}$ -value was calculated by subtraction of the reference gene (Rev) and each gene of interest (GOI) (Formula 3).

$$\Delta\text{Ct} = \text{Ct}(\text{GOI}) - \text{Ct}(\text{rev})$$

**Formula 3: Calculation of the  $\Delta\text{Ct}$ -value**

The standard deviation (StDev) of the  $\Delta\text{Ct}$ -value was calculated from the standard deviations of the GOI and the endogenous control in accordance with error propagation (Formula 4).

$$\text{StDev}(\Delta\text{Ct}) = \sqrt{(\text{StDev}(\text{Ct}(\text{GOI}))^2 + (\text{StDev}(\text{Ct}(\text{Rev})))^2}$$

**Formula 4: Calculation of the StDev of the  $\Delta\text{Ct}$ -value.**

The  $\Delta\Delta\text{Ct}$ -value was then calculated to obtain differences between two samples (e.g., treatments, time, donors). The  $\Delta\text{Ct}$  of a calibrator sample was subtracted from the test sample (Formula 5).

$$\Delta\Delta\text{Ct} = \Delta\text{Ct}(\text{test sample}) - \Delta\text{Ct}(\text{calibrator sample})$$

**Formula 5: Calculation of the  $\Delta\Delta\text{Ct}$ -value from a test and calibrator sample (e.g., day 0 and day 4)**

The standard deviation of the  $\Delta\Delta\text{Ct}$  and  $\Delta\text{Ct}$ -value can be assumed to be the same. The fold difference of gene expression was calculated based on a negative or positive  $\Delta\Delta\text{Ct}$  as shown in Formula 6 and Formula 7 respectively.

$$\Delta\Delta\text{Ct} \leq 0 \rightarrow \text{fold - difference} = 2^{-\Delta\Delta\text{Ct}}$$

**Formula 6: Calculation of the fold-difference ( $\Delta\Delta\text{Ct} \leq 0$ ).**

$$\Delta\Delta\text{Ct} > 0 \rightarrow \text{fold - difference} = -2^{\Delta\Delta\text{Ct}}$$

**Formula 7: Calculation of the fold-difference ( $\Delta\Delta\text{Ct} > 0$ ).**

For the non-symmetric standard deviation of the fold-difference, the standard deviation was expressed as a range by adding or subtracting the error to/from the middle value of  $\Delta\Delta\text{Ct}$  and subjecting that value to Formula 6 and Formula 7 to obtain upper and lower fold-difference.

### 3.13 Agarose Gel Electrophoresis of cDNA

The gel was prepared by weighing 0.5 g agarose, adding 50 mL of TAE buffer (40 mM Tris, 20 mM acetic acid and 1 mM EDTA) and microwaving the solution until agarose was fully dissolved. After 5 min of cooling, 3  $\mu$ L of peqGREEN (VWR, Radnor, Pennsylvania, USA) dye was added, the gel was cast into the mold-form and the comb was added. After 60 min, the gel was fully polymerized and the comb was removed. The gel was removed from the mold-form, placed in the electrophoresis chamber and submerged in TAE buffer. 1  $\mu$ L of loading dye was added to the samples (10  $\mu$ L qPCR product) and 9  $\mu$ L of the samples were pipetted into the designated pockets. 5  $\mu$ L of 1 kb DNA Hyperladder (Meridian Bioscience, Cincinnati, Ohio, USA) was added to the designated pockets and the gel ran at 80 volts for 1 hour. Gel images were obtained via the Quantum gel documentation imaging system (Vilber Lourmat, Eberhardzell, Germany) and BioVision software (Vilber Lourmat, Eberhardzell, Germany).

### 3.14 ELISA

For IgG, IgM and IgA ELISA, we used kits (ELISA Flex: Human IgG (ALP), #3850-1AD-6; ELISA Flex: Human IgM (ALP), #3880-1AD-6; ELISA Flex: Human IgA (ALP), #3860-1AD-6; ELISA substrate: pNPP for ALP, #3652-P10 all from Mabtech, Nacka Strand, Sweden). Supernatants were obtained via centrifugation (400 g, 5 min), after culture, stored at -20 °C until use and thawed on ice.

ELISA was conducted according to the manufacturers' description. First 96-well high protein binding plates (VWR, Radnor, Pennsylvania, USA) were labeled with capture antibody overnight and blocked with blocking-buffer (SuperBlock™, #37580, ThermoFisher, Waltham, Massachusetts, USA). The plate was washed 5 times (ELISA Wash Buffer, #421601, BioLegend, San Diego, California, USA) before samples were applied. Washing was always performed this way. Samples were diluted 400, 4000 and 40000-fold in blocking buffer. Each concentration was prepared in triplicate. Background control (PBS) and dilutions for the standard curve were prepared in blocking buffer. All samples were applied and incubated (2 h, RT). The plate was washed 5 times. Detection antibody was applied and incubated (1 h, RT). The plate was washed 5 times and pNPP substrate was applied and left for incubation (1 h, RT). The optical density was assessed via plate reader (GENios, Tecan, Männedorf, Switzerland) at 405 nm with a reference wavelength of 580 nm. Data were collected



via XFluor software (GENios, Tecan, Männedorf, Switzerland) and exported into Excel (Microsoft, Redmond, Washington, USA).

### **3.15 3D Printing of Microencapsulation Unit**

We designed the 3D-Modle of our microencapsulation unit using the 3D CAD software Fusion 360 (Autodesk, San Rafael, California, USA). The 3D-Modle was converted to STL-format and sliced with PreForm slicing software (Formlabs, Somerville, Massachusetts, USA). For 3D-Printing, we used a Form 3 SLA 3D-Printer with clear resin V4 and a Form 3 resin tank V2 (Formlabs, Somerville, Massachusetts, USA). For post-processing of the 3D-Prints, we used the Form Cure and Finish Kit (Formlabs, Somerville, Massachusetts, USA). Before UV treatment in the Form cure, all the support structures were removed and the microencapsulation unit was washed. Especially the inner systems were flushed with isopropyl alcohol to remove the excessive resin before the final polymerization step. The finalized microencapsulation unit was sterilized for 30 min under UV light before use.

### **3.16 Alginate Encapsulation**

A 1.5 wt% Na-alg solution was prepared in PBS and stirred overnight. For the production of capsules, the suspension was added dropwise to 50 ml of a well-agitated CaCl<sub>2</sub> solution (90 mM CaCl<sub>2</sub>, 154 mM NaCl, 0.02 vol% Tween 20) using an encapsulation apparatus consisting of a syringe pump (KDS model 100, KD Scientific, Holliston, MA), a 2 ml syringe (B. Braun, Melsungen, Germany) and our in-house 3D-printed encapsulation unit. The settings were as follows: flow velocity cell suspension, 40 mL/h; flow velocity coaxial N<sub>2</sub>-stream, 1 – 4 L/min; drop height, 8 cm. Capsules were stirred in the CaCl<sub>2</sub> solution for another 2 min and stored there afterward.

### **3.17 Cell Encapsulation in SCS-PDADMAC**

Procedures for encapsulation and release of the cells from the SCS-PDADMAC capsules were as reported previously (Jérôme et al., 2017). A schematic depiction of the encapsulation process can be seen in Figure 39.

1.8 % (w/v) SCS solution was prepared in PBS and stirred overnight at room temperature. The solution was sterilized by autoclaving (5 min, 121 °C, 2.05 bar) and allowed to cool to room temperature for 2 h under constant stirring (150 rpm; 5 mm magnetic stirrer). IL-4, IL-21, BAFF and CD40L were added at the same concentrations

as in the growth medium, unless otherwise indicated. The PDADMAC stock solution was diluted to 0.85 % (w/v) in PBS and sterilized by autoclaving (20 min, 121 °C, 2.05 bar). For encapsulation, the B cells (viability > 85 %), pre-cultured for 4 days if not indicated otherwise, were first resuspended in human AB serum. Afterward, they were either recovered by centrifugation (400 g, 10 min) and resuspended in 3 mL SCS solution at a concentration of  $1 \times 10^6$  cells/mL without serum (cells/capsules<sub>withoutserum</sub>). Alternatively, the cell suspension in serum was directly diluted 1:10 in the SCS solution (cells/capsules<sub>withserum</sub>). The cell/SCS-solution was gently stirred for 5 min (50 rpm) and filled in a 2 ml syringe (B. Braun, Melsungen, Germany). The syringe was placed in a syringe pump (KDS model 100, KD Scientific, Holliston, MA) and connected to the in-house 3D-printed encapsulation unit via a silicone tube with a 5 mm inner diameter. The syringe was pushed by hand until the encapsulation unit was filled and then pumped at 40 mL/h through the nozzle of the encapsulation unit (Figure 33), where droplets formed in a coaxial N<sub>2</sub> stream (4 L/min). The polyelectrolyte capsules formed instantaneously when the droplets entered the well-agitated (300 rpm) PDADMAC hardening bath (50 mL). Afterward, the capsules were stirred for another 2 min in the hardening bath before adding 50 mL PBS. After 10 min stirring, the PDADMAC/PBS solution was replaced by 100 mL fresh PBS and stirred for another 10 min. Washing was repeated once more. Afterward, capsules were transferred to a 10 cm tissue culture dish containing 10 mL base medium 2 (i.e., without GF supplementation).

### **3.18 Cell Release from SCS-PDADMAC Capsules**

For cell release, aliquots of the capsules were taken and the medium was aspirated as thoroughly as possible. The wet-weight of the capsules was determined, while 1 mg of capsule material was assumed to be the equivalent of 1 mL of culture. A 10-fold surplus (by weight) of a 1 % (w/v) cellulase solution (Cellulase Cellulysin®, Merck, Darmstadt, Germany) in PBS was added. The mixture was incubated for 1 h at 37 °C under agitation (200 rpm) in a lab shaker (Kuehne, Basel, Switzerland). The brittle capsules were broken by repeated up-and-down pipetting with a P1000 pipette (Eppendorf, Hamburg, Germany). To remove residual capsule material, suspensions were passed through a 70 µm cell strainer before further analysis.

### **3.19 Capsule Microscopy and Image-Based Size Determination**

We used an inverted light microscope for standard microscopy of cells and capsules (CKX41, Olympus Live Sciences, Tokyo, Japan). For imaging, we used a Primovert inverted light microscope with the imaging software Zenlite (V.3.3) (Carl Zeiss AG, Oberkochen, Germany). Zenlite software was also used to determine the capsules' size.

### **3.20 Diffusion Assay with Vitamin B<sub>12</sub> and Resorufin**

Resorufin solution was produced from a 5 mg/mL resazurin solution by autoclaving (5 min, 121 °C, 2.05 bar). A calibration curve from 1 to 0.1 mg/ml in 0.1 mg/mL steps of the dedicated solution and 90 µL of PBS was prepared in the wells of a 96-well plate. Empty SCS-PDADMAC capsules were produced and stored in PBS as described above. The PBS was aspirated as thoroughly as possible and the wet weight of the capsules was determined. We aimed for 500 µg of capsules to keep experimental conditions as constant as possible. The capsules were transferred into a micro reaction tube

For the start of diffusion, on surplus (by weight) of a 5 mg/mL vitamin B<sub>12</sub>- or resorufin-solution was added to the capsules, the lid was closed and the tube was inverted 3 times. 1 mg of capsule material was assumed to be the equivalent of 1 mL of dye solution. For sampling, 10 µL of the dye solution was aspirated and added to the prepared wells with 90 µl PBS. The first sample was taken immediately after inverting and was defined as  $t = 0$  s. After the last sample, the 96-well plate was measured via plate reader (GENios, Tecan, Männedorf, Switzerland). Vitamin B<sub>12</sub> absorption was measured at 405 nm, while resorufin fluorescence was measured with an excitation at 535 nm and emission at 590 nm. Data were collected via XFluor software (GENios, Tecan, Männedorf, Switzerland) and exported into Excel (Microsoft, Redmond, Washington, USA).

### **3.21 Statistical Analysis**

Group data are reported as mean  $\pm$  standard deviation. If not otherwise stated,  $n$  represents the number of technical replicates. OriginPro software (version 2021, OriginLab, Northampton, Massachusetts, USA) was used for ANOVA with Bonferroni multiple comparison tests to determine whether data groups differed significantly. Statistical significance was defined as \*( $p \leq 0.05$ ), \*\*( $p \leq 0.01$ ) or \*\*\*( $p \leq 0.001$ ).

## 4 Results and Discussion

### 4.1 Unspecific Stimulation with PWM

This chapter is a slightly modified version of “Isolation of primary human B lymphocytes from tonsils compared to blood as alternative source for *ex vivo* application” published in Journal of Chromatography B and has been reproduced here with the permission of the copyright holder (Helm et al. 2021).

#### 4.1.1 Primary Human B Cells from Blood and Tonsils

A detailed comparison of blood and tonsils as a source of B cells was conducted by S. Riedl and is published in Helm et al. (2021). An average number of  $33.8 \pm 20.3 \times 10^6$  living B cells per donor was isolated by magnetic sorting procedure from buffy coats. The corresponding yield of viable B cells derived from tonsillar tissues from children was  $90.2 \pm 74.6 \times 10^6$  cells and from adults  $269.7 \pm 155.6 \times 10^6$  cells. Differences between adult and child donors were due to more input material from adult donors.

For the preparation of any B cells from tissues, T cells are considered to be the most prominent contamination (Boyaka et al. 2000). When adult starting materials were compared, the fraction of B cells within the total lymphocyte fraction was 6-fold higher in tonsils than in buffy coats. The relative B cell content in tonsillar tissue of children was even higher. Yet, isolation from buffy coats resulted in a statistically significant ( $p < 0.001$ ) higher purity of the B cells ( $94.9 \pm 1.6$  %) compared to the isolation from tonsils, where the separation on nylon wool column led to non-negligible residual contamination of the B cell fraction with T cells (Median<sub>adult</sub>: ~19 %, Median<sub>child</sub>: 5 %).

B cells were mostly CD20<sup>+</sup> indicating an extremely low frequency of PB and PC (CD20<sup>-</sup>) in blood and tonsils. The frequency of the CD38<sup>+</sup> subset (e.g., naïve and GC-like cells) was slightly lower in adult donors compared to child donors and about two-fold lower than among the cells isolated from blood. Adult tonsils displayed a high frequency of CD27<sup>+</sup> cells (i.e., cells that have already encountered their specific antigen), whereas blood contained mainly naïve B cells (i.e., CD27<sup>-</sup>). Interestingly, children’s tonsils contain low amounts of CD27<sup>+</sup> B cells, reflecting a still-developing immune system. Therefore, blood and child tonsils are considered the preferred source for isolating naïve B cells. In contrast, adult tonsils provide higher numbers of matured B cells, i.e., GC and memory cells (Helm et al. 2021).

Blood is a well-established source for B cells, with magnetic-assisted cell sorting (MACS) kits readily available for quick isolation and high B cell purities. However, tonsils as lymphoid organs are more plentiful as cell sources, capable of providing enough lymphocytes for multiple experiments with one individual donor. This reduces donor-dependent variation when techniques are established with primary cells, while cells can be collected from juvenile and adult individuals. B cell purities are lower with our nylon wool-based procedure compared to commercially available MACS kits (Helm et al. 2021). If high purities are required, anti-CD3 or -CD19 MACS kits can be utilized instead of nylon wool, or T cell depletion can be achieved by adding CSA to the culture medium (Flores et al. 2019). However, tonsils and our isolation protocol can be a more suitable starting point for cultures for co-culturing approaches with T and B cells.

#### 4.1.2 Tracking Cellular Division via CFSE Intensity Reduction

CFSE labeling was conducted following the protocols developed in previous works (Parish et al. 2009; Quah et al. 2007; Quah and Parish 2010). In brief, the cells were washed twice in PBS, then  $5 \times 10^6$  cells were incubated for 5 minutes in  $2.5 \mu\text{M}$  CFSE. Subsequently, FCS was added to stop the labeling process. The cells were washed in IMDM and finally resuspended in base medium 1. Figure 9 shows the results of the CFSE labeling and cells after 12 days of culture with and without PWM for donor B3.

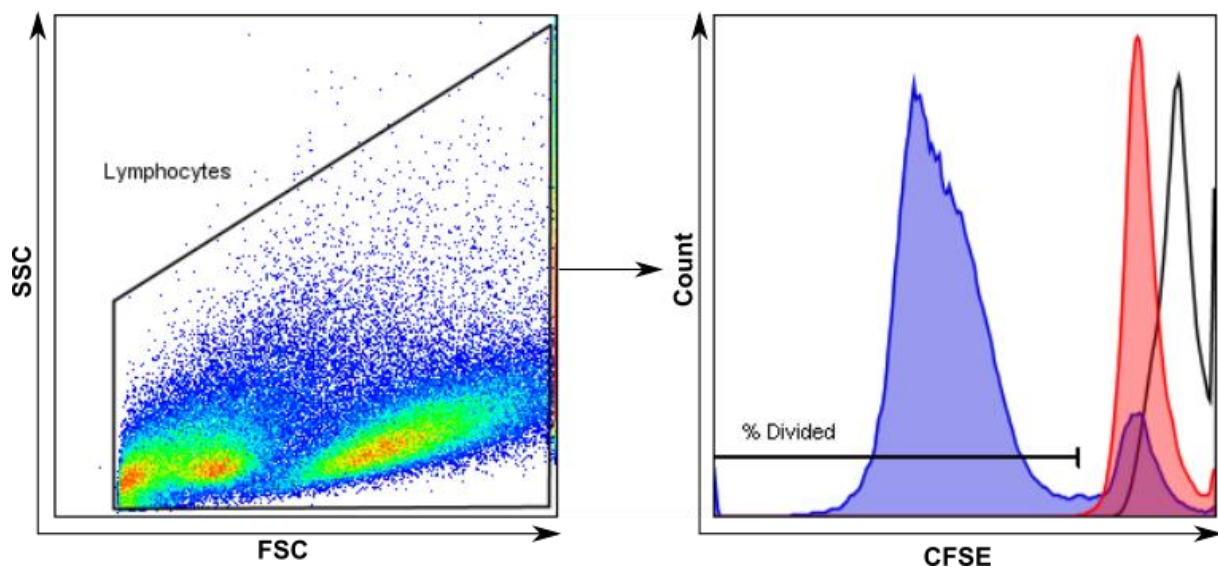


Figure 9: Gating strategy for the CFSE dilution assay analysis. Lymphocytes were gated via FSC vs. SSC and CFSE intensity was analyzed after. B cells of donor B3 on day 0 after CFSE staining (white) and after 12 days of cultivation without PWM (red) and with PWM (blue) are shown. Divided cells were defined as cells having undergone at least one round of division during the cultivation period, as evidenced by a reduced CFSE fluorescence.

The labeling was performed right after cell isolation, prior to culture. The cells were measured 24 h after the CFSE-labeling, when adding GF to the assigned wells. Figure

9 shows the stained cells prior to PWM supplementation (white) and on day 12 of culture with (blue) and without PWM (red). B cells were cultured without PWM, to observe presumed spontaneous B cell proliferation events, possibly induced by interaction with the remaining T cells (Banchereau and Rousset 1992). Non-stimulated cells never showed significant proliferation. Undesired activation of the cells could therefore be excluded. The presence of T cells in the sample was consequently insufficient to induce B cell proliferation.

Cell division results in a sequential halving of fluorescence. Normally up to 8 individual divisions can be monitored before the fluorescence is decreased to the background fluorescence of unstained cells (Parish et al. 2009). With our protocol, the identification of cells that underwent 1 – 8 divisions was not possible since there were no individual peaks in the histogram related to a number of divisions. The protocol was therefore constrained to identify the percentage of overall cells that underwent at least one division to quantify the proliferative response of B cells.

#### **4.1.2 Proliferative Response to PWM in Primary Human B Cells**

Cells prepared by the two protocols, namely BC<sub>MACS</sub>, NW-B<sub>adult</sub>, and NW-B<sub>child</sub>, were cultured for up to 12 days in a culture medium supplemented with PWM (5 µg/mL) as unspecific stimulus. Figure 10 shows the Proliferation by CFSE dilution assay followed by flow cytometry analysis as described in Figure 9.

Overall, cell division was not observed during the first 4 days of culture in the presence of PWM, indicating an extensive lag phase. On day 5, weak proliferation was detectable for some donors. After that, all tonsillar cells isolated from adult donors (NW-B<sub>adult</sub> preparations) commenced dividing actively, albeit with pronounced donor variability. The strongest proliferative response was observed for cells from donor A2. Cells isolated from juvenile tonsils showed the lowest tendency for proliferation. Only donor C4 showed measurable division. Lower amounts of CD27<sup>+</sup> cells in child-derived B cells can be a possible explanation for the lower proliferative response (Helm et al. 2021).

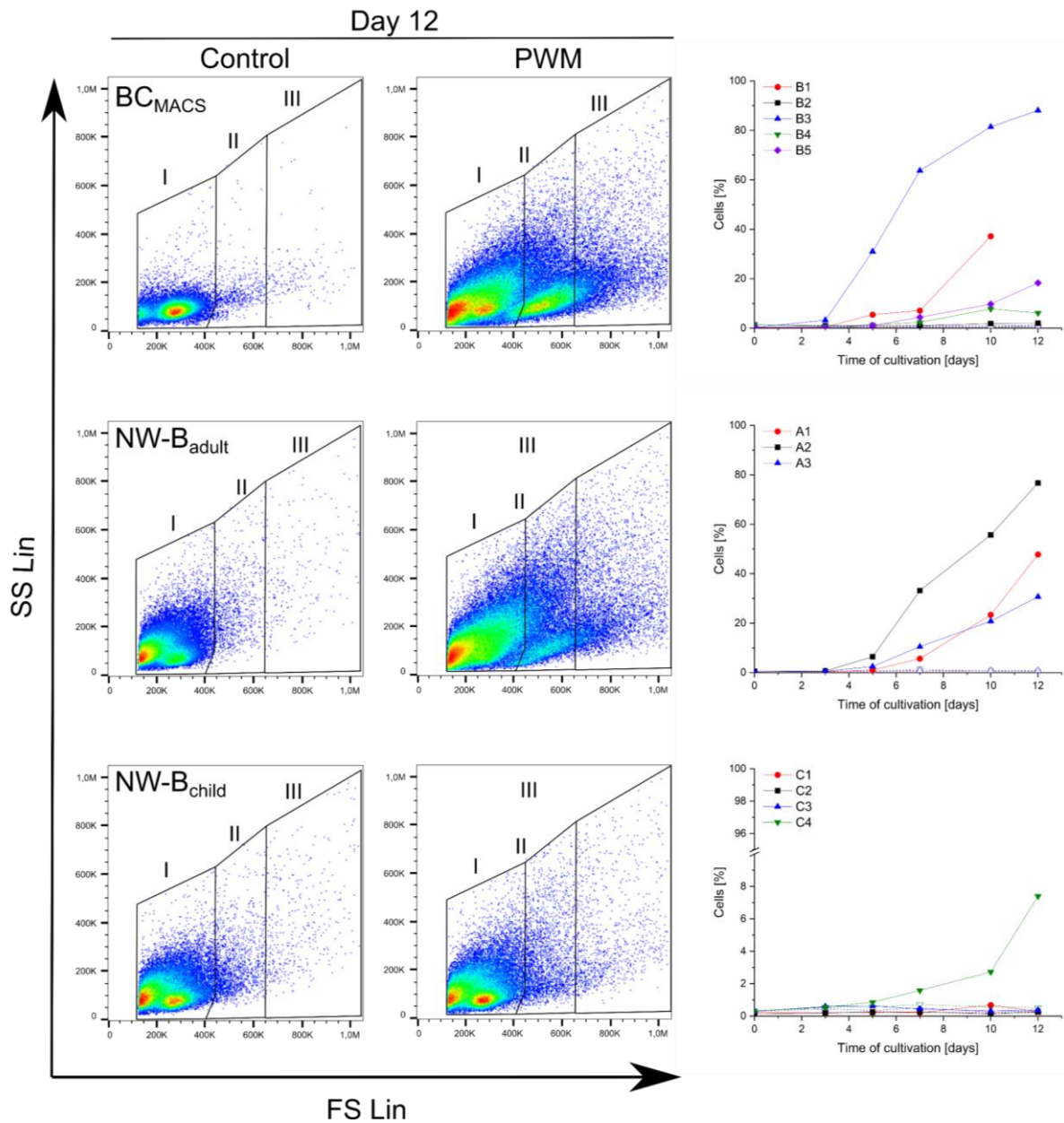


**Figure 10:** Left: Representative forward vs. side scatter plots for donors B3 (BC<sub>MACS</sub>), A2 (NW-B<sub>adult</sub>), and C4 (NW-B<sub>child</sub>). For day 12, dot-plots of non-treated cells (control) and cells stimulated with 5  $\mu\text{g}/\text{mL}$  PWM (PWM) are given. Right: Cell proliferation (i.e., percentage of divided cells) in the absence (dashed lines) and the presence (solid lines) of PWM. Data represent the percentage of divided cells in the Lymphocytes gate. This figure is adopted from Helm et al. (2021).

For peripheral B cells isolated from blood, the proliferative response to mitogens declines with age (Cobleigh et al. 1980). A similar effect is described here for the first time for B cells isolated from tonsils. Furthermore, the response to the B cells isolated from blood shows significant donor specificity. At the same time, cells from donor B3 and, to a lesser extent, B1 and B5 showed a proliferative response, while others did not.

Cultivation in the presence of PWM induced overall cell proliferation and was accompanied by changes in the scattering properties of the cells, suggesting a

subdivision into three populations (I, II, and III) according to variations in size and granularity, as seen in Figure 10. Analysis of the scattering properties of the divided cells revealed that population I contained the majority (up to 55 %) of the cells that had undergone at least one division. Most of the remaining cells that had divided, were found in population II, whereas population III contained < 7 % of divided cells (Table 7).

**Table 7: Percentages of divided cells in FS/SS sub-populations after 12 days of cultivation with PWM as mitogenic stimulus. Bold fonts highlight donors, proliferating best under PWM stimulation (Helm et al. 2021).**

Cell fractions	Donor	Frequency of divided cells (%)		
		Population I	Population II	Population III
BC <sub>MACS</sub>	B1	17.5 (0.3)	5.9 (0.0)	2.3 (0.0)
	B2	1.7 (1.2)	0.3 (0.1)	0.0 (0.0)
	<b>B3</b>	<b>54.8 (0.6)</b>	<b>27.4 (0.0)</b>	<b>6.3 (0.0)</b>
	B4	3.9 (0.8)	1.3 (0.0)	0.9 (0.0)
	B5	13.8 (0.8)	3.5 (0.1)	1.1 (0.0)
NW-B <sub>adult</sub>	A1	26.6 (0.3)	11.9 (0.0)	6.6 (0.0)
	<b>A2</b>	<b>52.7 (0.4)</b>	<b>19.7 (0.0)</b>	<b>4.8 (0.0)</b>
	A3	21.3 (0.7)	7.3 (0.1)	2.4 (0.0)
NW-B <sub>child</sub>	C1	0.2 (0.2)	0.0 (0.0)	0.0 (0.0)
	C2	0.2 (0.2)	0.0 (0.0)	0.0 (0.0)
	C3	0.3 (0.3)	0.0 (0.0)	0.0 (0.0)
	C4	4.6 (0.5)	1.8 (0.0)	1.0 (0.0)

These results indicate that cell proliferation within a dedicated population is induced upon PWM stimulation. However, we can also hypothesize that after division, cells further differentiate, which might change their scattering properties. As reported before, PWM can trigger long-lasting B cell expansion, while concomitantly inducing terminal differentiation into ASC (Bekeredjian-Ding et al. 2012). Both differentiation and fate commitment are controlled by a complex regulated process occurring in a cell division-linked manner (Tangye et al. 2003).

#### 4.1.3 Effect of T Cell Impurities in PWM-Stimulated B Cell Cultures

PWM is a T cell-dependent B cell mitogen and a weak T cell mitogen (Mellstedt 1975; Keightley et al. 1976). Since most of the NW-B fractions contain a non-negligible amount of contaminating T cells, we could not exclude that the PWM additionally helped the T cells to proliferate and that this had an impact on the B cell response to stimulation. Figure 11 shows the gating strategy for the identification of T and B cells in the lymphocyte population for blood and tonsillar cells.



## BC/FDG

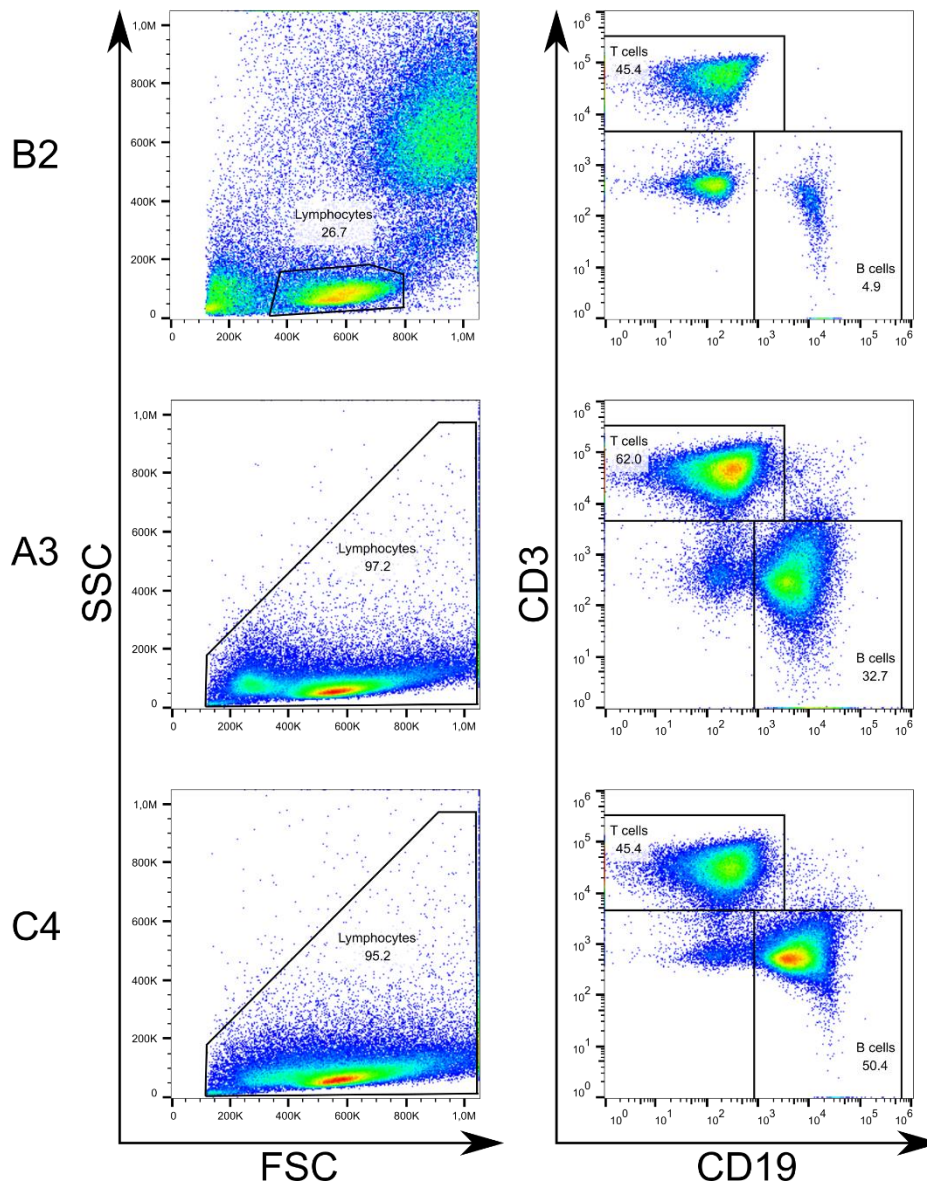


**Figure 11: Gating of lymphocytes via FSC vs. SSC and subsequent gating of T and B cells via CD19 vs. CD3 expression. Shown are donor B2 before MACS and tonsillar B cells of A3 and C4 after FDG (before NW separation).**

B cell populations containing a higher number of T cells might be more prone to activate B cells because the T cells can secrete cytokines, which are required for B cell proliferation and differentiation (Mellstedt 1975; Keightley et al. 1976). Therefore, we also analyzed B and T cell incidence after 12 days of mitogenic stimulation (Table 8).

NW-B<sub>child</sub> cells, i.e., cells showing low proliferation tendency in general, also maintained high B cell numbers during the cultivation. In the case of cells in the NW-B<sub>adult</sub> and the BC<sub>MACS</sub> preparations, a strong proliferative response was accompanied by significant changes in relative B cell content, e.g., A2, B3. Concomitantly, the frequency of T cells increased 2- (A2) or 15-fold (B3), and a new population negative for both CD19 and

CD3 (non-B-non-T cells) emerged. However, for the other more mildly proliferating samples (donors A1, A3, B1 and B5), neither an apparent decrease of the B cell frequency nor an increase of the T cells population was observed.

**Table 8: T cells and B cells distribution after 12 days of cultivation with PWM as mitogenic stimulus. Cells were cultivated for 12 days in the presence of 5 µg/mL PWM. CD19<sup>+</sup>(B cell), CD3<sup>+</sup> (T cell) and CD19<sup>-</sup>CD3<sup>-</sup> cell distribution was determined by bicolor immunostaining and flow cytometry ('Lymphocyte' gate). Bold fonts highlight donors proliferating best under PWM stimulation (Helm et al. 2021).**

Cell fraction	Donor	B cells (%)	T cells (%)	Non-B-non-T-cells
BC <sub>MACS</sub>	B1	97.8	0.6	1.6
	B2	98.6	0.1	1.3
	<b>B3</b>	<b>46.5</b>	<b>42</b>	<b>11.5</b>
	B4	86.2	8.7	5.1
	B5	94.4	1.9	3.7
NW-B <sub>adult</sub>	A1	84.5	14.7	0.8
	<b>A2</b>	<b>38.8</b>	<b>46.4</b>	<b>14.8</b>
	A3	73.5	18.9	7.6
NW-B <sub>child</sub>	C1	94.7	5.1	0.2
	C2	96.5	3.4	0.1
	C3	94.2	5.7	0.1
	<b>C4</b>	<b>92.6</b>	<b>6.6</b>	<b>0.8</b>

This indicates the proliferative response of not only B cells in PWM-stimulated cultures. PWM seems to harness cellular interactions, of presumably T and B cells, leading to proliferative response of Both cell types and possibly others as well.

#### 4.1.4 Effect of PWM on B Cell Differentiation

As shown above, PWM-stimulation led to proliferation accompanied by changes in the scattering properties of the cells. This might be the first hint that besides proliferation, some further maturation of the B cells alongside their differentiation pathway had occurred. Mostly focusing on cell preparations displaying a noticeable proliferative response (i.e., BC<sub>MACS</sub> and NW-B<sub>adult</sub>) upon PWM stimulation, we analyzed the frequency of the most relevant B cell subsets (CD20, CD27 and CD38), i.e., naïve, memory and PC-like cells in the populations mentioned above I, II, and III as seen in Figure 12.

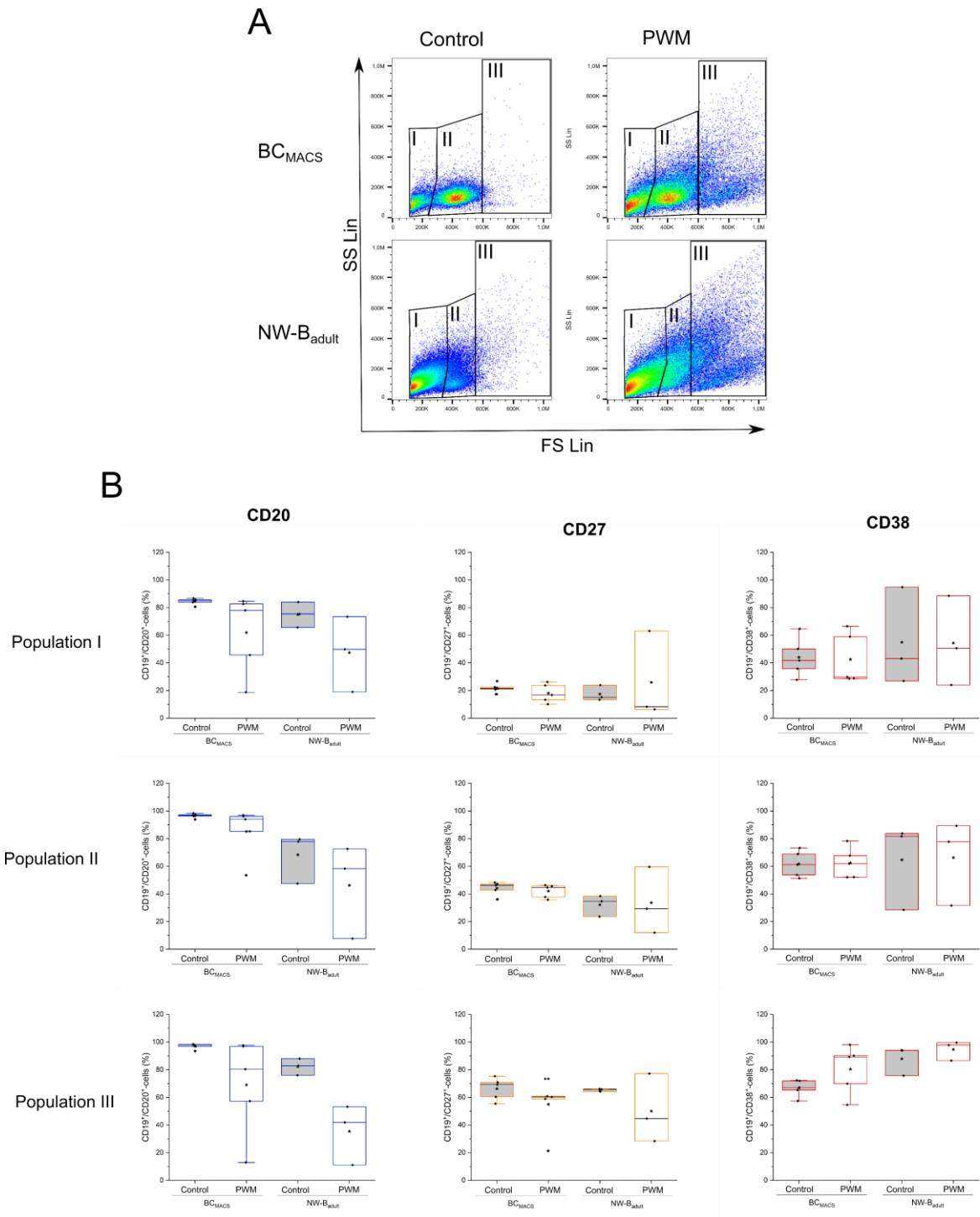


**Figure 12: Expression of CD markers in the various FS/SS subpopulations after 12 days of stimulation with PWM. Donors: A1-A3 and B1-B5. A: Representative FS/SS plots with the corresponding populations. Control: 12 days of cultivation without PWM. PWM: 12 days cultivation with 5  $\mu\text{g}/\text{mL}$  PWM. The cells in the Lymphocyte gate were divided into three subpopulations (I, II, III) according to their scattering properties. B: Expression of CD markers in the various subpopulations.  $BC_{MACS}$ : Flow-through fraction of the MACS column;  $NW-B$ : adherent fraction, mechanically eluted from the nylon wool column. Grey bars: control; white bars: PWM stimulated. Whiskers show the interquartile range.  $\square$ : mean;  $-$ : Median;  $\blacklozenge$ : count for a specific donor. The graphs show the distribution of the CD 20, 27 and 38 markers in the B cells  $CD19^+$ -population after 12 days of PWM treatment (PWM) – For comparison, cells without PWM were used (Control). This figure is adopted from Helm et al. (2021).**

Upon PWM stimulation, the occurrence of CD20<sup>+</sup> cells lowered in all populations, indicating the rise of ASCs, which are the only B without CD20 expression (i.e., CD20<sup>-</sup> cells). A trend toward a decrease of the CD27<sup>+</sup> cell subset in the three populations was only detectable for blood-derived cells after PWM stimulation. For PWM-treated tonsillar material, the frequency of CD19<sup>+</sup>/CD27<sup>+</sup> cells showed a broad variation across the donors, which was not detected for the non-treated cells. Moreover, whereas in populations I and II, the variation between the donors increased, the incidence of CD27<sup>+</sup> cells tended to decrease in population III.

For both blood and tonsil-derived B cells, the frequency of the CD38<sup>+</sup>-subset in populations I and II was independent of the PWM treatment. Still, it displayed a greater donor variability for the tonsillar cells. For both tissues, the percentage of CD38<sup>+</sup> cells in population III increases after 12 days of stimulation. CD38 expression is a B cell marker routinely used to identify ASCs, encompassing both PB and mature PC (Sanz et al. 2019). Taken together, these data show that changes in the scattering properties of the cells upon PWM stimulation are accompanied by an extensive variation of the B cell subsets distribution and show that the cells not only have proliferated but also have differentiated during the 12 days of cultivation with this lectin.

There is still a tremendous need for fast and inexpensive *in vitro* systems that can reproduce at least some features of the human immune response. In this context, blood is a well-established source for lymphocytes and highly pure B cells can be obtained by negative immunomagnetic cell sorting (MACS) using available commercial kits. We propose tonsils as a general alternative or complementary source to blood for the isolation of primary human B cells since our results show differences in the incidence of the B cell subsets (i.e., naïve, memory, GC and ASCs) as in their proliferative response to PWM. Moreover, in the case of tonsillar tissue as a source, B cells can also be derived routinely from infant, adolescent and adult tissue. Such B cells represent a different stage of human immune system development.

In contrast to blood, this allows investigation of B cell response during different developmental stages of the whole immune system. *Ex vivo* differentiation and their proliferative response upon targeted activation might help to further understand the complex mechanisms behind B maturation *in vivo*. In addition, tonsils are a more plentiful source regarding cell number and cell types, making them an ideal starting material when co-culturing systems are investigated.

## 4.2 Specific Stimulation with Soluble CD40L in Suspension

The CFSE-assay was replaced by automated cell counting to track proliferative response. This was mainly to avoid the unstimulated period of 24 hours before and after staining. Additionally, our CFSE assay paired with B cells did not offer the possibility to trace exact division numbers as described by others (Parish et al. 2009; Quah et al. 2007; Quah and Parish 2010).

Two media were developed and tested for specific stimulation of B cells with soluble CD40L (Table 5), ASC expansion medium containing IL-21 and memory expansion medium without IL-21.

### 4.2.1 Primer Specificity and Reference Gene Selection for RT-qPCR

For correct quantification of gene expression via RT-qPCR, correct amplification of cDNA and a stably expressed reference gene must be ensured. To rule out unspecific amplifications of the used primers and to assess the success of our PCR reactions, agarose gel electrophoresis of the amplicons was performed after RT-qPCR (Figure 13).

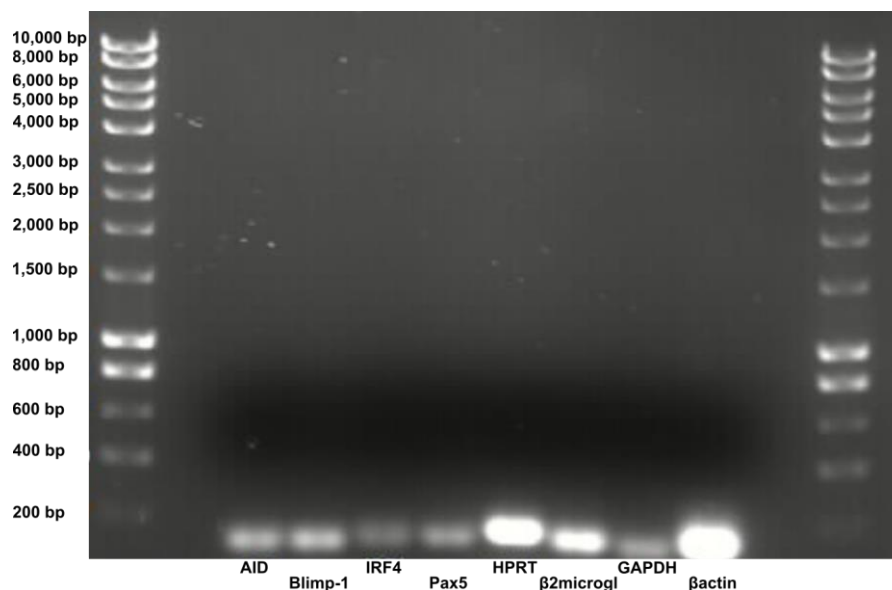


**Figure 13: Agarose gel of DNA, amplified by RT-qPCR with our 8 primers described in the method section. Cells of donor C2 were analyzed via RT-qPCR immediately after thawing.**

The agarose gel showed all analyzed amplicon DNAs in the expected range (< 200 bp) without unwanted fragments. Additional analyses of different donors and culturing conditions also showed no unwanted fragments (data not shown). The designed primers were therefore considered suitable for accurate quantification of gene expression via RT-qPCR.

For the  $\Delta\Delta C_t$ -method, a stably expressed reference gene had to be selected to obtain accurate results. To ensure precise analysis of relative gene expression in different samples, tissues, or experimental conditions, we analyzed 4 reference genes (HPRT,  $\beta_2$ -microglobulin, GAPDH and  $\beta$ -actin) to select the most stable gene throughout experiments (Figure 14). Commonly used reference genes may be stable in many situations, but their expression can vary considerably depending on species, genotype, developmental stage, experimental treatment, or circadian rhythm (Jain et al. 2018; Lacerda et al. 2015; Radonić et al. 2004). For the calculation of reference gene stability, we used the GeNorm algorithm (Vandesompele et al. 2002). Briefly, the ratio of a pair of reference genes and all pairwise variations was calculated across all samples (donors or days in media). The M value is the arithmetic mean of all pairwise variations. The lower the M value, the more stable the reference gene, where stability is defined as  $\ln(1/\text{Avg M})$ .

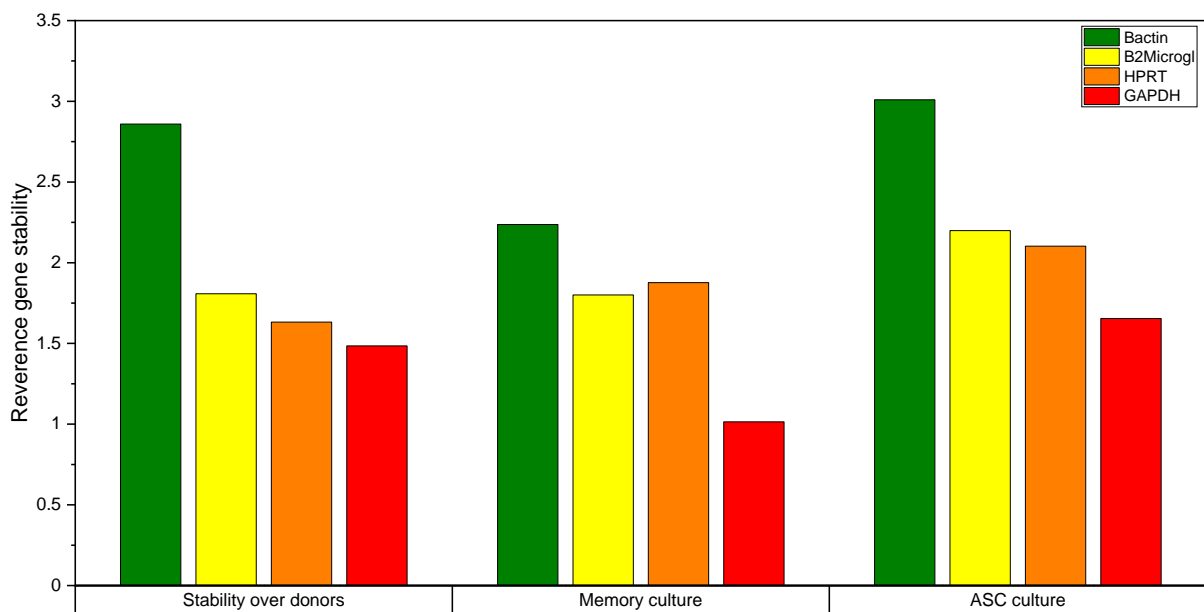


**Figure 14: Reference gene stability in B cells to select an endogenous control. For donor stability, 5 donors (C1, C2, A1, A4, A7) were tested immediately after thawing. For memory and ASC culture, samples were taken during medium change on days 0, 4, 8 and 11 of culture of two donors (C1, C2)**

We tested the stability of reference genes across five donors (C1, C2, A1, A4 and A7) to identify the most stable gene among different donors. Stability during proliferation was obtained in batch-culture of ASC- and memory expansion medium. B cells of donor C1 and C2 were cultured for 11 days without medium replacement. Gene expression was analyzed on days 0, 4, 8 and 11 of culture.

GAPDH showed the lowest stability across donors and cultures, while additionally performing a notable drop in stability, when cultured in memory expansion medium.

$\beta_2$ -microglobulin and HPRT showed comparable stability.  $\beta$ -actin showed notably higher stability compared to all other genes. Interestingly, when cultured in memory expansion medium,  $\beta$ -actin also performed a slight drop in stability. This drop, however, did not reduce its stability below any other gene.  $\beta$ -actin was therefore identified as the most suitable reference gene across all donors and culturing conditions. Based on these findings, we selected  $\beta$ -actin as our reference gene for tonsillar B cells in all subsequent RT-qPCR experiments.

Interestingly, recurrent mutations in the  $\beta$ -actin gene have been associated with cases of diffuse large B cell lymphoma (Lohr et al. 2012). Actins are highly conserved cytoskeleton proteins and were shown to be involved in B lymphocyte activation (Harwood and Batista 2011). This emphasizes the key role of  $\beta$ -actin expression in B cells and could explain the constant expression in our experimental setups.

#### **4.2.2 CSA and Human AB Serum in B Cell Cultures**

The effect of CSA on T cells is well known. Cyclosporin's key effect relies on the modulation of T lymphocyte activity, while other effects on the immune system remain to be determined (Flores et al. 2019; Leitner et al. 2011). Serum is arguably the most common supplement in cell-culture media and the least consistent, because of its batch-to-batch variations. Human serum harbors thousands of distinct proteins originating from a wide range of cells and tissues, as well as thousands of small-molecule metabolites, all in varying concentrations. Comparable to cell culture with primary cells, donor-dependent variations cannot be ruled out when human AB serum is collected (van Steirteghem et al. 1978).

We tested CSA and three human AB serum batches to identify effects on B cell expansion. For growth tests,  $0.1 \times 10^6$  B cells were cultured for up to 12 days in ASC expansion medium with and without CSA or with different batches of human AB serum (Figure 15).

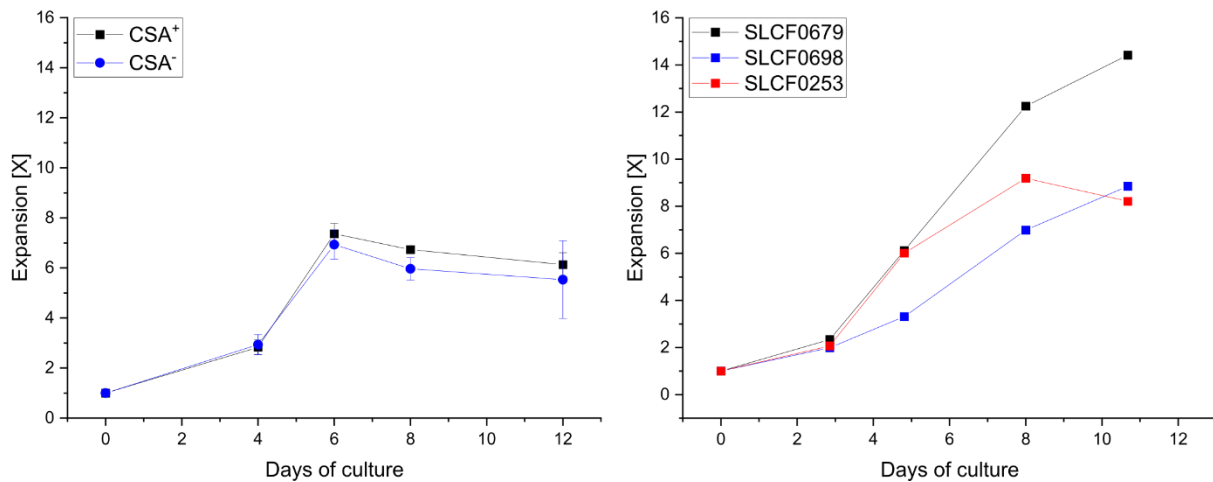


**Figure 15: Effect of CSA and three different batches of human AB serum on B cell expansion in ASC expansion medium.  $0.1 \times 10^6$  B cells were cultured for up to 12 days and expansion was measured during batch culture. We used donor A7 for CSA testing and donor A5 for serum testing.**

CSA showed no significant effects on B cell expansion, while different batches of human AB serum caused notable effects on B cell expansion. We defined CSA as a standard supplement in our B cell expansion media to suppress unwanted T cell proliferation in our experiments. The unwanted proliferation of T cells in B cell cultures could lead to B cell stimulation via secreted growth factors or surface-derived stimulation, reducing comparability between different donors with varying T cell impurities. Supplementation of CSA was therefore considered crucial for all subsequent experiments, to obtain reproducible results.

Regarding serum-dependent variations, Batch SLCF0679 showed the highest expansion, while continuing to proliferate throughout the whole experiment. SLCF0698 showed the lowest proliferative response, with continuous proliferation as well. SLCF0253 showed a comparable proliferative response to SLCF0679 at first but slowed down and reached maximal expansion on day 8 of culture with decreasing cell numbers afterward. Batch SLCF0679 expanded 14.4-fold, which was more than 1.5-fold higher than the other batches. Human AB serum, therefore, impacts B cell proliferation and needs to be standardized in some way. We defined serum batch SLCF0679 as our standard batch for all following experiments to rule out any further serum batch-derived variations and to emphasize B cell donor variations.

To generally overcome such concerns, scientists have tried to develop serum-free growth media (Néron et al. 2011b). Most serum-free formulations apply only to a specific cell type or closely related group of cell lines. Such supplements or media are not commercially available for every cell type yet. Chemically defined, serum-free



media are one of the fastest-growing segments in the cell culture space. The global serum-free media market was valued at 740 million USD in 2021 and is anticipated to reach 2370 million USD in 2030, growing at a Compound Annual Growth Rate of 14.1 % during the forecast period between 2022 and 2030 (Straitsresearch 2022).

Donor-derived variations in primary human cell culture can only be adequately analyzed when serum-free media are defined, or all experiments are conducted with a single batch of human serum. Limited availability of defined serum batches can prevent other scientists from repeating exact experimental setups, emphasizing the general need for serum-free media in cell culture.

#### **4.2.3 Optimizing Seeding Densities and Soluble CD40L Utilization**

For *ex vivo* expansion of B cells, several criteria can be considered to assess the quality. The total amount of cells after culture can serve as the simplest criterium, while the expansion respects the input cells. Lastly, the utilization of CD40L can be considered to respect input GF. This is of particular interest for soluble CD40L, since CD40L is the most abundant GF in B cell culture media with up to 1000-fold higher concentration compared to other GF like IL-4, IL-21 or BAFF (Néron et al. 2011a). To examine the most suitable culturing conditions in terms of B cell expansion with high CD40L utilization, B cells were seeded in different densities with standard CD40L concentration (0.4 µg/mL) or corresponding CD40L per million cells (Figure 16). B cells of donor C1 were seeded from 0.1 to 0.5 million cells and cultured in a 24-Well plate in 1 mL ASC expansion medium with either 0.4 µg/mL or 4 µg CD40L per million cells. Cell numbers were measured after 7 days in culture to observe B cell growth.

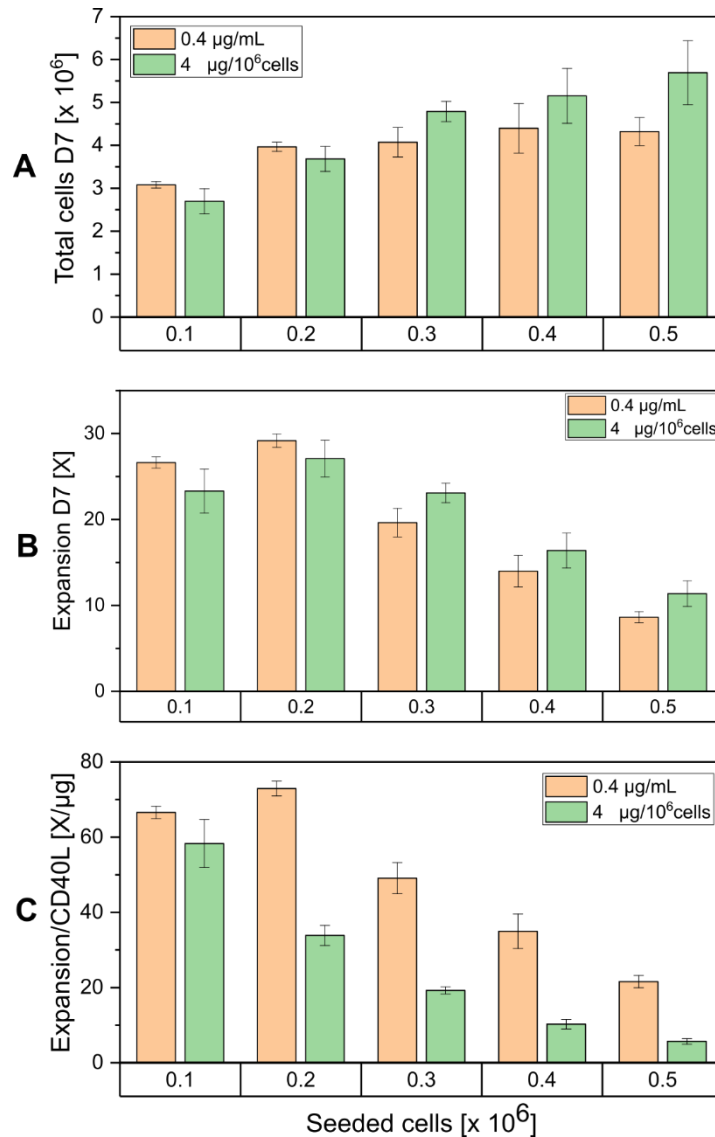


**Figure 16: 3 assessment methods for B cell proliferation. (A) shows the total cell number after culture, and (B) shows the expansion, respecting cellular input. In contrast, (C) shows the expansion divided by the input amount of CD40L in  $\mu\text{g}$ , respecting input cells and CD40L. B cells of donor C1 were seeded in different densities with standard CD40L concentration ( $0.4 \mu\text{g}/\text{mL}$ ) or corresponding CD40L per million cells in ASC expansion medium. Cell number was measured after 7 days in culture to observe B cell growth.**

Figure 16 shows the 3 different quality assessment methods for one B cell culture. After culture, the total amount of cells increased with seeding density and used amount of CD40L (Figure 16A). An increase of CD40L from  $0.4$  to  $2 \mu\text{g}/\text{mL}$  at a seeding density of  $0.5 \times 10^6$  cells led to a 30 % increase in total cellular outcome. Notably, up to  $5.7 \pm 0.7 \times 10^6$  cells/mL were supported in our ASC expansion medium after seeding  $0.5 \times 10^6$  cells with  $2 \mu\text{g}/\text{mL}$  CD40L. Therefore, up to  $5.2 \pm 0.7 \times 10^6$  cells/mL could be generated with the present building blocks in our medium.

The expansion increased slightly but not significantly when seeding density was increased from  $0.1$  to  $0.2 \times 10^6$  cells/mL and decreased subsequently (Figure 16B).

The corresponding increase of CD40L also led to slight but not significant increased B cell expansion.

When input CD40L is considered (Figure 16C), an increase in concentration significantly reduced the expansion per CD40L, showcasing low utilization of additional stimulus above 0.4  $\mu\text{g}/\text{mL}$  or 4  $\mu\text{g}/10^6$  cells in B cell cultures.

The quality evaluation of our expansion procedure can be viewed from different standpoints if cells or CD40L are considered a valuable or rare resource. When both are available in unlimited amounts, the total amount of generated cells can be considered without respecting input of them. Higher inputs lead to higher amounts of generated B cells. This can be explained by more cellular starting material and more stimulus. Doubling either starting cell numbers or an increase of CD40L did not double the outcome, indicating lowered utilization at higher concentrations. Expansion decreased with seeding density, while the corresponding increase of CD40L led to slightly higher expansion but was still decreasing, suggesting lower seeding densities for efficient use of available B cells. When the expansion is additionally divided by input CD40L, low utilization of soluble CD40L is observed and decreased with concentration, suggesting low concentrations for increased utilization of the T cell derived protein. Increased starting cell densities and CD40L concentration increased absolute B cell outcome. The highest utilization is reached at a low starting concentration of B cells and CD40L. We, therefore, set our seeding density to  $0.1 \times 10^6$  B cells/mL in all subsequent cultures, while CD40L was set to 4  $\mu\text{g}/10^6$  cells and sometimes varied to observe other effects.

#### **4.2.4 Memory and ASC Expansion Medium in Batch Cultures**

In the pertinent literature, CD40L and IL-21 have been reported as relevant factors for B cell activation and differentiation. The response of human adult tonsillar cells to varying concentrations of CD40L and IL-21 in growth medium was analyzed by cultivating  $0.1 \times 10^6$  cells per well and mL in 24-well plates. First, CD40L concentration was varied from 0 to 1  $\mu\text{g}/\text{mL}$  while the concentration of IL-21 was kept constant (20 ng/mL), i.e., in the range suggested in the pertinent literature (Néron et al. 2011a). In the absence of CD40L, a 2.9-fold expansion of the cells was observed after seven days (Figure 17A). In the presence of CD40L, expansion increased in a concentration-dependent manner, reaching a 69.4-fold expansion at 1  $\mu\text{g}/\text{mL}$  CD40L. Next, the IL-21 concentration was varied from 0 to 50 ng/mL while CD40L was kept constant at

0.4  $\mu\text{g}/\text{mL}$ , to be within the range reported by Néron et al. (2011) (Figure 17B). In the absence of IL-21, the cells expanded 11.7-fold within 7 days. Supplementing the medium with 10  $\text{ng}/\text{mL}$  IL-21 resulted in a 40.9-fold expansion. A further increase in the IL-21 concentration did not further improve proliferation. In our ASC expansion medium (Table 5), we set the IL-21 concentration to 20  $\text{ng}/\text{mL}$  when supplemented, to avoid the region with a rapid change of proliferative outcome between 0 and 10  $\text{ng}/\text{mL}$ . In all experiments, the cell viability was  $> 80\%$ .

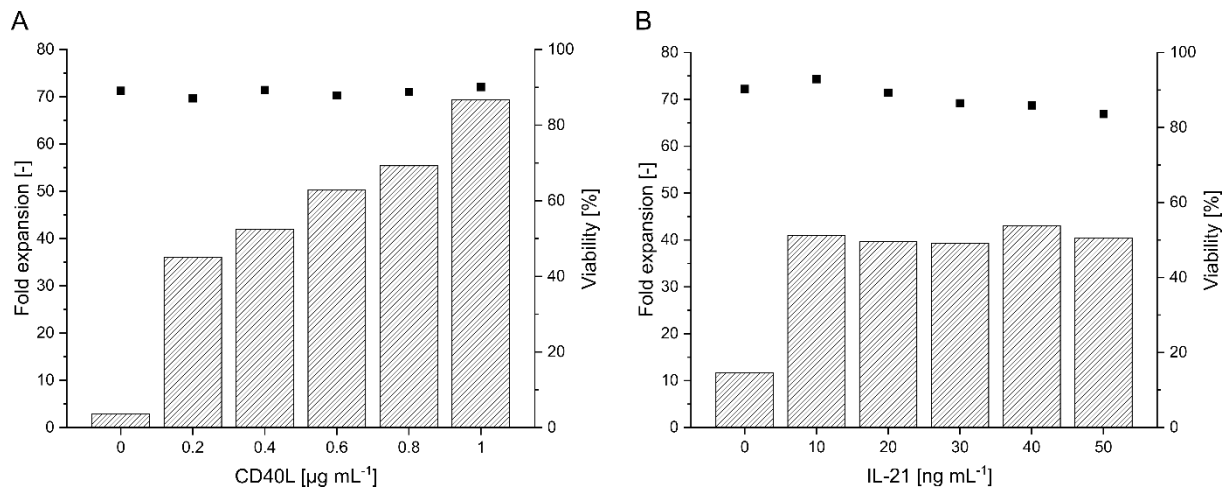


**Figure 17: Influence of CD40L- and IL-21 on B cell expansion and viability after seven days of suspension cultivation with donor A1.  $0.1 \times 10^6$  B cells were seeded in 24-well plates in growth medium supplemented with A) the indicated amounts of CD40L and 20  $\text{ng}/\text{mL}$  IL-21 and B) the indicated amounts of IL-21 and 0.4  $\mu\text{g}/\text{mL}$  CD40L. Shown are the expansion factor (bars) and the viability (■). This figure is adopted from Helm et al. (2022).**

IL-21 promotes terminal plasma cell differentiation and antibody secretion in B cell cultures (Parrish-Novak et al. 2000; Ettinger et al. 2005; Ettinger et al. 2007; Bryant et al. 2007). To define an alternative medium with reduced PC differentiation, we defined a memory expansion medium without IL-21 (Table 5). The effect of both media on B cell response was analyzed further.

Two adult donors were seeded at  $0.1 \times 10^6$  cells per well and mL in 24-well plates and cultured for 7 days in memory or ASC expansion medium with varying CD40L concentration. The expansion was measured via cell count and B cell differentiation was tracked via flow cytometry and RT-qPCR.

For both donors, expansion was significantly higher in ASC expansion medium, containing IL-21 (Figure 18), while expansion in memory medium without IL-21 was significantly lower compared to ASC medium.

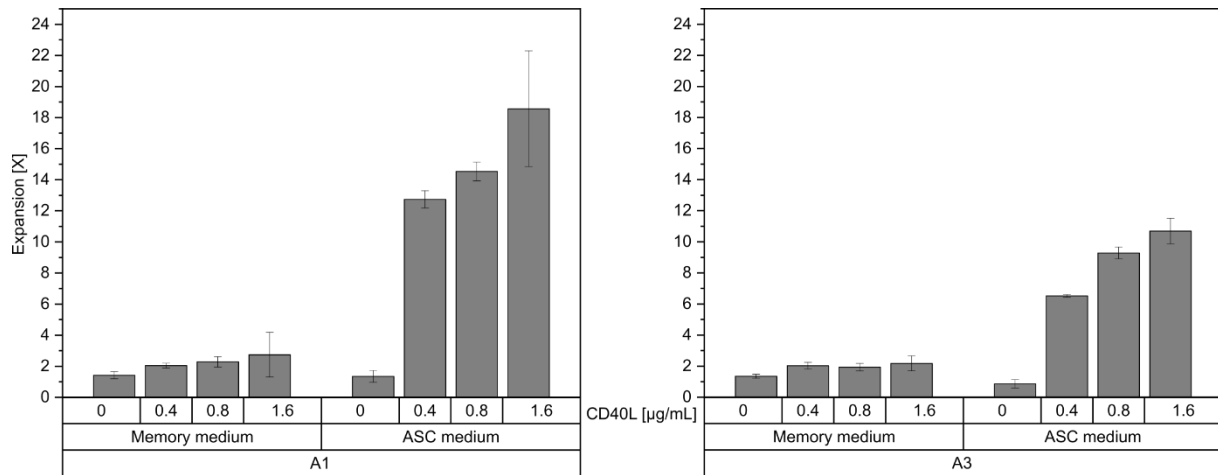


**Figure 18: Expansion of adult B cells in memory- and ASC expansion medium with varying CD40L concentration. Cells were cultured for 7 days without changing the medium (n = 3 replicates).**

Both cultures proliferated the least without CD40L as a stimulus. In memory medium, the increase of CD40L concentration led to a small but non-significant expansion increase. Both donors expanded between 2- and 3-fold in memory expansion medium even with increasing CD40L concentration. In ASC culture, increased CD40L concentration improved the proliferative outcome, as already described above (Figure 17). Donor A1 expanded  $12.7 \pm 0.6$ -fold, at  $0.4 \mu\text{g/mL}$  CD40L and  $18.6 \pm 3.7$ -fold at  $1.6 \mu\text{g/mL}$ . Donor A3 expanded  $6.5 \pm 0.1$ -fold at  $0.4 \mu\text{g/mL}$  CD40L and  $10.7 \pm 0.8$ -fold at  $1.6 \mu\text{g/mL}$ . Quadrupling the concentration of CD40L, therefore, increased expansion by 5.9-fold for donor A1 and 4.2-fold for donor A3.

Expansion of donor A1 was higher compared to donor A3, while donor A1 also responded stronger to increased CD40L stimulation, indicating notable donor-dependent variation. Memory medium showed little proliferative response, when CD40L was present, making this medium a seemingly worse alternative to ASC medium in terms of B cell expansion. For the highest possible expansion in batch culture, IL-21 seemed to be crucial. The amplification of B cell expansion by supplementation of IL-21 was reported before (Good et al. 2006). However, further increase of CD40L concentration above  $0.4 \mu\text{g/mL}$  only led to minor benefits in expansion, reinforcing this concentration as our standard in B cell cultures. This is in accordance with the improved utilization of CD40L at low concentrations, described above (Figure 16).

To analyze the effect of both media on B cell differentiation, we performed flow cytometry analyses after culture of donor A3 (Figure 19).  $\text{CD19}^+$  B cells were analyzed toward their CD27 and CD38 expression. We defined 3 populations, namely memory

cells (CD27<sup>+</sup>CD38<sup>+</sup>), plasmablasts (CD27<sup>+</sup>CD38<sup>++</sup>) and plasma cells (CD27<sup>++</sup>CD38<sup>++</sup>). Naïve cells (CD27<sup>-</sup>CD38<sup>+/-</sup>) were not included, due to low abundance (< 1 %) in this experiment.

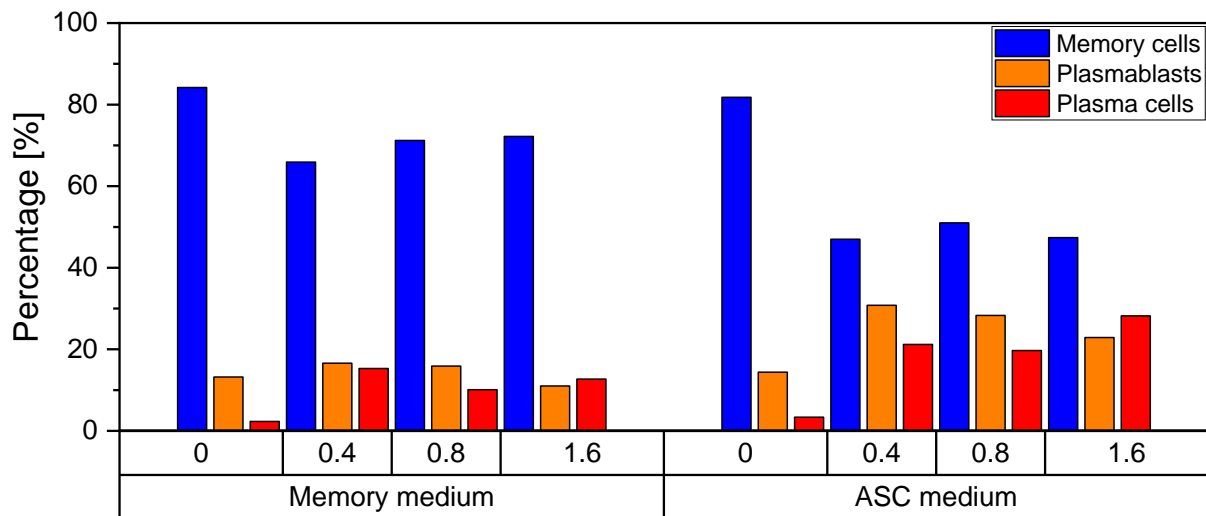


**Figure 19: Phenotype of adult B cells from donor A3 in memory- and ASC expansion medium with varying CD40L concentration. Cells were cultured for 7 days without a change of medium. Memory cells were defined as CD27<sup>+</sup>CD38<sup>+</sup>, PB as CD27<sup>+</sup>CD38<sup>++</sup> and PC as CD27<sup>++</sup>CD38<sup>++</sup>.**

Without CD40L, both media maintained high memory cell content with few ASC (PB + PC). The amount of PC was significantly lower than PB, when CD40L was not supplemented. PC development was therefore restricted to the presence of CD40L. IL-21 in ASC medium alone could not promote PB or PC development. When CD40L was supplemented, memory cell content fell in both culture media, due to the development toward PB and PC. In memory medium, the memory cell content decreased by 18.3 % from 84.2 % (0 µg/mL) to 65.9 % (0.4 µg/mL) and increased again with additional CD40L stimulus to 72.2 % (1.6 µg/mL). In ASC medium, the memory cell content decreased by 34.8 % from 81.8 % (0 µg/mL) to 47 % and stagnated around 50 % at increasing concentration. When CD40L concentration was increased, ASC content decreased in memory medium and stayed constant in ASC medium. The highest content of ASC was observed at a CD40L concentration of 0.4 µg/mL for both cultures. Memory culture reached 31.9 % ASC, with 16.6 % PB and 15.3 % PC, while ASC culture reached 52 % ASC, with 30.8 % PB and 21.2 % PC. Only at a CD40L concentration of 1.6 µg/mL in ASC culture, PC content was higher with 28.2 %, indicating enhanced development from PB toward PC when CD40L was increased in the presence of IL-21.

Interestingly, the ratio of memory cells to ASC was always close to 50 % in ASC culture. Overall, both media relied on the presence of CD40L to cause the differentiation of cells. Memory cell percentage was higher in memory medium and increased with CD40L concentration. In ASC medium, the ratio between memory- and ASC stayed constant at around 50 % and ASC shifted slightly toward PC when CD40L concentration was increased. This indicates that additional CD40L stimulus pushed the memory culture toward memory cells and the ASC culture toward PC, confirming the dedicated functionality of both media.

Figure 20 shows the expansion and flow cytometry analyses of child-derived B cells after 7 days in memory or ASC medium. Without CD40L in the media, child cells also showed the least proliferation. Interestingly, child cells expanded much better in memory medium compared to adult B cells. Expansion even surpassed the ASC medium at 0.4  $\mu\text{g}/\text{mL}$  CD40L but seemed to reach a plateau at higher CD40L concentrations. In ASC medium, B cells increased their expansion when more CD40L was supplemented. This is similar to the observations made with adult cells cultivated in ASC medium.

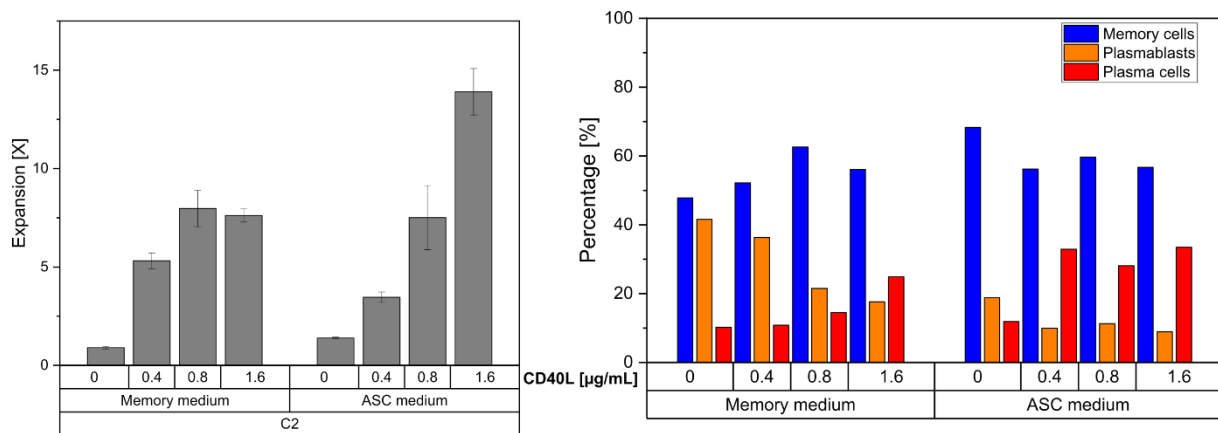


**Figure 20: Expansion and phenotype of child B cells in memory- and ASC expansion medium with varying CD40L concentration. B cells of donor C2 were cultured for 7 days without changing the medium (n = 3 replicates). Memory cells were defined as  $\text{CD}27^+\text{CD}38^+$ , PB as  $\text{CD}27^+\text{CD}38^{++}$  and PC as  $\text{CD}27^{++}\text{CD}38^{++}$ .**

Regarding subclass development, both media showed more B cell differentiation without CD40L compared to adults, shown in Figure 19. Memory cell percentage was 50 % and 68 % compared to two times 80 % in adults without CD40L. When CD40L was supplemented in memory medium, B cells decreased their PB content and increased their PC content, while memory cells increased slightly and peaked at 0.8  $\mu\text{g}/\text{mL}$  CD40L. In ASC medium, memory cell content was slightly higher compared to memory medium and did not change notably, when more CD40L was added. PB

content was lower compared to memory medium and did not vary much. PC, however, increased up to 30 % when CD40L was supplemented and raised.

As opposed to adult B cell cultures in ASC and memory expansion medium, child B cells seemed more responsive to memory medium and showed more PC development in such cultures. When child cells were cultured in ASC medium, we also observed more pronounced PC development compared to memory medium. This indicates that B cells derived from child tissue are more responsive to cultures without IL-21 compared to adult B cells.

Additionally, we addressed the gene expression characteristics for both media with varying CD40L concentrations in batch culture of C2. After culture, B cells were subjected to RT-qPCR and gene expression was analyzed, compared to cells before culture (Figure 21).

AID was upregulated for all measurements while being stronger expressed in culture with memory medium compared to ASC medium. The highest upregulation of AID in memory medium was  $7.7 \pm 0.5$ -fold at  $0.4 \mu\text{g/mL}$  CD40L, while ASC medium resulted in a maximal upregulation of  $3.8 \pm 0.5$ -fold. Therefore, AID upregulation was roughly doubled after 7 days in memory medium, compared to ASC medium. Notably, AID fluctuated in memory medium while being stable in ASC medium, when the CD40L stimulus was increased.

Pax5 was downregulated for all measurements, while being stronger downregulated in culture with memory medium compared to ASC medium. The highest downregulation of Pax5 was observed in memory medium with  $-19.7 \pm 0.8$ -fold at  $0.8 \mu\text{g/mL}$  and  $-8.2 \pm 1.2$ -fold at  $1.6 \mu\text{g/mL}$  in ASC medium. The downregulation of Pax5 increased with CD40L concentration in ASC medium and fluctuated in memory medium. Interestingly, in memory medium without CD40L and IL-21, Pax5 was downregulated by  $21 \pm 3$ -fold, indicating cellular changes in our medium even without these cytokines. When IL-21 was present in ASC medium without CD40L, Pax downregulation was hampered compared to memory medium, and the B cells started upregulating IRF4 and Blimp-1. The presence of IL-21 alone, therefore, caused this effect. When CD40L concentration was increased in ASC medium, Pax5 was further downregulated with increasing CD40L, while IRF4 and Blimp-1 showed the highest expression at  $0.4 \mu\text{g/mL}$  and decreased afterward. In memory medium, IRF4 and Blimp-1 showed no significant upregulation whatsoever.



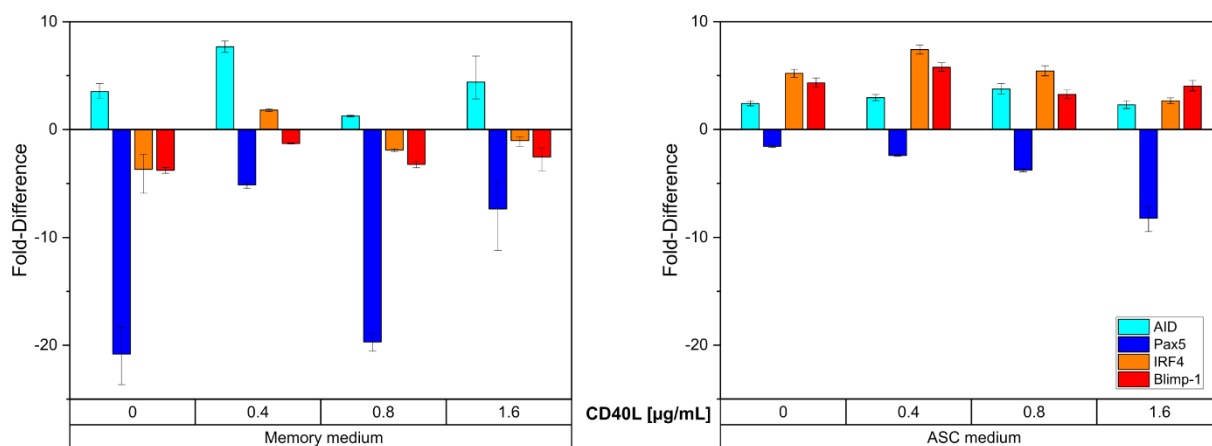


**Figure 21: Gene expression of B cells from donor C2 after 7 days of batch culture in memory- or ASC expansion medium. CD40L concentration was increased from 0 to 1.6 µg/mL. Gene up- or downregulation was calculated via  $\Delta\Delta C_t$ -method compared to cells before culture and  $\beta$ -actin as reference gene.**

B cells in memory medium without IL-21 seemed to follow no clear differentiation pattern, when CD40L concentration was increased. AID, as an enzyme that controls SHM and CSR in B cells, was upregulated, indicating a GC-like response of B cells to our memory medium as described by others (Kuraoka et al. 2011; Xu et al. 2012). Combined with the absence of IRF4 and Blimp-1 expression, PB or PC differentiation can be ruled out. IRF4 is known to control CSR, GC B cell formation and ASC differentiation (Shaffer et al. 2009), while Blimp-1 is required for further differentiation into fully functional ASC (Shapiro-Shelef et al. 2003). B cells seemed to develop toward activated GC B cells in our memory medium. In contradiction, Pax5 downregulation indicated a beginning B cell commitment toward the ASC fate or activation (Kallies et al. 2004). This was even observed in memory culture without CD40L stimulation, indicating possible effects of IL-4, BAFF or constituents in the human AB serum. Differentiation in memory medium was possibly less directed toward an inevitable fate, due to little proliferative activity in adults (Figure 18), hindering B cells from following a programmed gene expression pattern as observed in ASC medium. Nevertheless, B cells seemed to be activated and committed toward ASC by downregulation of Pax5, but the absence of IRF4 and Blimp-1 upregulation suggests a developmental step between memory cells and ASC, possibly being a GC expression pattern.

In the absence of CD40L, IL-21 alone reduced the downregulation of Pax5 and caused upregulation of IRF4 and Blimp-1, compared to memory medium without CD40L stimulus. This displays the many times reported key role of IL-21 in B cell development toward ASC (Ding et al. 2013; Bryant et al. 2007; Ettinger et al. 2005; Good et al. 2006). Good et al. reported that the receptor for IL-21 is expressed by naïve and germinal

center B cells but not memory or plasma cells (Good et al. 2006). Our findings, however, suggest that the receptor for IL-21 is present on our tonsillar memory B cells and ASC development can be induced by IL-21 alone. Supplementation and increase of CD40L concentration in ASC medium promoted gene expression in a proportional fashion. Only AID stayed constant between 2- and 4-fold upregulation, indicating a low impact on hypermutation of B cells compared to culture in memory medium. Pax5 got downregulated, while IRF4 and Blimp-1 were upregulated when CD40L concentration was increased. This indicates a skip of the GC-like expression pattern observed in memory medium by direct commitment toward ASC. IRF4 and Blimp-1 were upregulated, indicating development toward PB and PC, as already shown by the flow cytometry assessment (Figure 19 & Figure 20).

Taken together, memory expansion medium showed a low proliferative response in adult-derived cells, while child cells seemed more responsive. Expansion did not exceed 3-fold when CD40L concentration was raised to 1.6  $\mu\text{g}/\text{mL}$  in adult-derived cells, while child-derived cells showed up to 6-fold expansion. B cells maintained their memory phenotype and showed little development toward ASC. Increased CD40L concentration led to a higher fraction of memory cells after the culture of adult-derived cells. Gene expression of child cells showed signs of SHM and CSR, indicated by increased AID expression. IRF4 and Blimp-1 did not change expression, while Pax5 was downregulated. This indicates an activated B cell phenotype without full commitment toward ASC in our memory expansion medium. The observed gene expression pattern in memory medium suggests a GC reaction performed by our tonsillar memory B cells.

ASC expansion medium showed significantly higher proliferation reaching 19-, 11- and 14-fold expansion for donor A1, A3 and C2, respectively. Roughly half of the cells developed toward a PB or PC phenotype. This ratio stayed in balance when the CD40L concentration was increased, while ASC ratio shifted toward PC when the CD40L concentration was increased. Gene expression showed upregulated, but lower, AID expression compared to memory expansion medium, indicating some degree of SHM and CSR in ASC medium, which was not altered with CD40L stimulus. Pax5 got progressively downregulated, while IRF4 and Blimp-1 were progressively upregulated with increasing CD40L concentration. B cells' phenotype and gene expression pattern confirmed the PC and PB development in ASC expansion medium.

Both media showed lower expansion potential in batch culture compared to other reports. Alonso-Guallart et al. used naïve B cells derived from macaque blood or spleen and cultured them with CD40L-expressing feeder cells. The B cells expanded 20- to 40-fold during 14 days in culture, exceeding our simple batch protocol by a small margin (Alonso-Guallart et al. 2021). Nojima et al. outperformed this by far and managed to expand naïve mouse B cells by 200-fold in only 6 days, setting a new standard. B cells were cultured on a layer of CD40L-BAFF-co-expressing fibroblasts in the presence of IL-4, being very close to our culturing system (Nojima et al. 2011).

Feeder cells support the growth of cells in culture by contributing an undefined and complex mixture of ECM components and growth factors. They can support *in vitro* survival and growth of cells that would require the presence of a variety of known or unknown soluble or membrane-bound growth factors and receptors (Llames et al. 2015). This is an advantage and disadvantage at the same time. Cells receive complex but undefined stimuli, providing them with some essential but unknown GF, creating problems in reproducibility. The availability of feeder cells can also be problematic for some groups. And when primary cells are transferred back into the organism, allogeneic or xenogeneic problems can occur (Llames et al. 2015). When using animal feeder cells, cross-transfer of animal pathogens can also become a problem (Zhang et al. 2013). This urges the need for cell-free stimulation systems. In this section, we laid the basis for human B cell expansion media with well-defined ingredients, capable of guiding B cell differentiation toward a desired subtype (e.g., memory or antibody secreting cells). Human AB serum is the last undefined component, which can be replaced in the future to obtain a fully defined culturing media for the expansion of primary human B cells. Commercially available human B cell expansion medium (ImmunoCult™) provides such a stimulation. Based on CD40L and IL-4, the medium was shown to expand B cells in a range from 38- to 1190-fold at day  $14 \pm 1$  in culture, as described by the manufacturer (STEMCELL Technologies 2021). Human primary naïve or memory B cells are cultured in a medium with undisclosed GF, which is replaced every 2 – 4 days. This outperforms our Batch approach regardless of the CD40L stimulus used and points out the necessity for a continuous culturing approach with the replacement of medium, to obtain optimal B cell expansion.

#### 4.2.5 B Cell Expansion with Medium Change and Memory Pre-Culture

Nojima et al. showed that switching from a culture without IL-21 to a secondary culture of mouse B cells with IL-21 maintains the proliferation, while shifting the developmental fate from memory toward long-lived PC (Nojima et al. 2011). This is in accordance with our observations for memory- and ASC expansion medium containing soluble CD40L stimulus instead of feeder cells. We additionally observed signs of SHM, indicated by AID upregulation, which was not reported by Nojima et al. (2011). Robinson et al. (2019) adopted this protocol recently and showed that a switch to cultures with IL-21 generated 3 – 10 times more mouse B cells (Robinson et al. 2019). This motivated us to develop a novel expansion protocol with human tonsillar B cells and soluble CD40L protein as stimulus. The absence of feeder cells, secreting unknown amounts of CD40L and BAFF increases the reproducibility of this culturing approach. A pre-culture with memory expansion medium (Memory pre-culture), without IL-21, holds the potential to boost the expansion of our human tonsillar B cells and was therefore tested extensively.

Figure 22 shows the expansion and growth rates of B cells from donor C1 in batch culture with ASC expansion medium and various CD40L concentrations. B cells were seeded at  $0.1 \times 10^6$  cells per well and mL in 24-well plates and cultured for 8 days. CD40L concentration was varied from 0.05  $\mu\text{g}/\text{mL}$  up to 3.2  $\mu\text{g}/\text{mL}$  in doubling steps. We tracked the proliferative response daily to identify the exponential growth phase and to set the ideal frequency for medium changes.

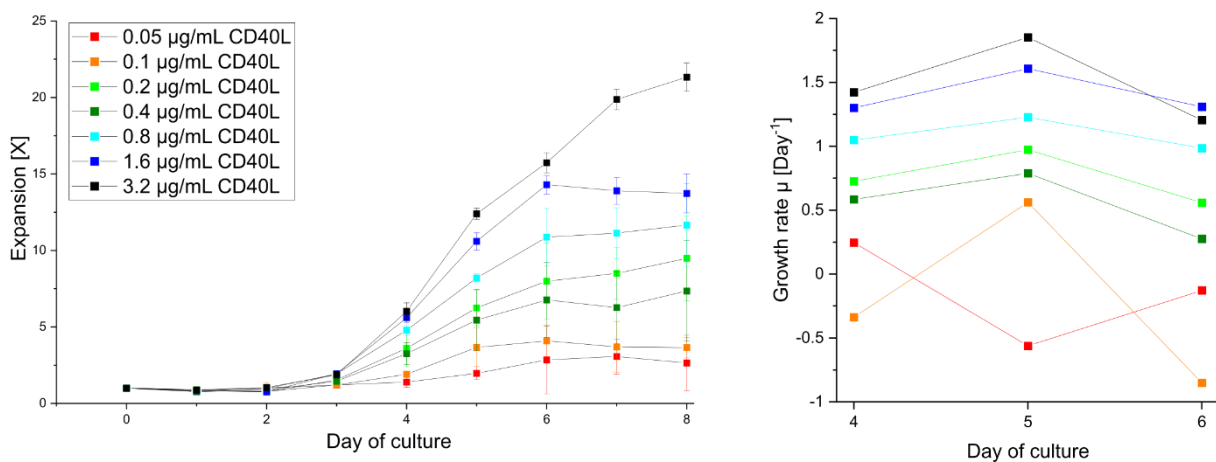


**Figure 22: Dynamic expansion of donor C1 over the course of 8 days with different CD40L concentrations. The right graph shows the growth rate  $\mu$  during the exponential phase between days 4 and 6.**

As expected, additional CD40L stimulus increased the growth rate  $\mu$  and expansion notably. No proliferation was observed in the first 2 days of culture. The maximal

growth rate was observed between day 4 and 5 of culture for every CD40L concentration except for 0.05  $\mu\text{g}/\text{mL}$ , which already stopped expansion, likely due to lack of CD40L stimulus. Based on this, we decided to replace the B cell growth medium every 3 – 4 days to provide the cells with fresh stimulus before leaving the exponential growth phase. This frequency is in accordance with other groups and recommended in commercially available kits (Robinson et al. 2019; Nojima et al. 2011; STEMCELL Technologies 2021). GF concentration for memory- and ASC expansion medium was set to the concentrations shown in Table 5 if not indicated otherwise.

We cultured B cells of 6 donors, 3 children (C 1 – 3) and 3 adults (A 4 – 6), in batch culture, ASC culture and memory pre-culture until cells stopped proliferation (Figure 23). For Batch culture, B cells were cultured in ASC medium without medium change. In ASC and memory pre-culture, B cells received fresh medium after 4, 8, 11 and 15 days. ASC culture was conducted in ASC expansion medium exclusively. Notably, ASC culture and batch culture were the same in the first 4 days of culture. Memory pre-culture was performed in memory expansion medium for the first 4 days of culture. Subsequent culture after memory pre-culture was performed in ASC expansion medium. When B cells were seeded or medium was changed, cells were (re-)seeded at  $0.1 \times 10^6$  cells per well and mL in 24-well plates. We tracked cell numbers daily and performed flow cytometry of B cells upon the start of culture and during each change of medium. We additionally performed RT-qPCR during the culture of donor C2 to analyze gene regulation of AID, Pax5, IRF4 and Blimp-1. For donors C2 and A5, we analyzed IgM, IgA and IgG secretion via ELISA on days 8 and 11 of ASC and memory pre-culture.

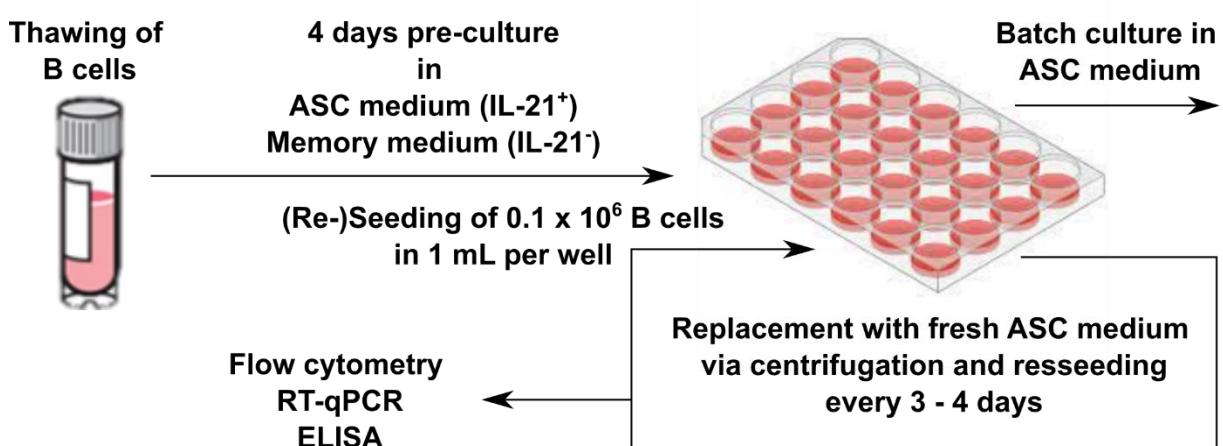
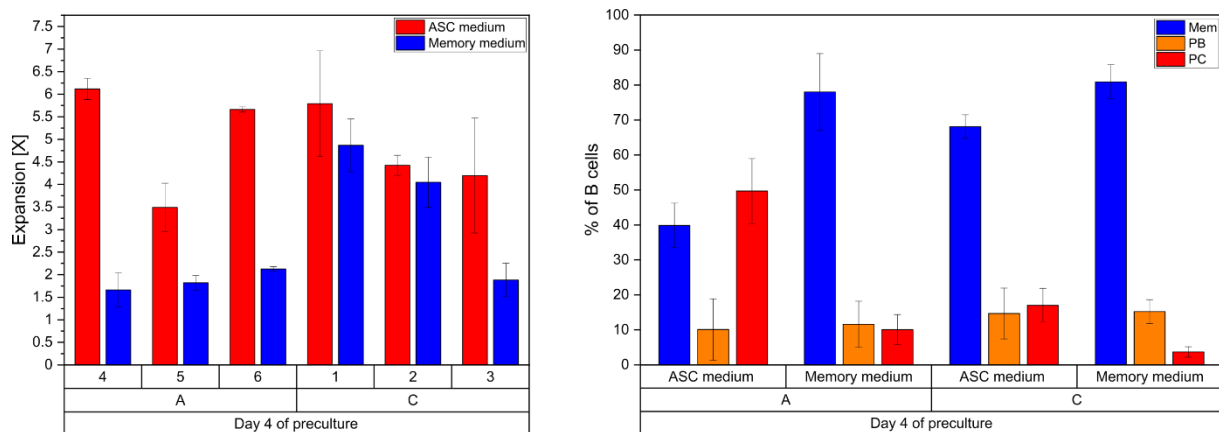


Figure 23: Schematic illustration of the 3 different culturing approaches for B cell expansion.

The first 4 days of culture already showed significant differences in expansion and differentiation between the culturing approaches and the donor age (adult/child), as seen in Figure 24. B cells expanded better in ASC expansion medium ( $5 \pm 1$ -fold) compared to memory expansion medium ( $2.8 \pm 1.3$ -fold). In memory expansion medium, additional differences between adult ( $1.8 \pm 0.2$ -fold) and child ( $3.6 \pm 1.3$ -fold) donors were observed. In ASC medium, no significant difference between adult ( $5.1 \pm 1.1$ -fold) and child ( $4.8 \pm 0.7$ -fold) donors were observed. C3 was the only child performing low expansion ( $1.9 \pm 0.4$ -fold) in memory medium.



**Figure 24: B cell expansion and subclasses on day 4 of ASC and memory pre-culture, shown for 6 individual donors. Expansion was calculated from  $n = 3$  experimental replicates, while subclasses were calculated from  $n=3$  adults (A) or children (C). Memory cells were defined as  $CD27^+CD38^+$ , PB as  $CD27^+CD38^{++}$  and PC as  $CD27^{++}CD38^{++}$ .**

B cell differentiation also showed pronounced differences between culturing approaches and the donor age in the first 4 days of culture.

ASC culture developed stronger toward PC compared to memory culture. This was more pronounced for adult donors. Memory cell development showed converse behavior, with robust maintenance in memory culture compared to ASC culture. PB showed no significant differences at this point in culture.

These results indicate that B cells derived from children or adults can enter different developmental paths dependent on which culturing system is chosen. B cell medium without IL-21 emphasizes this effect notably. Adult-derived B cells were less responsive to memory medium in terms of expansion and responded with higher PC differentiation in ASC medium. The lower expansion potential in memory medium is already shown in Figure 18. Child-derived B cells showed higher expansion potential in memory medium and responded with less PC differentiation in ASC medium. One explanation is a less developed immune system in children compared to adults. Adult

cells likely encountered more pathogens in the past and are, therefore, further matured, increasing their tendency to become PC. This, in turn, seems to reduce their memory expansion potential. Child-derived cells showed expansion potential almost comparable to that observed in ASC medium containing IL-21 while maintaining higher memory cell content. Expansion of memory cells by stimulation without IL-21 is therefore favored in cultures of B cells derived from younger donors. These developmental differences got more pronounced toward the end of culture, as shown in the remaining chapter.

Figure 25 shows the expansion of the 3 culturing approaches for each donor individually to emphasize the variation between donors. Measurement for expansion was stopped when the cell number did not increase overnight or did not exceed doubling over a period of 3 days. Cultures and expansion lasted between 12 and 22 days. Especially in child donors, the period of culture was extended by a memory pre-culture. Batch culture led to the lowest expansion of B cells.

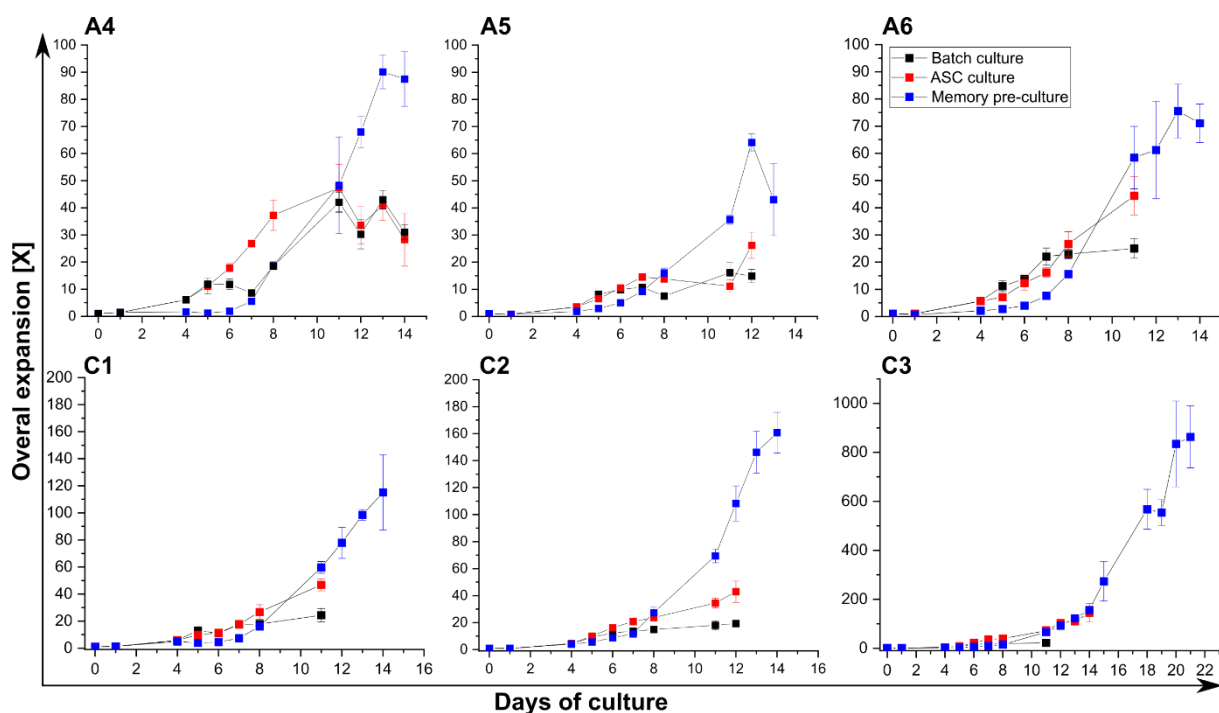


**Figure 25: Expansion of the 3 culturing approaches for each donor individually over the course of 11 – 22 days. Measurement for expansion was stopped, when cell number did not increase overnight or did not exceed doubling over a period of 3 days (n=3 replicates)**

In Batch cultures, which were conducted in ASC medium, B cells expanded between 15- and 25-fold. Only Donor A4 exceeded that range with an expansion of  $43 \pm 3$ -fold. In ASC culture, with additional medium changes for supply of fresh GF, expansion was between 40- and 50-fold for most donors. Only donor A5 expanded less with

26 ± 5-fold and C3 expanded more, reaching 145 ± 38-fold. Lastly, memory pre-culture led to the highest expansion in all donors. Adults-derived B cells expanded 77 ± 11-fold, reaching a maximum of 90 ± 6-fold for donor A4. All child-derived B cells expanded over 100-fold. Here donor C3 showed the highest expansion potential by far, reaching 863 ± 127-fold. We repeated the memory pre-culture for donor C3 with 0.4 and 1 µg/mL CD40L (Appendix 1) to see if additional CD40L would be beneficial and if the expansion would exceed all donors again. Both cultures expanded 400-fold, confirming a higher expansion potential of this donor. Additional CD40L stimulus, however, was not beneficial once more.

These results further show that adult- and child-derived cells inhere different potentials for expansion based on what medium and culturing approach is introduced to them. Batch culture had the lowest expansion potential, which can be explained by the lowest amount of CD40L stimulus and no supply of fresh medium components. Adults and children reacted with comparable expansion, while donor A4 surpassed the other donors. The culture with medium renewal approximately doubled the expansion, staying below expectations. Only donor C3 profited in this culturing approach increasing expansion by 6-fold compared to batch culture. The benefit gained by three medium changes is arguably low for most donors when expansion can be boosted more efficiently via memory pre-culture. Use of memory pre-culture showed the most notable effect on overall B cell expansion. In the first 4 days, child-derived B cells showed a similar expansion to the other cultures, while adults expanded in a lower magnitude, as shown in Figure 18. In the final expansion, both donor categories drew benefit of a memory pre-culture, however. As indicated in the first 4 days of preculture, child-derived B cells proceeded with the trend. They increased the overall expansion potential by more than double compared to adult-derived B cells. This further confirms the difference between adult and child-derived B cells. For *ex vivo* expansion of B cells, the donor's age seems to play a vital role in regards to how the cells can be stimulated most efficiently, which is a memory-pre culture.

Differentiation, in consequence, can also be impacted by different culturing approaches. Figure 26 shows the CD20 expression over the culturing time in the 3 culturing approaches. We noticed two different expression states of B cells at the beginning and end of culture (Figure 26A). Before culture, CD20 expression was high in most of the B cells and reduced to a low value being CD20 low or negative. We,



therefore, defined two populations ( $CD20^{++}/CD20^{+/-}$ ) and tracked their quantity during the 3 culturing approaches in adults and children (Figure 26B).

Throughout all the culturing approaches, the quantity of  $CD20^{++}$  B cells decreased continuously. In Batch culture, adults showed a stronger decrease in CD20 expression. The single-stimulated B cells showed the lowest reduction in CD20 expression overall. In ASC and memory pre-cultured cells of children, a comparable decrease to adult cells was observed on day 11 of culture. Memory pre-cultured B cells showed a slowed reduction during the first 4 days of culture. The reduction of  $CD20^{++}$  B cells accelerated when the medium was switched to ASC medium. Toward the end of ASC- and memory pre-culture, the content of  $CD20^{++}$  B cells approached 10 %, while Batch culture seemed to follow a similar trend but was not measured for the same duration. This indicates a loss of memory cell identity in all the culturing approaches, showing a cell development toward ASC.

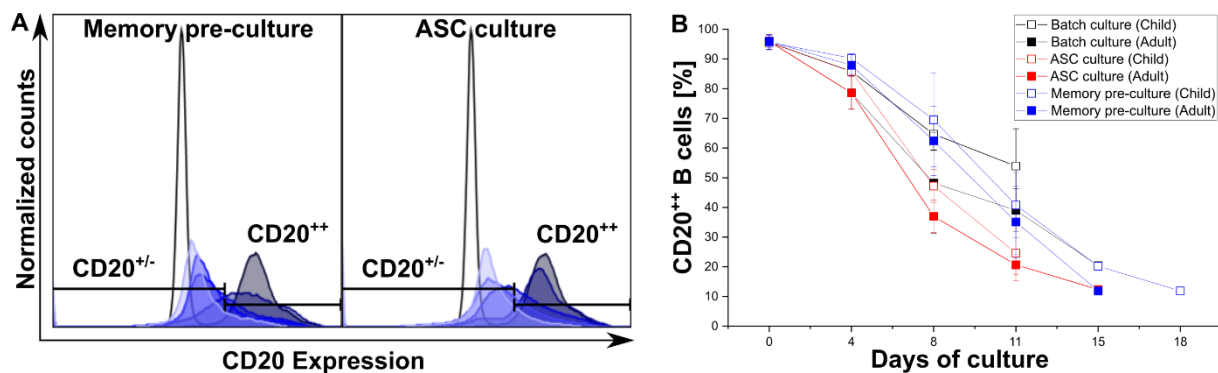


**Figure 26: CD20 expression during Batch-, ASC- and memory pre-culture of tonsillar B cells derived from adults and children. (A) Exemplary histograms of ASC- and memory pre-cultured B cells of donor A4, showing the gates for  $CD20^{++}$  cells and  $CD20^{+/-}$  cells. Dark blue shows the CD20 expression before culture, while lighter blue shades indicate later points of culture. Mock staining ( $CD20^{-}$ ) is shown in white. (B)  $CD20^{++}$  percentage of adult or child-derived B cells during the 3 different culturing approaches (n=3 adults/children).**

PB and PC development was expected in our culturing system as indicated by previous data and supplemented IL-21, which is known to cause PC development (Parrish-Novak et al. 2000; Ding et al. 2013; Ettinger et al. 2005). CD20 is expressed in all developmental stages of B cells, except the first and last. It is present on late pro-B cells through memory cells, but not early pro-B cells or PB and PC (Kaminski et al. 2012; Kjeldsen et al. 2011; Sanz et al. 2019). This shows that our culturing system causes the B cells to proceed with their development and mature from memory cells toward PB and PC. Batch culture showed the lowest decrease in CD20 expression, indicating a dependency on further stimulus, which is more abundant in restimulated cultures. To further investigate the subset development in our culturing approaches,

we analyzed the quantities of memory cells, PB and PC throughout the culturing period (Figure 27).

Memory cell content decreased during all culturing approaches. Child and adult batch cultures decreased in a similar fashion and reached a plateau after 8 days with approximately 70 % memory cells remaining. In ASC culture of adult B cells, memory cells reached a plateau after 4 days of culture with approximately 40 %. Child cells, in contrast, reached that plateau 4 days later, after 11 days in culture. In memory pre-culture, a decrease of memory cells started after the preculture, simultaneously with the change to ASC expansion medium. Adult B cells in memory pre-culture reached the lowest content of memory cells, approximately 10 % less compared to ASC-cultured cells. In contrast, child cells decreased to 40 % and increased their memory content again after day 11 in culture.

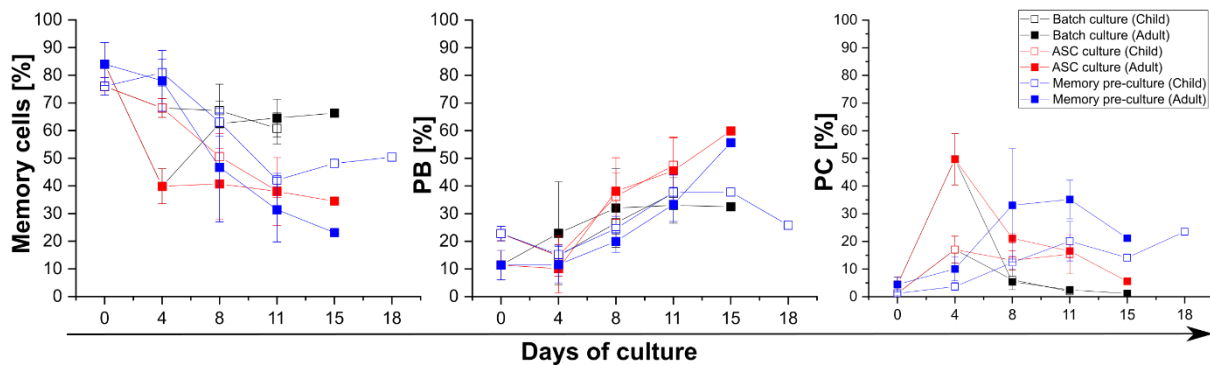


**Figure 27: Subclass development during batch, ASC and memory pre-culture. Samples were taken during medium change (n=3 adults/children). Memory cells were defined as CD27<sup>+</sup>CD38<sup>+</sup>, PB as CD27<sup>+</sup>CD38<sup>++</sup> and PC as CD27<sup>++</sup>CD38<sup>++</sup>.**

PB content on day 0 of culture was approximately 10 % higher in children compared to adults. On day 4 of culture, the PB content of child-derived cells decreased, while adult-derived B cells increased in PB content. In subsequent culture, all approaches increased in PB content. Batch culture reached a plateau at 30 %. ASC culture of adult and child cells increased the PB content progressively throughout the culture and showed the highest value overall. Similar behavior was observed for memory pre-culture of adult cells. Child-derived cells stagnated at 40 % and decreased PB content after day 15 in culture.

PC content was close to 0 for all donors at the start of culture. As already shown in Figure 24, PC performed a burst on day 4 of Batch and ASC culture. Adults performed a much more robust development toward PC compared to children. In memory pre-culture, a substantial increase was observed after change to ASC expansion medium

on Day 8 (adults) or Day 11 (children). Here also, PC development was more pronounced and occurred earlier in adult-derived cells, compared to child cells.

Several conclusions can be made about the culturing approaches based on these data. The batch culture showed the highest maintenance of Memory cells while performing a PC burst, peaking on day 4 of culture. Afterward, the PC content decreased, while PB increased in a reversed manner. This indicates that PC went into apoptosis, which is well known for short-lived PC bursts (Auner et al. 2010), while further PB were generated until day 8 of culture, holding memory cells constant. Toward the end of culture, the cell pool was comprised of approximately 70 % memory cells and 30 % PB with very low levels of PC left. ASC culture showed similar behavior in the first 4 days of culture but maintained a low memory content of 40 % afterward. Here also the PC content decreased after the burst on day 4, while PB increased in reversed manner. PC decrease was slower in ASC culture than in the ASC expansion medium batch culture. This indicates that additional stimulus by replacement with fresh medium pushes the culture further toward PB and maintains the PC burst for an extended period compared to Batch culture.

Consequently, memory cell maintenance is also lower in ASC culture with medium changes. After 11 days of culture, memory content was lower, while PB content was higher compared to the batch, which can again be ascribed to the repeated stimulation in this form of culture. Memory pre-cultured B cells showed a delayed PC burst, peaking 4 days later, compared to both other cultures. This can be explained by missing IL-21 stimulus in the first 4 days, known to cause the PC differentiation observed in the ASC expansion medium (Parrish-Novak et al. 2000; Good et al. 2006; Ettinger et al. 2007). Interestingly, the adult cells decreased the remaining memory cells toward the end of culture even further compared to ASC culture. In contrast, child cells increased their memory cell content after 11 days in culture. This can be explained by a slower generation of PB from the memory pool compared to the apoptosis of PC, causing this shift in subpopulations. Notably, this was only observed with donor C3 (Data not shown). These results confirm differences between adult and child B cells. Adult cells responded with a more vigorous PC burst and developed toward PB in a higher quantity, compared to child cells. This further supports the theory that the child's immune system is still developing, indicating somewhat less specialized memory cells. This means that cells derived from younger individuals are less prone to induce PB and PC development and are slower in this process. This should be

respected by researchers in the future, when results with primary B cells from donors of different ages are interpreted or used in processes.

To further study the impact of ASC and memory pre-culture, we analyzed the gene expression of AID, Pax5, IRF4 and Blimp-1 on days 4, 8 and 11 of culture for one donor (C2). The up- or downregulation of the 4 genes on each day, compared to day 0, is shown in Figure 28. Notably, these data show the same donor as in Figure 21, where CD40L concentration was varied and cells were measured after 7 days in culture.

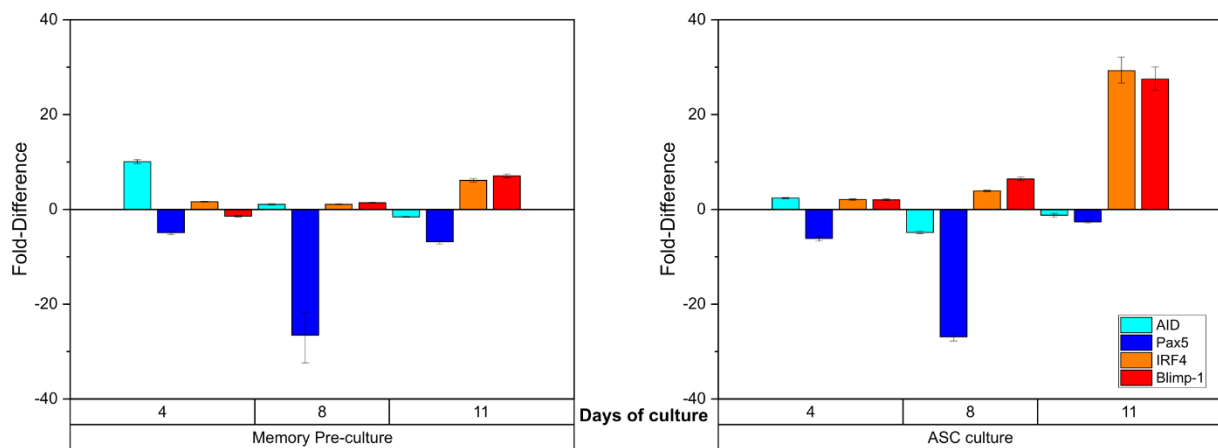


**Figure 28: Gene-regulation of B cells from donor C2 during ASC- or memory pre-culture on days 0, 8 and 11. Gene up- or downregulation was calculated via  $\Delta\Delta C_t$ -method in comparison to cells before culture and  $\beta$ -actin as reference gene.**

On day 4 of memory pre-culture, AID was upregulated by  $10.1 \pm 0.5$ -fold, while ASC culture showed less upregulation of AID ( $2.4 \pm 0.1$ -fold). Pax5 was downregulated in both cultures with  $-4.9 \pm 0.4$ -fold and  $-6.1 \pm 0.5$ -fold, respectively. IRF4 and Blimp-1 did not change expression in memory-pre culture, while both were upregulated by  $2 \pm 0.2$ -fold in ASC culture.

On day 8 of memory pre-culture, AID expression decreased back to the level before the start of culture, while ASC culture even decreased by  $-4.9 \pm 0.3$ -fold. Pax5 decreased its expression to  $-26.5 \pm 5.8$ -fold and  $-26 \pm 0.8$ -fold. IRF4 and Blimp-1 did not change expression in memory-pre culture again while being further upregulated to  $3.9 \pm 0.1$ -fold and  $6.4 \pm 0.4$ -fold in ASC culture.

On day 11, both cultures showed no significant AID change compared to levels before culture. Pax5 was downregulated further in memory pre-culture ( $-6.8 \pm 0.6$ -fold) compared to ASC culture ( $-2.7 \pm 0.2$ -fold). IRF4 and Blimp1 were less upregulated in memory pre-culture with  $6 \pm 0.5$  and  $7 \pm 0.4$ -fold, respectively, compared to ASC culture with  $29.2 \pm 2.8$  and  $27.5 \pm 2.5$ -fold respectively.

This shows that memory pre-culture has, in addition to increased expansion, the potential to induce SHM and CSR by upregulation of AID in the first 4 days of culture. This is a well-known AID function in B cell development and occurs mainly during GC reaction (Kuraoka et al. 2011; Xu et al. 2012). This could prove advantageous in further research aiming to improve antibody affinity by *ex vivo* GC reaction to find improved clones of a specific antibody. ASC expansion medium with IL-21 seemed to hamper this upregulation in ASC culture from the start and reversed AID upregulation in memory pre-culture after day 4. Since IL-21 is known to promote ASC development (Parrish-Novak et al. 2000; Ettinger et al. 2007; Ettinger et al. 2005), this suggests a skip of a GC-like state of the B cells by pushing them directly into PB and PC faith.

Interestingly, both cultures showed similar regulation of Pax5 with slight downregulation of Pax5 on day 4, maximal downregulation on day 8 of culture and went up again on day 11. Downregulation of Pax5 indicates B cell activation and development toward ASC (Nutt and Kee 2007; Fuxa and Busslinger 2007), which seems to be a similar extent in both culturing approaches. Upregulation of IRF4 and Blimp-1, as a marker of PB and PC faith (Shinnakasu and Kurosaki 2017; Turner et al. 1994; Shapiro-Shelef et al. 2003), seemed to be delayed in memory pre-culture compared to ASC culture. However, both seemed to be regulated to a similar extent and fashion compared to Pax5. They were strongest upregulated when Pax5 returned to the expression observed at the start of culture. This contradicts the widely accepted theory that Pax5 needs to be downregulated before B cells can commit toward PC (Fuxa and Busslinger 2007). However, a recent study by Liu et al. (2020) found that repression of Pax5 is not essential for robust PC development and antibody secretion, while it is required for optimal IgG production and accumulation of long-lived PC (Liu et al. 2020). We observed a high percentage of PB toward the end of cultures, shown via flow cytometry in Figure 27. This gene expression pattern of only upregulated IRF4 and Blimp-1 toward the end seems to be associated with this PB phenotype.

It is important to note, however, that we only tested one child donor. It would be interesting to see, in this regard, if adults show less AID upregulation in memory pre-culture. Child-derived B cells were less prone to develop into PC and perform PC burst, indicating a different developmental state compared to adults. This, in turn, could also impact how Pax5, IRF4 and Blimp1 are regulated between children and adults. We observed major differences in PC development, burst and proliferation dependent on age, suggesting different expression patterns in the starting material. This would

enhance later differences in the up and downregulation of genes between adults and children. Since we did not investigate this, further research could address this issue.

Figure 29 shows the Ig concentration in the cell culture supernatants on days 8 and 11 of ASC- and memory pre-culture of donor C2 and A5. According to different references, the average concentrations of serum IgG IgM and IgA are reported to be 5.6 – 18 g/L, 0.39 – 2.83 g/L and 0.51 – 5.8 g/L, respectively (Amino et al. 1978; Kardar et al. 2003; Jazayeri et al. 2013), which suggests an elevated base level of Ig in our culture media containing 10 % human ab serum. Most notably, IgG was 10-fold higher compared to IgM and IgA, supporting this suggestion. Absolute amounts of secreted antibodies were not considered due to supplemented human AB serum in our media, increasing the base level of all subclasses. We exclusively focused on differences between donors, days of culture and culturing methods.

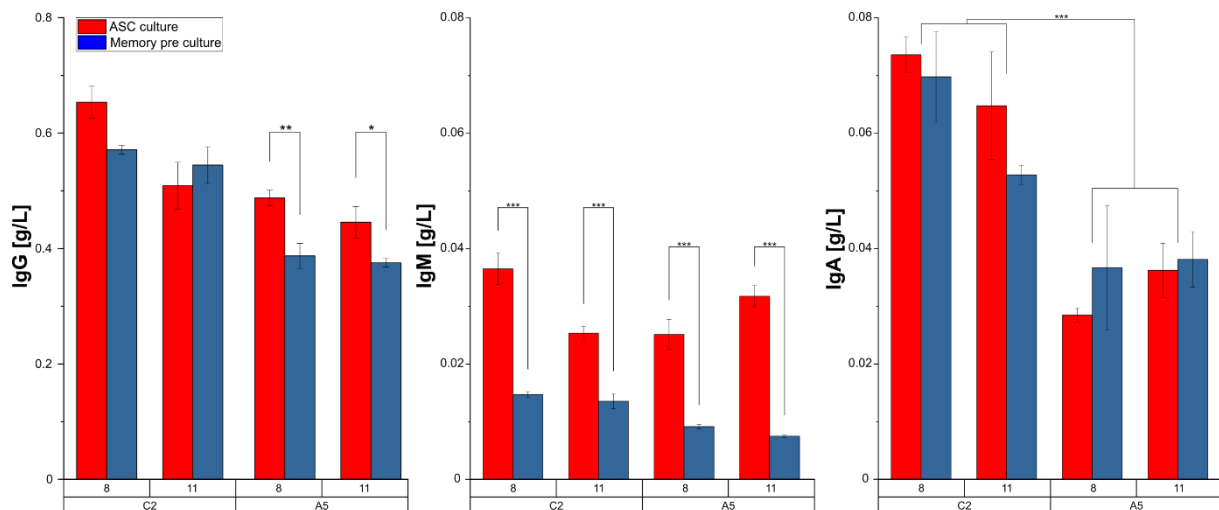


**Figure 29: IgG, IgM and IgA concentration in cell culture supernatants determined via ELISA. Supernatants were collected on days 8 and 11 of ASC- and memory pre-culture of donor C2 and A5. Serum-derived Ig levels were not subtracted. Data group difference between culture day culturing method and donors was determined via three-way ANOVA with Bonferroni multiple comparison test (\* p≤0.05; \*\* p≤0.01; \*\*\* p≤0.001).**

No significant differences in IgG, IgM or IgA secretion were discovered between days 8 and 11 of culture for both donors. This indicates that B cells produced comparable amounts of antibodies on day 8 and 11 of culture, independent of the culturing method and donor.

Cells of donor C2 showed no significant difference in IgG secretion between ASC- and memory pre-culture, while A5 produced significantly fewer IgG when B cells were subjected to memory pre-culture. This suggests donor-derived variations, causing different IgG secretions dependent on the culturing approach. This possibly hints toward further differences between adults and children.

IgM secretion levels showed the most significant differences of all antibody subclasses between the two culturing approaches. Both donors showed this behavior, confirming a reduction of IgM production when B cells were subjected to memory pre-culture. This seems to be the case for adults and children, since C2 and A5 both showed significant differences. IgM is secreted more by non-switched B cells (Noviski et al. 2018), pointing toward an occurring class switch away from IgM cells when cells were subjected to memory pre-culture. This is in accordance with the elevated AID expression in memory pre-culture observed for donor C2 (Figure 28). AID expression is well known to facilitate CSR and SHM in B cells (Muramatsu et al. 2000; Durandy 2003). Since donor A5 also showed this trend, it is tempting to assume that this donor also elevated AID levels during memory pre-culture and performed a CSR away from IgM.

The secretion of IgA showed no significant differences between both culturing approaches, while donor C2 secreted significantly more IgA compared to A5. This confirms donor-derived variations and could indicate a higher IgA secretion of child-derived B cells. Another possibility is, that C2 developed toward an IgA isotype, while A5 developed toward an isotype we did not test (e.g., IgE, IgD).

Based on the Ig secretion levels after ASC- and memory pre-culture, we can conclude that secretion stays at a constant level on days 8 and 11 of culture. A5 reduced the IgG secretion when B cells were subjected to memory pre-culture and IgA levels were significantly different between donors, showing donor-derived variations again, possibly due to donor age. Furthermore, a class switch away from IgM seemed evident for both donors when B cells were memory pre-cultured, indicating incidence of CSR and SHM, as already suggested by the upregulation of AID in memory pre-culture of Donor C2. This once more showcases the potential of a memory pre-culture in terms of expansion boost and changes in the antibody repertoire of the B cells.

#### **4.2.6 ASC and Memory Pre-Culture with Blood-Derived B Cells**

Since all previous results regarding ASC- and memory pre-culture were obtained with tonsillar B cells, we applied both protocols and batch culture to blood derived B cells to see if similar effects can be seen here. Functional differences between B cells isolated from blood and tonsils are well known and have been shown by others and us before (Pérez et al. 2014; Helm et al. 2021).

Cells were collected from buffy coats (Donor B6) via MACS as described in the method section and subjected to the culturing approaches described in Figure 23. We tracked

cell number for the calculation of expansion daily. Surface receptor expression and gene expression of AID, Pax5, IRF4 and Blimp-1 were measured on days 4, 8 and 11 of cultures.

Figure 30 shows the Expansion of B cells in all culturing approaches and the percentage of CD20<sup>++</sup> B cells during these cultures. Expansion in the first 4 days of preculture was 4-fold lower in memory-pre culture ( $2.8 \pm 0.2$ -fold) compared to ASC and batch culture ( $12.6 \pm 1.3$ -fold). Expansion potential in the ASC medium was again higher than in memory expansion medium, as already described for adult tonsillar donors (Figure 24). This opens the question of whether this observation is based on the donor's age or the source, which is blood in this case. Investigation of this matter is impossible since blood samples of child donors are only available under rare circumstances. Overall, batch culture showed the lowest expansion, again showcasing the advantages of cultures with medium changes, almost doubling the expansion capacity. Memory pre-culture started with a lower proliferation and surpassed ASC culture after 8 days in culture, indicating increased expansion potential in blood cells as well. To further back this hypothesis, more blood donors should be tested.

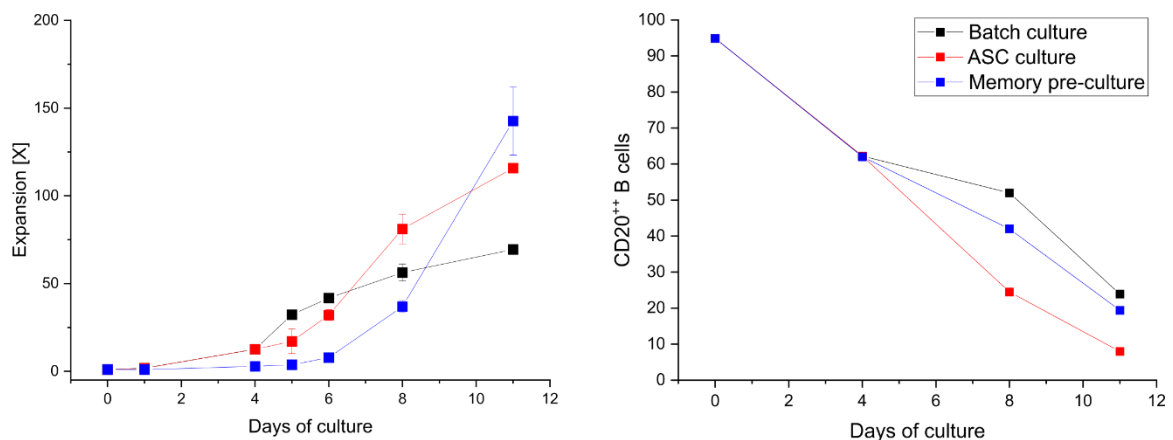


**Figure 30: Expansion and CD20<sup>++</sup> B cell content during Batch, ASC and memory pre-culture of blood derived B cells (B6).**

CD20<sup>++</sup> B cells declined in all three cultures, while their share was somewhat equivalent after 4 days in culture and fell strongest in ASC culture, followed by memory pre-cultured cells and batch culture maintained the highest quantity of CD20<sup>++</sup> B cells. This is comparable to the observations made with tonsillar B cells, shown in Figure 26. Loss of memory cell identity in blood-derived B cells, showing a cell development toward ASC, is therefore evident. The presence of IL-21 boosted this effect in both tonsillar and blood derived B cells.



Analyses of blood B cell subclasses like memory cells, PB and PC are shown in Figure 31, similar to tonsillar cells shown in Figure 27.

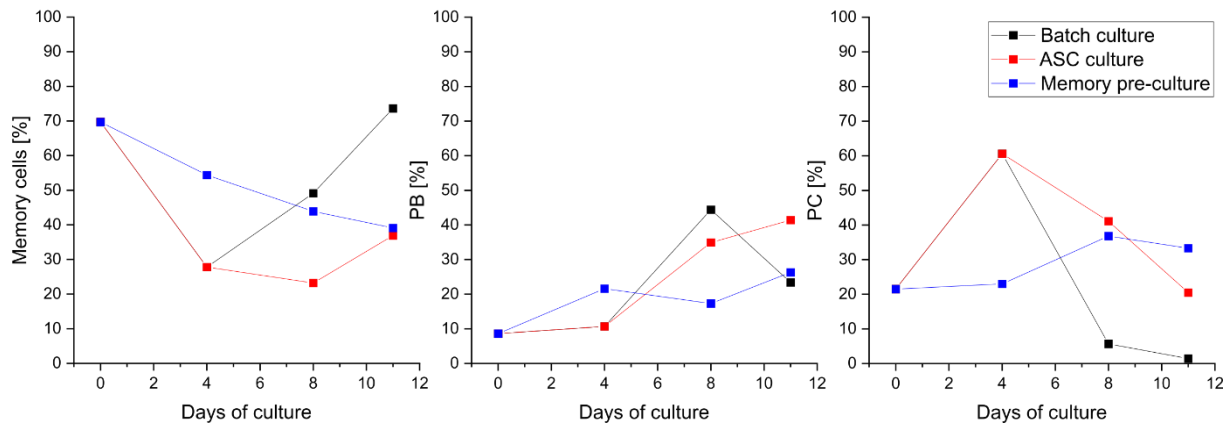


**Figure 31: Subclass development during batch, ASC and memory pre-culture of B6. Samples were taken at the start and during medium change on days 4, 8 and 11. Memory cells were defined as CD27<sup>+</sup>CD38<sup>+</sup>, PB as CD27<sup>+</sup>CD38<sup>++</sup> and PC as CD27<sup>++</sup>CD38<sup>++</sup>.**

Memory cell content decreased stronger in the first 4 days of ASC- and Batch culture, while memory pre-cultured cells maintained double the memory content. In later culture, the batch culture increased the memory content again, showing a reversible burst of PC representing most of the cells for a short period and then returning to mostly memory cells (70 %) again. ASC culture showed similar behavior with a longer-lasting burst of PC and lower levels of memory cells (37 %) after culture, with a higher share of PB (41 %). Memory pre-cultured cells reduced their content progressively with more PB development in the first 4 days and a PC burst after day 8 of culture. Memory pre-cultured blood B cells showed the highest PC share at day 11 of culture, indicating a less pronounced but longer-lasting PC burst. These findings again indicate a somewhat memory cell-focused expansion in the first 4 days of culture and a longer-lasting PC burst when blood B cells are subjected to a memory pre-culturing approach.

Gene expression analyses, shown in Figure 32, revealed further differences between both culturing approaches in blood-derived B cells. AID showed no upregulation during both, ASC and memory pre-culture at all times. This indicates that blood-derived B cells do not perform CSR or SHM when subjected to memory pre-culture. Blood-derived B cells are possibly more prone to developing into ASC than their tonsillar counterpart. This seems plausible, since B cells in the blood are not located in close proximity to T cells, which is necessary for GC formation leading to such effects. Moreover, blood cells are derived from adult donors, which could also cause this disparity.

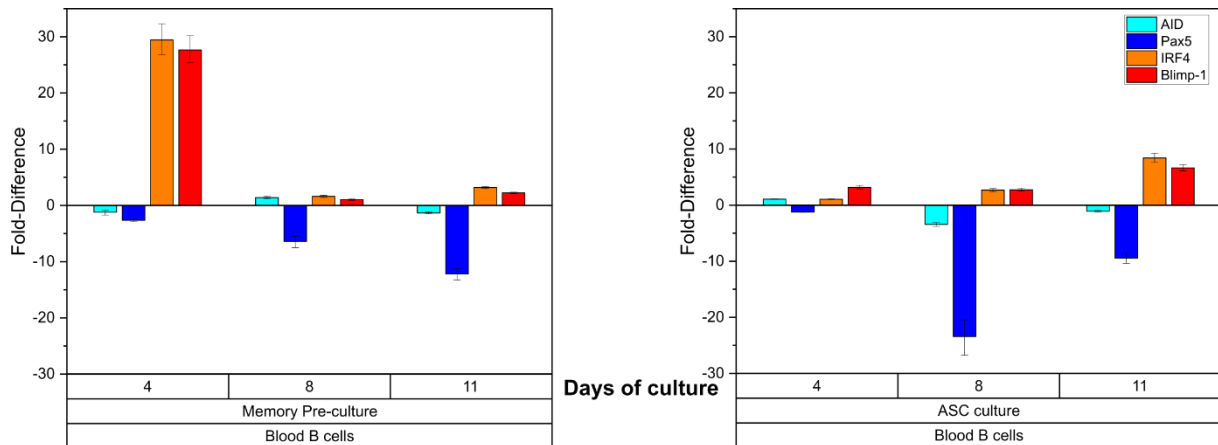


**Figure 32: Gene-regulation of B cells from donor B6 during ASC- or memory pre-culture on days 0, 8 and 11. Gene up- or downregulation was calculated via  $\Delta\Delta C_t$ -method in comparison to cells before culture and  $\beta$ -actin as reference gene.**

Pax5 was progressively downregulated in memory pre-cultured B cells. ASC culture peaked in Pax5 downregulation on day 8 of culture and increased back toward the starting level. This is similar to what we observed for both culturing approaches with tonsillar B cells, shown in Figure 28. Observable activation of B cells is only seen after 8 days in both culturing approaches. Activation was stronger pronounced in ASC culture, however.

Interestingly, IRF4 and Blim-1 were most upregulated after 4 days of memory pre-culture, without any signs of activation via Pax5 downregulation, which contradicts what we observed in tonsillar B cells (Figure 28), where ASC culture caused higher upregulation of these, ASC indicator, genes. Additionally, the upregulation of both genes occurred immediately after 4 days in memory expansion medium, whereas tonsillar cells showed this behavior only toward the end of the culture. This suggests a key role played by CD40L without IL-21, causing ASC development in blood-derived B cells. One could hypothesize that memory B cells derived from human blood are triggered to develop toward ASC by CD40L stimulation immediately, even better in the absence of IL-21. ASC culture, in contradiction, increased IRF4 and Blimp-1 expression toward the end of culture, similar to tonsillar B cells.

This confirms major difference between blood and tonsillar B cells. They react differently to stimulation with CD40L and IL-21, seen by gene expression patterns. However, proliferative response and subclass development seemed comparable to that of tonsillar B cells. One has to keep in mind that the quantification of gene expression is always in comparison to the expression of genes before the start of culture. If the genetic program of the input cells starts at minute levels, a slight

upregulation of the same gene is much stronger compared to already upregulated genes.

Nevertheless, this shows that gene expression differs notably between blood derived and tonsillar B cells. A memory pre-culturing approach for expanding blood-derived B cells seems to grant the same benefits as observed in tonsillar B cells. B cells seemed to expand slightly better after a somewhat more extended lag phase, compared to purely ASC-cultured cells. If this is not the case with additional donors, the reduction of IL-21 in the first 4 days still states an advantage, by saving IL-21 as a valuable resource.

#### **4.2.7 Conclusion of Specific Stimulation with Soluble CD40L in Suspension**

In the process of medium development and testing, we showed no impairing effects of CSA as a standard supplement in all culturing media, while the importance of standardized serum was shown. To obtain comparable results between experimental replicates or when different donors are tested, all experiments must be conducted with the same batch of human serum. This is also particularly important when investigating primary cells with notable donor variations.

Growth and expansion of B cells were shown to benefit from lower cell seeding densities and low advantages were shown at increasing CD40L concentrations above 0.4  $\mu\text{g}/\text{mL}$  or 4  $\mu\text{g}/10^6$  cells. Supplementation of IL-21 boosted the proliferative response (in adults), while a further increase of IL-21 above 10  $\text{ng}/\text{mL}$  did not increase expansion. Taking this into account, we defined an ASC- and memory expansion medium (Table 5) and explored their effects on primary tonsillar B cells in batch culture. We observed notable differences in expansion between adult and child donor-derived B cells, when cultured in memory expansion medium. Adults showed little to no proliferative response, while children showed a comparable response to ASC medium. ASC medium yielded between 5- and 20-fold expansion for children and adults, with notable donor-derived variations. Subclass analyses of B cells in both media revealed increased PB and PC development in medium containing IL-21, as shown by others before. In contrast, memory expansion medium maintained a higher number of memory B cells. This was further confirmed via RT-qPCR of one child donor. In memory expansion medium, AID was upregulated, indicating SHM and CSR. Pax5 was downregulated, showing activation of B cells, while IRF4 and Blimp-1 were not upregulated, indicating no full commitment toward ASC. In ASC medium, B cells

showed lower but also upregulated AID, compared to memory medium. Pax5 was downregulated, while IRF4 and Blimp-1 were upregulated, showing commitment toward PB and PC.

As the next step, we tested two alternative culturing approaches with medium replacement every 3 – 4 days compared to a batch approach in ASC expansion medium. B cells were either pre-cultured for 4 days in memory expansion medium or directly subjected to ASC expansion medium for the full extent of culture. In the first 4 days, child-derived B cells again showed a better proliferative response in memory medium, while expansion in ASC medium was comparable despite donor-derived variations. Subclass development showed differences between adults and children as well. In ASC medium, adult-derived B cells performed a notably stronger PC burst, marked by higher PC numbers on day 4. Children maintained comparably high numbers of memory cells. In memory expansion medium, both maintained higher memory cell numbers. Later stages of the cultures revealed higher expansion potential when tonsillar B cells were pre-cultured in memory expansion medium compared to ASC culture. This effect was stronger pronounced in children than in adults. ASC culture led to a sharp peak of PC on day 4, while memory pre-culture caused a lower and longer-lasting increase in PC. PC development was always stronger pronounced in adult donors. Gene expression analyses and ELISA revealed that a memory pre-culture causes upregulation of AID and reduces IgM secretion compared to ASC culture, strongly hinting toward additional CSR and possible SHM in such a culturing approach in addition to benefits in expansion potential of primary tonsillar B cells.

Finally, we were able to show that similar benefits can be achieved by a memory pre-culture with blood derived B cells, while the genetic program showed major differences compared to tonsillar B cells. For RT-qPCR, we always ran 4 reference genes (e.g.,  $\beta$ -actin,  $\beta$ 2-microglobulin, HPRT and GAPDH) as endogenous control and identified  $\beta$ -actin as the most stable gene for all analyses.

A memory pre-culture without IL-21 is, therefore, beneficial for B cell expansion. This was shown by Nojima et al. before (Nojima et al. 2011). We improved this approach by replacing feeder cells with soluble CD40L and BAFF, making this system easily reproducible for other groups. We showed that this method works with primary human cells and that our approach was additionally capable of activating GC-like features by upregulation of AID, leading to CSR, which states the major advantages of this

research project being one step closer to the development of processes for human B cell therapies.

Suspension cultures of animal cells are the standard in cell culture, yet they are missing important features, only present in closely packed tissue environments. With the findings acquired in this section, we went on to transfer B cell cultures into closely packed tissue mimicking SCS-PDADMAC capsules to further investigate B cell development in closer approximation to the tissue environment. Encapsulated cultures of tonsillar human B cells are described in the next section of this work.

### 4.3 Encapsulated B Cell Cultures Stimulated with Soluble CD40L

This chapter is a slightly modified version of “Cultivation of Encapsulated Primary Human B Lymphocytes: A First Step towards a Bioartificial Germinal Center” published in *Macromolecular Bioscience* (Helm et al. 2022) and has been integrated into this chapter in accordance with the Copyright Transfer Agreement. All experiments regarding B cell expansion in suspension and encapsulated cultures were conducted by S. B. Huang and are only mentioned briefly in this chapter.

Microencapsulation can mimic complex body niches, bringing *ex vivo* cultivation closer to conditions found in the human body (Wilson and McDevitt 2013). Providing such engineered environments is promising for many cell types' *ex vivo* proliferation and differentiation. *Ex vivo* cultivation of B cells is typically performed in suspension in culture media containing multiple stimuli. Microcapsules consisting of SCS and PDADMAC are comprised of a liquid core of unreacted SCS polyelectrolyte enveloped by a semipermeable membrane made of PEC. For primary human T cells, microencapsulation in SCS-PDADMAC capsules has been demonstrated before and shown to support cellular growth and differentiation (Jérôme et al. 2017). Cellulose sulfate shares some structural similarities with heparan sulfate (HS), a highly abundant component of the ECM (Thomas Groth et al. 2020). Binding studies showed that HS-binding motifs are present on many cytokines (e.g., IL-2, IL-4, IL-10, CD40L) (Gehrcke and Pisabarro 2015; Najjam et al. 1997; Lortat-Jacob et al. 1997; Simon Davis and Parish 2013). HS immobilizes these cytokines leading to a range of functional consequences, including mitogenic effects (for a review, see (Laura E. Collins and Linda Troeberg 2019)). HS-like binding properties and effector function of SCS-PDADMAC microcapsules were previously demonstrated for IL-2 (Jérôme et al. 2017). Since cytokines involved in B cell development and maturation, such as IL-4 and CD40L, have been described to bind to HS, we tested the hypothesis that SCS-PDADMAC-capsules provide a suitable microenvironment for the *ex vivo* proliferation and differentiation of human primary tonsillar B cells.

In order to reduce donor-based heterogeneity, all experiments discussed below were carried out using several cryovials of B cells, derived from the tissue of a single adult donor (Donor A5).

### 4.3.1 Microencapsulation Unit and Alginate Encapsulation

Figure 33 shows the structure and partials of the technical dimensions of a newly designed microencapsulation unit. The upper part has two hose connectors to attach standard silicon tubes with an outer diameter of 5 mm and 1 mm wall thickness. The connection of silicon tubes is by push-on of the silicon tube. The vertical connector serves as an inlet for sterile SCS-solution, while the horizontal connector serves as an inlet for sterile nitrogen. For sterile nitrogen supply, a 0.2  $\mu\text{m}$  sterile filter can be interposed in the tubing leading to the nitrogen connector. The nozzle has an inner extruder for the SCS-solution with an outlet diameter of 600  $\mu\text{m}$  and an outer diameter of 900  $\mu\text{m}$ , resulting in a wall thickness of 150  $\mu\text{m}$ . The outer nitrogen flow channel has an inner diameter of 3 mm and an outer diameter of 5.5 mm, resulting in a wall thickness of 1.25 mm. The microencapsulation unit was printed via a Form 3 3D-Printer and was readily usable after the removal of excess resin. Detailed procedure can be found in the method section 3.15.

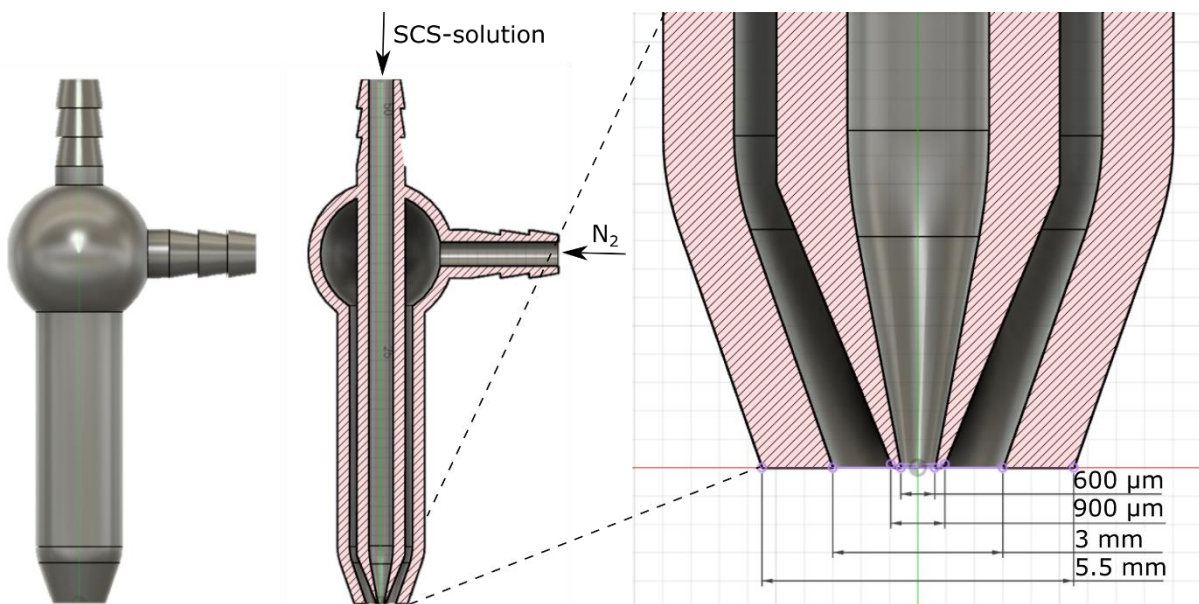


**Figure 33: 3D-printable microencapsulation unit as full and sectional view. Technical dimensions are shown for the nozzle. This figure is adopted from Helm et al. (2022).**

For sterile encapsulation, the 3D-printed unit was sterilized by 30 minutes of irradiation with UV-light, while other accessories were sterilized by autoclaving. Sterility was tested by incubating sterilized parts in LB-medium for multiple weeks without signs of contamination.

Sodium alginate was used as pre-testing material for the SCS encapsulation. Briefly, a 1.5-wt% sodium alginate solution was dropped into a 0.09 mol/L stirred calcium

solution using the 3D-printed microencapsulation unit. The encapsulation process was conducted with N<sub>2</sub>-flow rates of 1, 2, 3 and 4 L/min according to the variable area flow meter scale. The size of the resulting capsules was measured via microscopy.

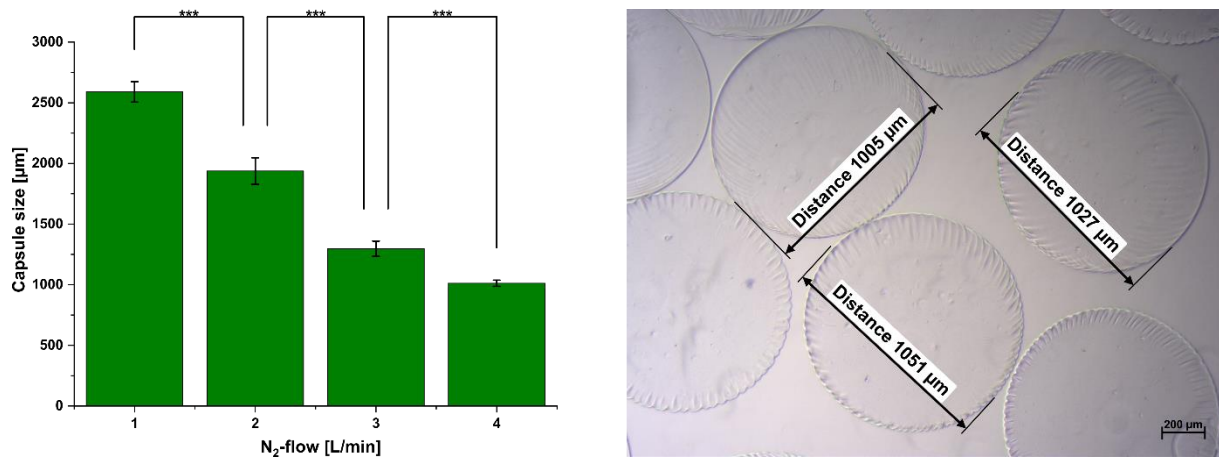


**Figure 34: N<sub>2</sub>-Flow dependent size distribution of sodium alginate capsules hardened in calcium solution and size measurement via microscopy.** Capsule size is shown for different N<sub>2</sub>-flows, 1 L/min (n=17 capsules), 2 L/min (n=20 capsules), 3 L/min (n=29 capsules) and 4 L/min (n= 32 capsules). Data group difference was determined via one-way ANOVA with Bonferroni multiple comparison test (\*\*\*) p≤0.001).

The results of the alginate encapsulation are depicted in Figure 34 and show a strong and significant correlation of capsule size with N<sub>2</sub>-flow. The capsule size decreased from 2589 ± 84 µm at 1 L/min N<sub>2</sub>-flow down to 1012 ± 26 µm at 4 L/min N<sub>2</sub>-flow. The size distribution of the produced capsules always stayed in a narrow range, guaranteeing good reproducibility for future encapsulations. Microscopic imaging also confirmed the spherical shape of the produced capsules, endorsing good functionality of the microencapsulation unit in the future. For a sphere, the specific surface area (the surface area per unit volume) increases as the diameter decreases. Therefore, a decrease in microcapsule diameter should reduce resistance to the transport of oxygen and nutrients to the encapsulated cells. Hence, smaller capsules are advantageous for cell cultures (Zhang and He 2011). We, therefore, selected the N<sub>2</sub>-flow rate of 4 L/min as our standard flow rate and used these settings to produce SCS-PDADMAC capsules.

This microencapsulation unit can be easily 3D-printed by other researchers, reducing costs and enabling them to use and test this technology. Additionally, the size of the capsules can be easily adjusted by variation of the N<sub>2</sub>-flow, making this system quick, adjustable and low-budget.



### 4.3.2 Molecular Weight Cut-Off (MWCO) and Size of SCS-PDADMAC Capsules

SCS-PDADMAC capsules were produced with the settings described in the methods section and were based on the pre-tests with alginate capsules. We selected the highest N<sub>2</sub>-flow rate to obtain the smallest possible capsules. The capsule size of our SCS-PDADMAC capsules was  $1223 \pm 47 \mu\text{m}$  ( $n = 39$  capsules) which is slightly bigger compared to alginate capsules at the same settings. This is likely due to the higher viscosity of the SCS solution, leading to a later shearing of the drops at the nozzle of the microencapsulation unit.

To determine the SCS-PDADMAC capsule MWCO, resorufin (0.229 kDa) and vitamin B12 (1.35 kDa) were tested for their ability to diffuse through SCS-PDADMAC capsules. 0.5 g capsules were mixed with stock solution (5 mg/mL) of vitamin B12 or resorufin. The supernatant samples were drawn at defined times, transferred to a 96-well plate and analyzed in the Tecan plate reader. Detailed procedures are described in the method section. Results of the time-dependent transfer into empty capsules are shown in Figure 35.

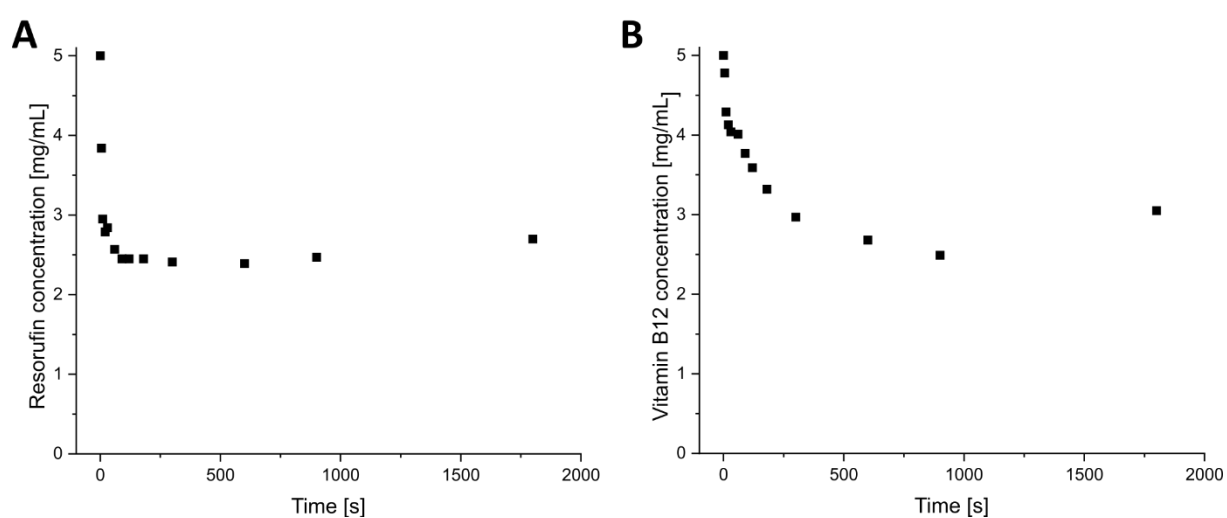


**Figure 35: SCS-PDADMAC capsule characterization. A: Diffusion of resorufin (0.229 kDa) into capsules characterized by a decreasing concentration in the supernatant. B: Vitamin B12 (1.35 kDa) diffusion into capsules characterized by decreasing concentration in the supernatant. This figure is adopted from Helm et al. (2022).**

Resorufin reduced its concentration by half in the first 150 seconds and remained at this concentration for the rest of the incubation time. Vitamin B12 could also diffuse freely through the capsule pores and reached concentration equilibrium within 10 minutes. Following these experiments, the MWCO can be deduced above 1.35 kDa, while smaller molecules diffuse faster through SCS-PDADMAC capsules. Previous investigations with our system have shown that RITC-Dextran, with a

molecular weight of 10 kDa, could not penetrate the capsule membrane (Werner 2013). The porous membrane of the polyelectrolyte microcapsules, therefore, has an MWCO between 1.35 and 10 kDa, which assures that most cytokines produced or required by the cells are trapped inside the capsules. At the same time, low molecular weight nutrients and metabolites can pass. All later supplemented cytokines have a molar mass above 10 kDa (e.g., CD40L 23 kDa, IL-4 15.1 kDa, IL-21 15.5 kDa, BAFF 17 kDa). In the case of insulin as one of our medium components with a molecular weight of 5.7 kDa, we could not predict its penetration. Therefore, we supplemented insulin in the form of ITS-G in- and outside the capsules during all cultivation of encapsulated B cells.

#### 4.3.3 FC Analyses of B Cells in Suspension and SCS-PDADMAC Capsules

In suspension culture, subsets were first identified by CD27 vs. CD38 dot plots and subsequently analyzed for CD20 expression in the identified subpopulations. Cells were assigned to subsets as follows: Memory cells: CD19<sup>+</sup>/CD20<sup>+</sup>/CD27<sup>+</sup>/CD38<sup>-</sup>; Germinal center (GC) cells: CD19<sup>+</sup>/CD20<sup>+</sup>/CD27<sup>+</sup>/CD38<sup>+</sup>; PB: CD19<sup>+</sup>/CD20<sup>-</sup>/CD27<sup>++</sup>/CD38<sup>-</sup>; PC: CD19<sup>+</sup>/CD20<sup>-</sup>/CD27<sup>++</sup>/CD38<sup>++</sup>.

Contrary to the development in suspension culture, the PC phenotype was not detected among the released encapsulated cells. Further analysis revealed that the cellulase treatment, used for cell release, prevented the detection of the CD27<sup>++</sup> subtype (Figure 36).

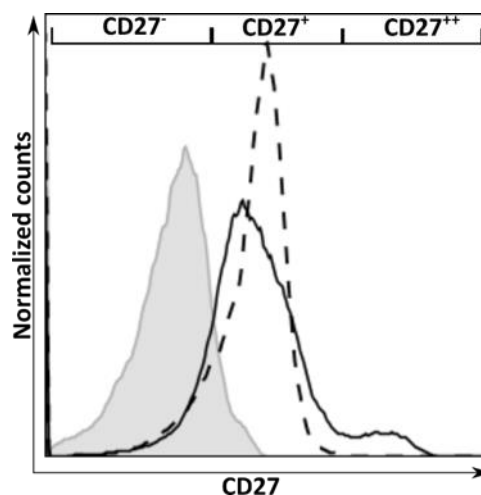
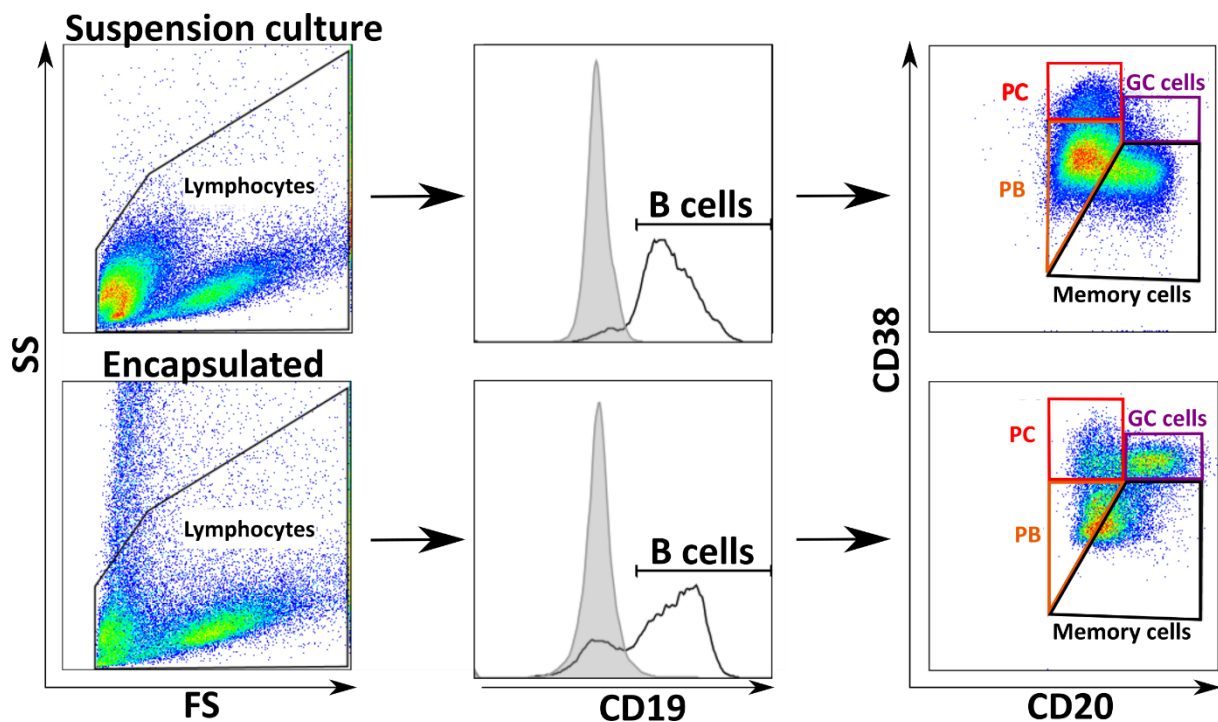


Figure 36: Histogram of B cells analyzed with flow cytometry regarding their CD27 expression. B cells incubated in PBS (solid black line) and incubated in 1 % (w/v) cellulase (dotted black line) are presented. Mock staining is shown in grey. This figure is adopted from Helm et al. (2022).

B cells incubated in cellulase still exhibited low CD27 expression (CD27<sup>+</sup>), while cells with high CD27 expression (CD27<sup>++</sup>) indicative of PC were no longer measurable after

incubation with the enzyme cellulase. CD27 is a glycosylated molecule (Teplyakov et al. 2017). If the glycosylation site is involved in antibody binding, cellulase treatment could presumably interfere and hamper this binding. As a result of this phenomenon, CD27 expression was not considered in the subclass analysis of encapsulated cells.

Encapsulated B cells were identified within the CD19<sup>+</sup> population and distinguished from capsule fragments. Subclass identification was based on the level of their expression of the CD20 and CD38 surface markers only, as shown in Figure 37.



**Figure 37: Gating strategy for B cells.** B cells in suspension culture (top panel), encapsulated B cells (bottom panel). Prior to subclass analysis, the lymphocyte population was identified (left panel) and B cells were gated via CD19 expression (white histogram in the middle panel and mock staining in grey). B cells were then divided into subclasses via CD20 and CD38 expression to distinguish between memory cells, germinal center (GC) cells, PB and PC, shown in the dot plot on the right. This figure is derived from Helm et al. (2022).

The first step was to define a gate in FS vs. SS to identify the lymphocytes and remove possible aggregates. Cells in the lymphocyte gate were then gated regarding CD19 expression to identify the B cells and distinguish them from capsule fragments, possibly in a similar size range. CD20 vs. CD38 expression was then used to identify memory cells, GC cells, PB, and PC within the B cells population. This gating strategy was used from now on, when encapsulated cells were analyzed and when B cells cultured in suspension were cultured in comparison.

#### 4.3.4 Suspension Culture of B Cells Compared to Encapsulated Culture

Since B cells cultured in suspension could be analyzed in further detail, due to additional CD27 staining, we conducted a complete subclass analysis for all four suspension cultures.

Cultures were issued from four individual cryovials (Donor A5) with a seeding density of  $0.1 \times 10^6$  cells/mL in ASC expansion medium. After thawing, cells were initially allowed to recover in growth medium for 4 days. Then, they were reseeded at  $0.1 \times 10^6$  cells in fresh ASC expansion medium and left in this batch culture for the rest of the duration. Expansion and differentiation into cellular subsets were followed for up to 18 days.

Cells in all cultures entered the exponential growth phase within four days after initiation of the culture and reached their maximum expansion between 5 and 20-fold after 11 – 14 days. Cell viability remained above 90 % during all cultures. Notable variations in expansion potential despite using one single donor were observed and suggested as a possible effect of the thawing and freezing process. Temperature fluctuations during freezing and handling variations in the thawing process are known to influence cellular behavior (Hermansen et al. 2018). The likelihood of such interexperimental variations should be considered when interpreting experimental results, even when only one donor is used (Helm et al. 2022). Figure 38 shows the development of the B cell subclasses (memory cells, GC cells, PB and PC). Notably, the GC phenotype is included in this gating strategy. GC were not included in previous gating strategies due to low abundance in suspension cultures.

All cultures followed a similar trend described in the previous chapters regarding ASC and batch culture of B cells. Memory cells constantly decreased, GC cells, as a newly defined subclass, peaked at day 4, PC reached a maximum on day 6 to 7 and then decreased and PB increased steadily from day 4 onwards.

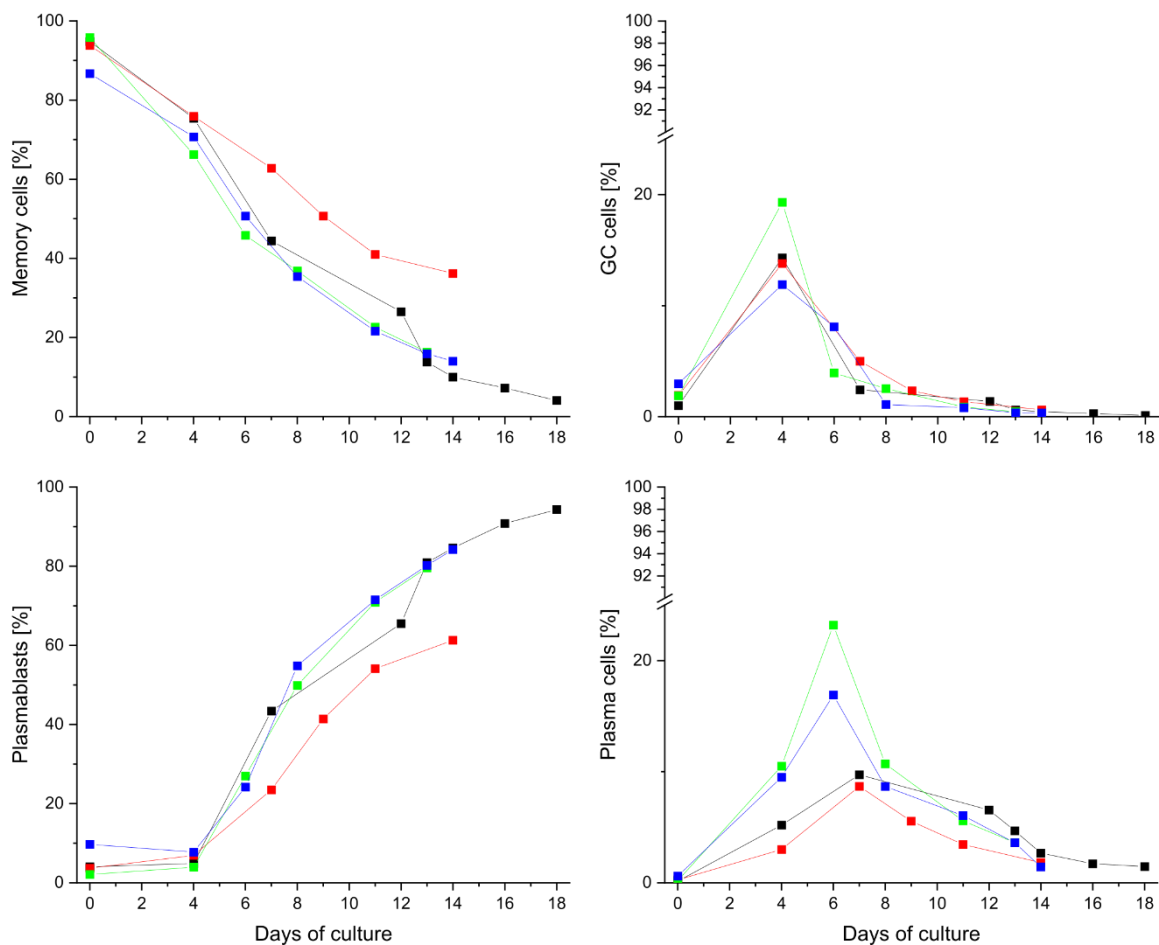


**Figure 38: Development of four individual suspension cultures derived from independent cryovials (identical donor). On day 4, cells were reseeded at  $0.1 \times 10^6$  cells/mL in fresh medium. In all cases, the viability was consistently above 90 %. B cells were gated as described for cells cultured in suspension in the previous chapter. This figure is adopted from Helm et al. (2022).**

The short-lived burst of PC observed in B cell culturing systems is a well-known phenomenon during B cell expansion in the presence of IL-21 (Avery et al. 2003). This was also described in previous chapters of this work. Development is similar to the *in vivo* situation, where most PC arising in the GC are short-lived, produce antibodies rapidly and then die (Ettinger et al. 2005; Bryant et al. 2007; Ding et al. 2013). Regarding the peak of GC cells on day 4, it is possible that this is due to delayed CD20 reduction compared to CD38 upregulation. This means that cells developing toward PC by upregulation of CD38 were, possibly by mistake, identified as GC cells due to delayed CD20 reduction. Hence, the correct identification as PC was only possible after day 4.

#### 4.3.5 SCS-PDADMAC Encapsulation with or without Human AB Serum Inside

Figure 39 shows the schematic process of B cell encapsulation in SCS-PDADMAC. This and the following chapters will elucidate possible variations in the process and their effects as described in Helm et al. (2022).

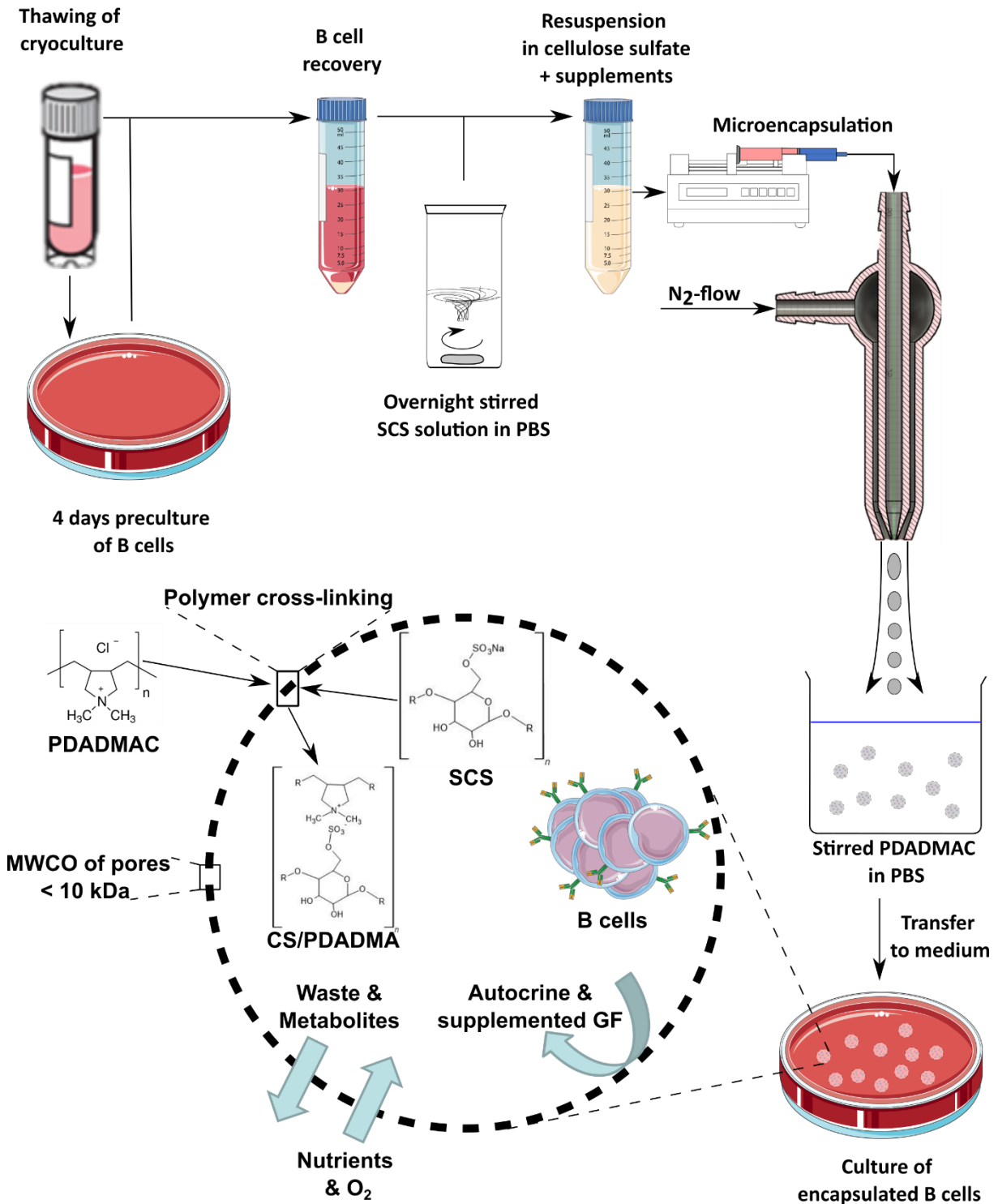


Figure 39: Depiction of the encapsulation process for primary tonsillar human B cells. Also shown is the PEC, forming the capsule membrane. This figure is adopted from Helm et al. (2022).

To allow reliable cell count and phenotyping post-release from the capsules, the cell density for encapsulation was chosen 10-fold higher ( $1 \times 10^6$  cells/mL<sub>capsule</sub>) compared to suspension culture. This questions the comparability between suspension and encapsulated B cell cultures, since either the volumetric concentration of the essential signal molecules or their amounts per cell would be similar. Initially, the volumetric concentration was adjusted to be identical in the capsules' core and the supernatant of the suspension cultures, accepting that this would reduce the amount of cytokine available per cell inside the capsules. As most cytokines have molar masses above 10 kDa (e.g., CD40L 23 kDa, IL-4 15.1 kDa, IL-21 15.5 kDa, BAFF 17 kDa), it was assumed that these molecules, when supplemented during encapsulation, would not be able to leave the capsules. The same applies to most signal molecules produced by the cells (Helm et al. 2022). The standard protocol for human T cell encapsulation with SCS-PDADMAC developed by our group, required a rinsing of the cells with human serum (referred to as serum-coating in the past) prior to the suspension in SCS, serving as protection against shear stress (Werner et al. 2015; Jérôme et al. 2017). In case of the B cells, besides this standard protocol (cells/capsules<sub>withoutserum</sub>), and to further emulate the environment experienced by B cells in the suspension culture, we also encapsulated the cells suspended in human serum, leading to a final serum concentration of 10 % (v/v) in the capsule core (cells/capsules<sub>withserum</sub>) (Helm et al. 2022).

Since thawing is stressful to the cells and the biomass is low, cells were encapsulated after cultivation in growth medium, long enough to allow the culture to enter the exponential growth phase (typically after 4 days as shown in Figure 38). Encapsulation was successful, with cells visible inside the capsules, as seen in Figure 40A. Throughout cultivation, the B cell density inside capsules increased visibly, observable as small cell aggregates forming after several days of cultivation, as highlighted in Figure 40B (Helm et al. 2022).

The expansion of encapsulated cells with and without human serum in the capsule core, compared to a suspension culture was performed as part of S. B. Huang's work (Helm et al. 2022). Briefly, cells remained highly viable throughout (> 85 %), with a small drop 24 h after encapsulation for cells/capsules<sub>withserum</sub>. Cells in suspension maintained high viability of over 90 % throughout the experiment. In terms of expansion, both encapsulation procedures showed a steady proliferation after a short lag phase of 24 hours. Cells doubled their number after 8 days in culture. The presence

of human serum in the capsules' core did not provide additional benefit for cell proliferation.

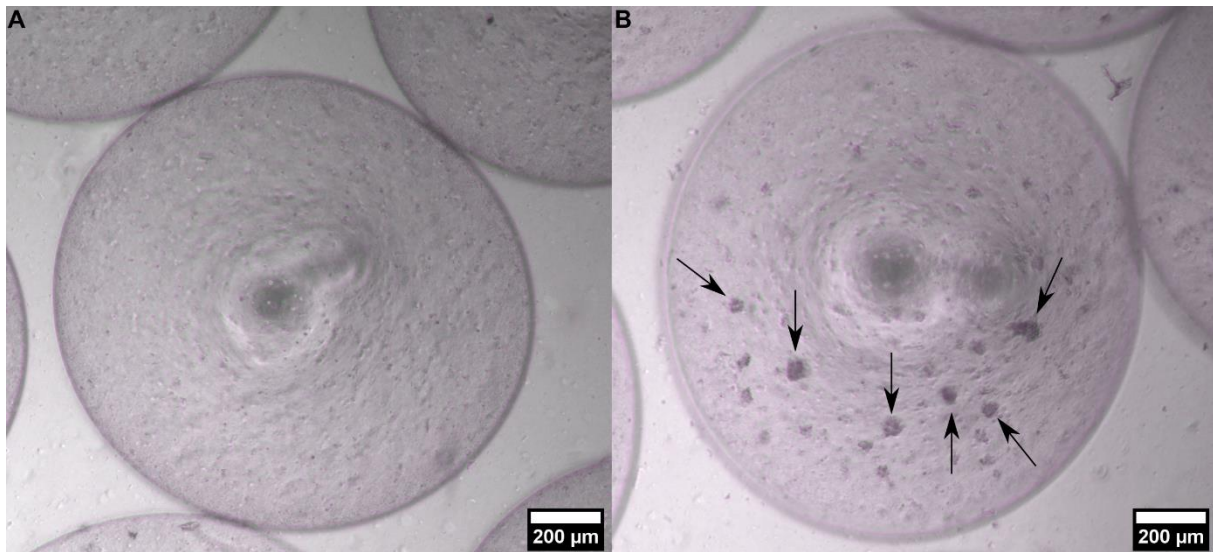


**Figure 40: Microscopic image of SCS-PDADMAC capsules with B cells inside. Representative capsules directly after encapsulation (A) and after 11 days of cultivation (with arrows pointing to aggregates) (B). All images were taken at 10x magnification. This figure is derived from Helm et al. (2022).**

Suspension culture showed a 3-fold higher expansion (6-fold absolute) throughout the cultivation. For encapsulated cultures, some limitations could not be excluded, as molecules larger than the MWCO of the capsule membrane (e.g., hormones, GF, proteins, lipids) cannot be replenished from the outside of the cell culture medium and thus will be gradually depleted inside the capsules during the cultivation time. Further, while the volumetric concentrations were identical, as already discussed, the amount of co-encapsulated cytokines per  $10^6$  cells was 10-fold lower inside the capsules compared to the suspension culture (Helm et al. 2022). This issue will be addressed in chapter 4.3.7.

Additionally, the subclass development of the encapsulated B cells was analyzed throughout the cultivation. Results are shown in Figure 41. While the presence of 10 % (v/v) human serum in the capsule core had made no difference in survival/expansion of the encapsulated B cells, an interesting influence on subtype development was observed. Before encapsulation, the cell pool contained 70.4 % memory cells, 7.7 % GC cells, 15 % PB, and 6.9 % PC. Comparison of all B cell subsets on Day 0 shows that encapsulated B cells ( $\text{cells/capsules}_{\text{withoutserum}}$  and  $\text{cells/capsules}_{\text{withserum}}$ ) differed from cells before encapsulation (Suspension). Notably, memory cell and PB content decreased, while PC and GC cells increased. This shift could be an indication of the lingering stresses of encapsulation.



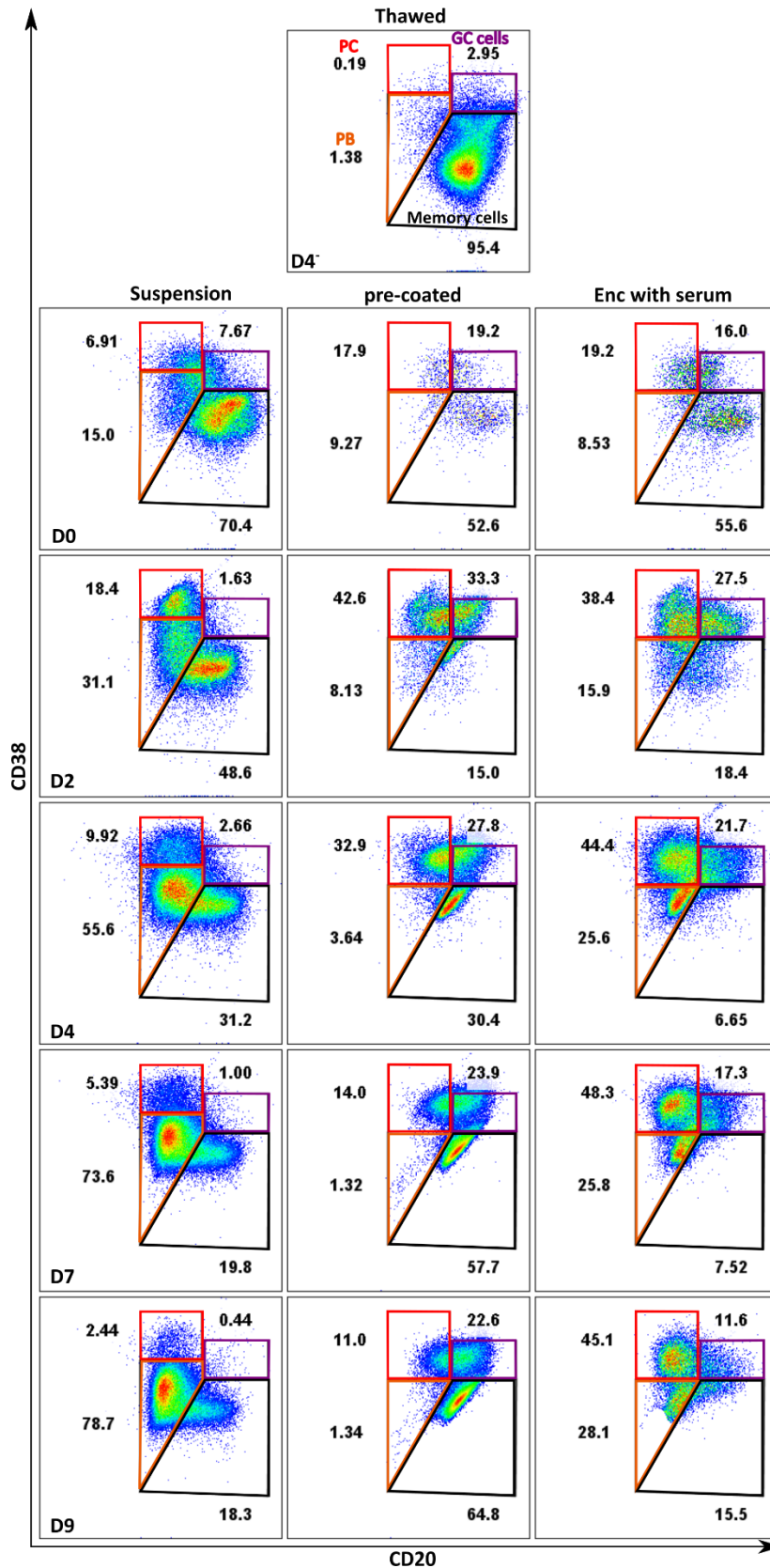


Figure 41: B cell subpopulation development for encapsulated cells compared to those cultivated in suspension. Day -4 refers to the day of thawing. Day 0 to Day 9 refer to the days of cultivation post-encapsulation or post-inoculation at  $0.1 \times 10^6$  cells/mL for the suspension culture. For each measurement, either one well of suspension culture of a 24-well plate was harvested or capsules were drawn and cells released by cellulase treatment. For flow cytometry measurements, 80,000 events were analyzed. This figure is adopted from Helm et al. (2022).

Thereafter, the capsule cultures showed differences in the subpopulation development depending on whether serum was present in the capsule core. For encapsulated B cells, that had solely been rinsed with human serum (cells/capsules<sub>withoutserum</sub>), PC and GC cell contents peaked on day 2 of cultivation and decreased afterward. At the end of the culture (Day 9), approximately 65 % of the cells had preserved their memory cells phenotype, 22.6 % of the cells were GC cells and 11 % could be classified as PCs. The amount of PB was very low throughout cultivation (< 10 %). In the case of the cells encapsulated with 10 % (v/v) human serum in the capsule core (cells/capsules<sub>withserum</sub>), the amount of memory and GC cells decreased steadily after Day 2, reaching 15.5 and 11.6 %, respectively, at the end of the cultivation. Concomitantly, the amount of PC and PB increased about 4-fold (PC) and 20-fold (PB) higher than for the pre-coated cells (cells/capsules<sub>withoutserum</sub>) at the end of the cultivation.

The typical short-lived PC burst followed by an immediate decline in numbers was observed in the suspension culture and, to a lesser extent, for cells/capsules<sub>withoutserum</sub>. However, this was not the case when 10 % (v/v) human serum was present in the capsules' core (cells/capsules<sub>withserum</sub>). Therefore, the presence or absence of human serum within the capsule core had a steering effect on subtype development. A rinse with human serum before encapsulation seemed to prevent the encapsulated B cells from maturing fully into the PB and PC subclasses. The content of memory cells remained high, while a decrease of the CD20 expression (i.e., differentiation into antibody-secreting cells) in the CD38<sup>++</sup> population seemed to be hampered, indicating impaired PB and PC development. A high GC cell content was observed, but the simultaneous maintenance of a high level of memory cell phenotype indicates developmental arrest. The presence of human serum in the capsules' core (cells/capsules<sub>withserum</sub>) led to distinct differentiation behavior (i.e., accumulation of PB and PC cells and decrease of GC and memory cells). It is thus tempting to conclude that B cell maturation in capsules is influenced by some high molecular weight components found in human AB serum.

Interestingly, both encapsulation strategies promote the development of GC-type cells, which was not the case when the cells were cultivated in suspension even though identical volumetric concentrations of the relevant cytokines (i.e., CD40L, IL-21, IL-4, and BAFF) were used. This indicates the existence of so far unknown cell stimulatory mechanisms provided inside the SCS capsules. Autocrine conditioning of their

microenvironment by the B cells and/or matrix interactions are possible contributions. For instance, high expression of Syndecan 1 (CD138) is characteristic of PC. This surface marker is upregulated during differentiation from PB into PC (Sanderson et al. 1989) and was shown to play a direct role in PC survival *in vivo* via cell-matrix interaction (Reijmers et al. 2013). Heparan sulfate (HS), which has chemical similarities with the cellulose sulfate used for encapsulation, also plays a major role in this process (Thomas Groth et al. 2020). Therefore, it is tempting to assume that the steady increase in PC content, observed in the capsules, is promoted by the capsule material binding to PC and supporting their survival *in vitro*.

#### **4.3.6 Capsules Cultured in Base Medium with or Without Human AB Serum**

To save human serum, the suffice of capsules cultured in base medium without human AB serum was tested. The cultured capsules contained B cells and all described GF to support optimal B cell development and growth inside the capsules. Draining essential components in human AB serum by concentration gradient and simultaneous permeability through the capsule wall could deplete certain molecules inside the capsules. Adverse effects on B cells by such draining effects leading to depletion of these molecules or GF should be revealed. Additionally, this approach could further support restraining important GF inside the capsules and give further insight into MWCO for crucial components in our SCS-PDADMAC capsule culturing system.

B cells were precultured for 4 days and reseeded at  $0.1 \times 10^6$  cells/mL for suspension culture, while the rest were encapsulated at  $1 \times 10^6$  cells/mL<sub>capsule</sub>. One part of the capsules was cultured in base medium. The other half was cultured in base medium without human AB serum. Detailed results are shown in Appendix 2.

B cells cultured in suspension showed similar behavior to other suspension cultures. On day 10 of cultivation, few PC and GC cells were observed. 80.5 % of the cells showed PB phenotype, while 12.7 % retained memory cell phenotype. On day 14, 91.2 % of the cells in suspension culture showed PB phenotype, while 7.4 % retained memory cell phenotype. Compared to other suspension cultures, cells developed similarly till D10 and developed further toward PB phenotype afterward.

Capsules cultured without serum showed a less pronounced differentiation in comparison to capsules cultured in base medium with serum. PC population was not as pronounced due to lower CD38 expression and less CD20 downregulation. PB population was also less distinct due to reduced CD38 and CD20 downregulation.

However, both culturing approaches reduced memory cell content to roughly 5 % from D10 onwards, showcasing clear differentiation potential for both approaches. Additionally, both culturing approaches led to notable amounts of GC cells. From D0 to D3, both cultures increased their GC cell content by 20 %, reaching roughly 25 %. Afterward, the culture in base medium without human AB serum increased GC cell content further to 29.3 % on D5 and decreased afterward to 19.5 % on D14. Capsules cultured in base medium with human serum started decreasing in GC cell content after D3, reaching 9.1 % on D14. Overall, B cell differentiation was less pronounced in capsules cultured without serum. CD38 upregulation and CD20 reduction were hampered, leading to less pronounced PC and PB populations, while GC cell content was higher in capsules cultured in base medium without serum. However, this could be caused by hampered CD20 reduction caused by missing cues.

This indicates that some components in the serum can penetrate the capsule wall and get diluted inside the capsules by lower concentration outside. However, compared to capsules without human serum inside the capsules, both culturing approaches led to the development of GC cells, PC, PB and reduction of memory cells. For impeccable development, however, we recommend to culture capsules in base medium containing human AB serum to avoid depletion of unknown components present in the serum. Important GF like CD40L, IL-4, IL-21 and BAFF can always be added exclusively to the SCS before encapsulation, which already helps to save resources.

#### **4.3.7 SCS-PDADMAC Encapsulation with Different Quantities of CD40L**

As mentioned above, CD40L per cell contributes toward the expansion of B cells and could impact their differentiation. This explains different expansion potentials observed between suspension cultures and encapsulated cultures observed so far. As already stated, while the volumetric concentrations were identical, the amount of co-encapsulated cytokines per  $10^6$  cells was 10-fold lower inside the capsules compared to the suspension culture. In an attempt to improve the proliferation of the encapsulated cells, the CD40L concentration inside the capsules was increased by 10-fold to reach 4  $\mu\text{g}$  CD40L per  $10^6$  cells, thereby approaching the conditions in the suspension cultures.

The expansion of encapsulated cells with different quantities of CD40L inside the capsule core compared to a suspension culture was performed as part of S. B. Huang's work. Briefly, B cells encapsulated at standard volumetric CD40L

concentration reached a maximum concentration of  $1.6 \times 10^6$  cells/mg<sub>capsules</sub> five days after encapsulation. In comparison, a maximal cell density of  $3.6 \times 10^6$  cells/mg<sub>capsules</sub> was reached on day 6 post-encapsulation in the presence of 4  $\mu$ g CD40L per  $10^6$  cells. During the intense growth phase of cells encapsulated with 4  $\mu$ g CD40L per  $10^6$  cells, the growth rate was comparable with control cells grown in suspension (0.35 and 0.32 d<sup>-1</sup>, respectively). However, the length of maximal growth phase was shorter for encapsulated cells (three days vs. five days in suspension). Therefore, with a total of 3.6-fold expansion, the encapsulated culture with 4  $\mu$ g CD40L per  $10^6$  cells still did not reach the growth rates of the suspension cultivation (5.6-fold expansion). This is in accordance with the findings in Figure 16, where increased seeding density with an equal amount of CD40L per cell led to a lower expansion of B cells in suspension cultures. This might reflect that the amount of the other supplements (e.g., IL-4, IL-21, BAFF or serum) also need to be increased during the encapsulation process. Further, as discussed above, additional factors, with an MW larger than 10 kDa, cannot diffuse through the capsule membrane and their lack might also impair cellular proliferation.

Subclass analysis of B cells encapsulated with 4  $\mu$ g CD40L per  $10^6$  cells was also performed. A detailed figure showing the FC-data can be found in Appendix 3. Encapsulated B cells exhibited an increased tendency for differentiation toward GC cells compared to suspension, with the peak achieved on day 2 after encapsulation (> 35 %) followed by a decrease of the GC cell content over time. The PC content increased over time in encapsulated cells, while the PB content fluctuated throughout the experiment and the memory cell content decreased over time. In comparison, suspension cells exhibited little tendency for the development of GC cells (maximum 10 % on day 2 after encapsulation) while experiencing a PC burst (13 % on day 2) and a steady increase of PB content. Increasing the CD40L concentration inside the capsules slightly enhanced the development of the GC cell content.

#### **4.3.8 SCS-PDADMAC Encapsulation with or without Pre-Culture**

A cryopreserved B cell pool is the closest one can get to the original tissue. The pre-culture proposed above, prior to encapsulation, is beneficial, as it increases the biomass, but it also directs the B cells toward the PC burst typical for suspension cultures (Figure 38). To avoid any differentiation of B cells during the pre-culture, we tested the option to encapsulate the cells directly after thawing and compared their behavior to those encapsulated after pre-culture.

The expansion of encapsulated cells with or without pre-culture before encapsulation, compared to a suspension culture was performed as part of S. B. Huang's work. Briefly, cells encapsulated directly after thawing exhibited an extended lag phase before entering the exponential growth phase compared to pre-cultured B cells in capsules. This was explained by the already exponentially dividing cells after pre-culture, while cells after freezing need some time to recover. The stress of encapsulation occurring during the cells' vulnerable state, i.e., directly after thawing, may also have contributed to this. The observed elongated lag phase and the somewhat higher cell mortality on the day of encapsulation in the case of the directly encapsulated cells can be explained by this. Moreover, B cells encapsulated after pre-culture were supplied with fresh growth medium with the original cytokine content on the day of encapsulation. Cells directly encapsulated were not. Interestingly, cells encapsulated with or without pre-culture exhibited similar specific growth rates ( $\mu_{max}$ ), also leading to maximal cell densities in the same range (direct encapsulation:  $2.7 \times 10^6$  cells/mg<sub>capsules</sub>; post-pre-culture encapsulation:  $2 \times 10^6$  cells/mg<sub>capsules</sub>) (Helm et al. 2022).

Figure 42 shows the subpopulation development for encapsulated B cells with and without pre-culture after thawing. The memory and GC cell distribution show similar trends in both cases. The differences in terms of the number of cells in each population are most probably related to differentiation occurring during the four days of pre-culture, as shown above for non-encapsulated cells (Figure 38). After 10 days of cultivation, the memory cell content was notably reduced in both cultures (< 20 %) and the GC cells represented 20 to 25 % of the overall B cell population. Most pronounced differences were detected for the PB and PC subsets. Both cultures started with low PB and PC numbers. As expected, the pre-cultured cells exhibited a higher starting content (10–15 % vs. < 5 %) for both subpopulations. Whereas a direct encapsulation drove B cells toward the PB phenotype, encapsulation after pre-culture induced an apparent accumulation of PC in the capsules. This may indicate a methodological option for directing B cell differentiation in capsules. Pre-cultures would guide B cells toward PC development, while direct encapsulation can promote the development of PB and GC cells.

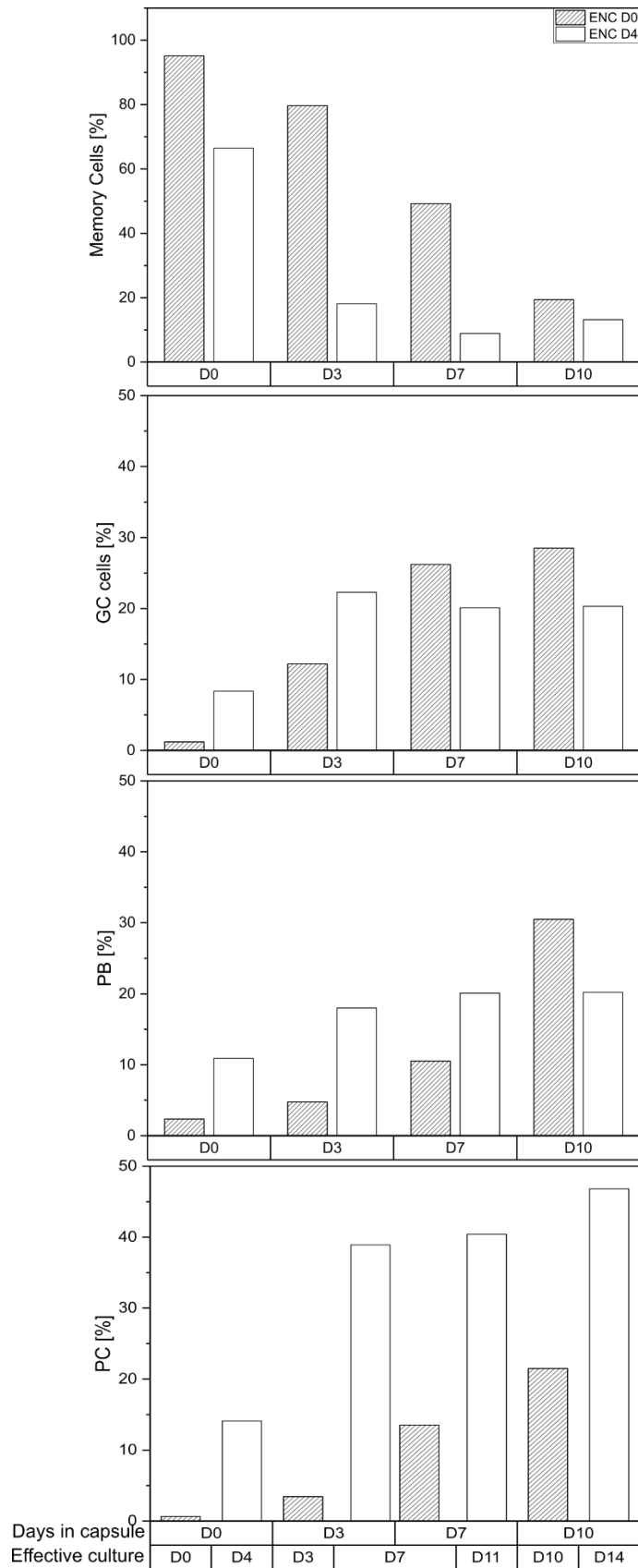


**Figure 42: Bar charts representing B cell subpopulations over 10 days in capsule culture with and without four days pre-culture prior to encapsulation. B cells were encapsulated at  $1 \times 10^6$  cells/mg<sub>capsules</sub> with 10 % (v/v) human serum (cells/capsules<sub>withserum</sub>) and standard GF concentrations ( $0.4 \mu\text{g}/\text{mg}_{\text{capsules}}$  and  $0.4 \mu\text{g}$  CD40L per  $10^6$  cells) in the capsules' core. The effective culturing time represents the overall duration of B cell culture after thawing. Days in capsule represents the actual time B cells were cultured inside capsules. This figure is adopted from Helm et al. (2022).**

### 4.3.9 Conclusion of Subclass Development in SCS-PDADMAC Capsules

In this section, we showed that it is possible to cultivate human primary tonsillar B cells in SCS-PDADMAC capsules, as previously only shown for T cells (Jérôme et al. 2017). Most importantly, such a cultivation system allows control of B cell subclass development *in vitro*, as summarized in Figure 43 for cultivation in suspension vs. capsules.

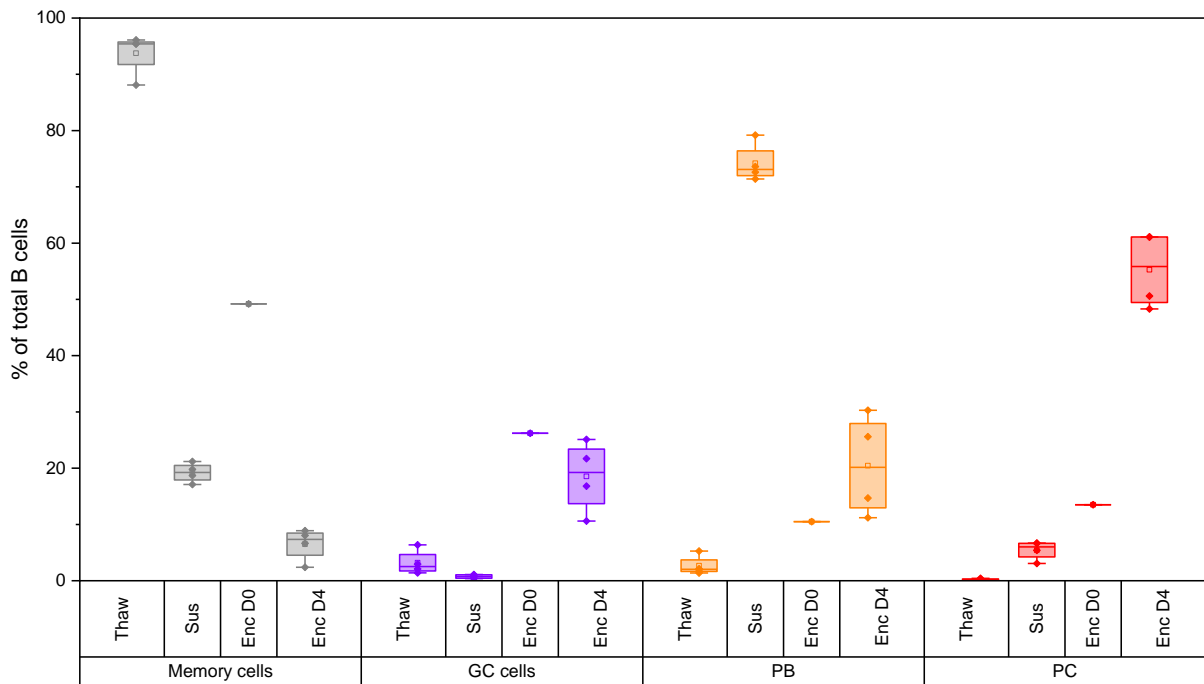


**Figure 43: B cell subsets development in suspension and encapsulated cultures. Grouped boxplots compare subpopulations of B cells straight after thawing (Thaw), on day 7 of encapsulated culture with (Enc D4) or without pre-culture (Enc D0) and suspension culture (Sus). Whiskers show the interquartile range. □: mean; -: Median; ◆: count for a specific donor. This figure is derived from Helm et al. (2022).**

In line with the tissue of origin used for cell isolation (i.e., tonsils), memory cells were most plentiful after thawing and steadily decreased independently of the cultivation types. GC cells were only observed in encapsulated cultures and tended to be more abundant when the cells were encapsulated directly after thawing. While PB accumulated in the suspension cultures, their count stayed moderate in the capsules. The most crucial aspect in this context is the PC subset development. Whereas suspension cultures only allowed a transient increase of PC (i.e., PC burst for 24 h), cultivation in SCS-PDADMAC capsules was accompanied by preservation of PC subsets for several days, especially when the cells were pre-cultured in suspension to induce their differentiation before encapsulation. Thus, cultivation in this polyelectrolytes-based capsule system might help to conduct controlled B cell differentiation in *in vitro* cultures without the necessity of adding specific costly cytokine



cocktails. In the future, such microcapsules could host improved organotypic GC development, supporting more tissue-like features than most other reported *in vitro* systems. Sufficient nutrient supply, conditioning of the microenvironment and mimicking of ECM are key features of this system. Finally, such an approach paves the way for the co-cultivation of multiple cell types involved in adaptive immunity. To conclude, microencapsulation of B cells is a promising method for improved GC reaction *in vitro*, bringing us one step closer to *ex vivo* immunization of human patients.

## 5 Outlook

Tonsils are a plentiful source of memory B cells, offering a unique advantage over other standard sources for B cells. They are readily available due to standard surgeries. They yield a significant amount of primary human cells with the addition of children and adults as possible donors, which is not offered when human blood is used. And other cell types can easily be isolated from tonsils in addition (e.g., T cells, FDC). This enables tonsils as an excellent source for developing co-culturing systems for the *in vitro* generation of immunogenic tissue-like structures while providing plenty of starting material. With the isolation method described in this work, we investigated different culturing methods for B cells, comparing adult child and blood derived B cells.

PWM is a well-established T cell-dependent B cell mitogen that can induce cellular proliferation in B cells. Its high availability and cheap costs make it an easy choice for researchers who want to expand their B cell starting pool. One has to keep in mind that the unspecific stimulation of B cells via PWM cannot induce B cell memory and is restricted to IgM secretion. We observed donor- and source-derived variations, which lowers the predictability of this stimulus. Proliferative response lowers with the donor age, while slight impurities with other cell types could alter proliferative outcome notably. Keeping these drawbacks in mind, PWM can serve as an inexpensive alternative for expanding or stimulating B cells and co-culturing with other immune cells. The media for this are described in detail and can be produced and adapted easily by others.

When specific or T-dependent stimulation and special features like immunological memory, CSR or SHM are desired, one should consider a system, exploiting CD40-CD40L interactions. With the here described media and culturing approaches, we offer an expansion platform described in detail and independent of feeder cells.

Access to feeder cell lines can be a problem for researchers, preventing them from applying such techniques. Our media and culturing approaches can be reproduced easily by others, opening the way for B cell expansion in a broader sense. In addition to expansion, slight changes in the media composition allow the stirred differentiation of B cells toward desired phenotypes and genetic programs. A memory pre-culture led to AID upregulation and CSR in B cells. This suggests the possibility of generating *in vitro* germinal center reactions by solely using soluble cytokines in suspension cultures of primary human tonsillar B cells. AID seemed to be upregulated only during the 4 days of memory pre-culture, indicating a comparatively low capacity to adapt immunity found *in vivo*. Future research could focus on elongated *in vitro* immunity protocols by adapting such cultures without IL-21. Cells for autologous B cell therapies or polyclonal antibodies could be produced with such protocols in the future.

However, the *in vivo* GC reaction between T- B- and follicular dendritic cells interacting in a closely packed tissue environment, leading to the selection and expansion of more potent antibody clones, is neglected in suspension systems. The here presented SCS-PDADMAC encapsulation is a novel platform for B cell cultures, mimicking such closely packed tissue environments. We were able to show retention of supplemented and autologous GF inside the capsules, while cellulose sulfate mimics functions of the ECM. At the same time, essential nutrients and metabolites can pass the capsule wall serving as a replacement for vascularization found in most tissues. Our microencapsulation unit can be produced cheaply, easily and fast by anyone with access to SLA 3D-printing, while necessary accessories are available in almost every lab. This, combined with the isolation protocol of tonsillar cells, lays the basis for future co-culturing systems for fully orchestrating immunologic adaptation and memory in the laboratory. FDC could serve as antigen-presenting cells to B cells, while B cells, in turn, would interact with T cells leading to CD40-CD40L engagement and cytokine secretion. These complex cellular interactions in the context of ECM-like structures and cytokine retention of SCS-PDADMAC capsules seem like the closest approximation to *in vivo* cultures one could get to date. This opens the way to alter the immunity of human patients outside the body, while maintaining the possibility of transferring cells back into the human body. Autologous B cell-based therapies could be based on this novel culturing platform and hold the potential to defeat certain diseases like HIV and most recently, covid-19.

## 6 List of Figures

- Figure 1: Schematic representation of the five immunoglobulin classes or isotypes in mammals. Each antibody consists of four polypeptides. Two heavy chains (green) and two light chains (yellow) joined to form a "Y" shaped molecule. Monomeric IgD, IgE, IgG, and the dimeric and pentameric forms of IgA and IgM are shown. This figure is adopted from Duarte (2016)..... 8**
- Figure 2: Antibody production in primary and secondary immune responses. Primary antibody responses are initially dominated by IgM, while secondary responses are dominated by elevated IgG. This figure is derived from Williams and Hussell (2012). ..... 9**
- Figure 3: Development of HSC toward mature B cells is defined by Ig rearrangements and negative selection of autoreactive B cells. After the transition from bone marrow to the periphery, mature naïve B cells migrate through the spleen into secondary lymphoid tissues. Some elements in the image have been obtained from Smart Servier Medical Art..... 10**
- Figure 4: The differentiation of mature naïve B cells upon antigen encounter. B cells can undergo unspecific (T-independent) or specific (T-dependent) activation. Unspecific activation leads to proliferation, PB differentiation and IgM secretion but is restricted to IgM and no affinity maturation occurs. Specific activation leads to the formation of GC, enabling affinity maturation and Ig class switch. B cells also differentiate into memory cells, PB and PC, enabling adaptive immunity. Some elements in the image have been obtained from Smart Servier Medical Art. .... 11**
- Figure 5: Surface receptor expression pattern for different developmental states of B cells from naïve B cells to PC. Some elements in the image have been obtained from Smart Servier Medical Art..... 18**
- Figure 6: The expression levels of major transcription factors during B cell differentiation. The height of the colored fields marks the expression level of Pax5 (green), AID (blue), IRF4 (orange) and Blimp-1 (red) over the different B cell stages. Some elements in the image have been obtained from Smart Servier Medical Art. .... 19**
- Figure 7: Schematic representation of a microcapsule, produced by polyelectrolyte complexation (PEC). Nutrients, oxygen, waste and metabolites cross the semipermeable membrane freely. Immune cells and antibodies are excluded, while autocrine and supplemented GF are entrapped. For semipermeable membrane formation, negative charges of anion polymer interact with positive charges of cation polymer, forming a PEC reaction. Some elements in the image have been obtained from Smart Servier Medical Art. .... 22**
- Figure 8: Overview of the isolation procedure for B cells from tonsils. Tonsillar tissue was minced and sieved to receive single cells for red blood cell lysis. After lysis, cells were separated via Ficoll density centrifugation to obtain a lymphocyte suspension containing T and B cells. Finally, B cells were purified via nylon wool column (Helm et al. 2021). .... 25**
- Figure 9: Gating strategy for the CFSE dilution assay analysis. Lymphocytes were gated via FSC vs. SSC and CFSE intensity was analyzed after. B cells of donor B3 on day 0 after CFSE staining (white) and after 12 days of cultivation without PWM (red) and with PWM (blue) are shown. Divided cells were defined as**

cells having undergone at least one round of division during the cultivation period, as evidenced by a reduced CFSE fluorescence.....	39
Figure 10: Left: Representative forward vs. side scatter plots for donors B3 (BC <sub>MACS</sub> ), A2 (NW-B <sub>adult</sub> ), and C4 (NW-B <sub>child</sub> ). For day 12, dot-plots of non-treated cells (control) and cells stimulated with 5 µg/mL PWM (PWM) are given. Right: Cell proliferation (i.e., percentage of divided cells) in the absence (dashed lines) and the presence (solid lines) of PWM. Data represent the percentage of divided cells in the Lymphocytes gate. This figure is adopted from Helm et al. (2021). .....	41
Figure 11: Gating of lymphocytes via FSC vs. SSC and subsequent gating of T and B cells via CD19 vs. CD3 expression. Shown are donor B2 before MACS and tonsillar B cells of A3 and C4 after FDG (before NW separation).....	43
Figure 12: Expression of CD markers in the various FS/SS subpopulations after 12 days of stimulation with PWM. Donors: A1-A3 and B1-B5. A: Representative FS/SS plots with the corresponding populations. Control: 12 days of cultivation without PWM. PWM: 12 days cultivation with 5 µg/mL PWM. The cells in the Lymphocyte gate were divided into three subpopulations (I, II, III) according to their scattering properties. B: Expression of CD markers in the various subpopulations. BC <sub>MACS</sub> : Flow-through fraction of the MACS column; NW-B: adherent fraction, mechanically eluted from the nylon wool column. Grey bars: control; white bars: PWM stimulated. Whiskers show the interquartile range. □: mean; -: Median; ♦: count for a specific donor. The graphs show the distribution of the CD 20, 27 and 38 markers in the B cells CD19 <sup>+</sup> -population after 12 days of PWM treatment (PWM) – For comparison, cells without PWM were used (Control). This figure is adopted from Helm et al. (2021). .....	45
Figure 13: Agarose gel of DNA, amplified by RT-qPCR with our 8 primers described in the method section. Cells of donor C2 were analyzed via RT-qPCR immediately after thawing. ....	47
Figure 14: Reference gene stability in B cells to select an endogenous control. For donor stability, 5 donors (C1, C2, A1, A4, A7) were tested immediately after thawing. For memory and ASC culture, samples were taken during medium change on days 0, 4, 8 and 11 of culture of two donors (C1, C2) .....	48
Figure 15: Effect of CSA and three different batches of human AB serum on B cell expansion in ASC expansion medium. 0.1 x 10 <sup>6</sup> B cells were cultured for up to 12 days and expansion was measured during batch culture. We used donor A7 for CSA testing and donor A5 for serum testing. ....	50
Figure 16: 3 assessment methods for B cell proliferation. (A) shows the total cell number after culture, and (B) shows the expansion, respecting cellular input. In contrast, (C) shows the expansion divided by the input amount of CD40L in µg, respecting input cells and CD40L. B cells of donor C1 were seeded in different densities with standard CD40L concentration (0.4 µg/mL) or corresponding CD40L per million cells in ASC expansion medium. Cell number was measured after 7 days in culture to observe B cell growth. ....	52
Figure 17: Influence of CD40L- and IL-21 on B cell expansion and viability after seven days of suspension cultivation with donor A1. 0.1 x 10 <sup>6</sup> B cells were seeded in 24-well plates in growth medium supplemented with A) the indicated amounts of CD40L and 20 ng/mL IL-21 and B) the indicated amounts of IL-21 and 0.4 µg/mL CD40L. Shown are the expansion factor (bars) and the viability (■). This figure is adopted from Helm et al. (2022). .....	54

Figure 18: Expansion of adult B cells in memory- and ASC expansion medium with varying CD40L concentration. Cells were cultured for 7 days without changing the medium (n = 3 replicates). .....	55
Figure 19: Phenotype of adult B cells from donor A3 in memory- and ASC expansion medium with varying CD40L concentration. Cells were cultured for 7 days without a change of medium. Memory cells were defined as CD27 <sup>+</sup> CD38 <sup>+</sup> , PB as CD27 <sup>+</sup> CD38 <sup>++</sup> and PC as CD27 <sup>++</sup> CD38 <sup>++</sup> . .....	56
Figure 20: Expansion and phenotype of child B cells in memory- and ASC expansion medium with varying CD40L concentration. B cells of donor C2 were cultured for 7 days without changing the medium (n = 3 replicates). Memory cells were defined as CD27 <sup>+</sup> CD38 <sup>+</sup> , PB as CD27 <sup>+</sup> CD38 <sup>++</sup> and PC as CD27 <sup>++</sup> CD38 <sup>++</sup> ... ..	57
Figure 21: Gene expression of B cells from donor C2 after 7 days of batch culture in memory- or ASC expansion medium. CD40L concentration was increased from 0 to 1.6 µg/mL. Gene up- or downregulation was calculated via $\Delta\Delta C_t$ -method compared to cells before culture and $\beta$ -actin as reference gene. ....	59
Figure 22: Dynamic expansion of donor C1 over the course of 8 days with different CD40L concentrations. The right graph shows the growth rate $\mu$ during the exponential phase between days 4 and 6. ....	62
Figure 23: Schematic illustration of the 3 different culturing approaches for B cell expansion. ....	63
Figure 24: B cell expansion and subclasses on day 4 of ASC and memory pre-culture, shown for 6 individual donors. Expansion was calculated from n = 3 experimental replicates, while subclasses were calculated from n=3 adults (A) or children (C). Memory cells were defined as CD27 <sup>+</sup> CD38 <sup>+</sup> , PB as CD27 <sup>+</sup> CD38 <sup>++</sup> and PC as CD27 <sup>++</sup> CD38 <sup>++</sup> . ....	64
Figure 25: Expansion of the 3 culturing approaches for each donor individually over the course of 11 – 22 days. Measurement for expansion was stopped, when cell number did not increase overnight or did not exceed doubling over a period of 3 days (n=3 replicates). ....	65
Figure 26: CD20 expression during Batch-, ASC- and memory pre-culture of tonsillar B cells derived from adults and children. (A) Exemplary histograms of ASC- and memory pre-cultured B cells of donor A4, showing the gates for CD20 <sup>++</sup> cells and CD20 <sup>+/-</sup> cells. Dark blue shows the CD20 expression before culture, while lighter blue shades indicate later points of culture. Mock staining (CD20 <sup>-</sup> ) is shown in white. (B) CD20 <sup>++</sup> percentage of adult or child-derived B cells during the 3 different culturing approaches (n=3 adults/children). ....	67
Figure 27: Subclass development during batch, ASC and memory pre-culture. Samples were taken during medium change (n=3 adults/children). Memory cells were defined as CD27 <sup>+</sup> CD38 <sup>+</sup> , PB as CD27 <sup>+</sup> CD38 <sup>++</sup> and PC as CD27 <sup>++</sup> CD38 <sup>++</sup> . ....	68
Figure 28: Gene-regulation of B cells from donor C2 during ASC- or memory pre-culture on days 0, 8 and 11. Gene up- or downregulation was calculated via $\Delta\Delta C_t$ -method in comparison to cells before culture and $\beta$ -actin as reference gene. ....	70
Figure 29: IgG, IgM and IgA concentration in cell culture supernatants determined via ELISA. Supernatants were collected on days 8 and 11 of ASC- and memory pre-culture of donor C2 and A5. Serum-derived Ig levels were not subtracted. Data group difference between culture day culturing method and donors was determined via three-way ANOVA with Bonferroni multiple comparison test (* p $\leq$ 0.05; ** p $\leq$ 0.01; *** p $\leq$ 0.001). ....	72

Figure 30: Expansion and CD20 <sup>++</sup> B cell content during Batch, ASC and memory pre-culture of blood derived B cells (B6). .....	74
Figure 31: Subclass development during batch, ASC and memory pre-culture of B6. Samples were taken at the start and during medium change on days 4, 8 and 11. Memory cells were defined as CD27 <sup>+</sup> CD38 <sup>+</sup> , PB as CD27 <sup>+</sup> CD38 <sup>++</sup> and PC as CD27 <sup>++</sup> CD38 <sup>++</sup> . .....	75
Figure 32: Gene-regulation of B cells from donor B6 during ASC- or memory pre-culture on days 0, 8 and 11. Gene up- or downregulation was calculated via $\Delta\Delta\text{Ct}$ -method in comparison to cells before culture and $\beta$ -actin as reference gene. ....	76
Figure 33: 3D-printable microencapsulation unit as full and sectional view. Technical dimensions are shown for the nozzle. This figure is adopted from Helm et al. (2022). ....	81
Figure 34: N <sub>2</sub> -Flow dependent size distribution of sodium alginate capsules hardened in calcium solution and size measurement via microscopy. Capsule size is shown for different N <sub>2</sub> -flows, 1 L/min (n=17 capsules), 2 L/min (n=20 capsules), 3 L/min (n=29 capsules) and 4 L/min (n= 32 capsules). Data group difference was determined via one-way ANOVA with Bonferroni multiple comparison test (***) p<0.001). ....	82
Figure 35: SCS-PDADMAC capsule characterization. A: Diffusion of resorufin (0.229 kDa) into capsules characterized by a decreasing concentration in the supernatant. B: Vitamin B12 (1.35 kDa) diffusion into capsules characterized by decreasing concentration in the supernatant. This figure is adopted from Helm et al. (2022). ....	83
Figure 36: Histogram of B cells analyzed with flow cytometry regarding their CD27 expression. B cells incubated in PBS (solid black line) and incubated in 1 % (w/v) cellulase (dotted black line) are presented. Mock staining is shown in grey. This figure is adopted from Helm et al. (2022). ....	84
Figure 37: Gating strategy for B cells. B cells in suspension culture (top panel), encapsulated B cells (bottom panel). Prior to subclass analysis, the lymphocyte population was identified (left panel) and B cells were gated via CD19 expression (white histogram in the middle panel and mock staining in grey). B cells were then divided into subclasses via CD20 and CD38 expression to distinguish between memory cells, germinal center (GC) cells, PB and PC, shown in the dot plot on the right. This figure is derived from Helm et al. (2022). ....	85
Figure 38: Development of four individual suspension cultures derived from independent cryovials (identical donor). On day 4, cells were reseeded at 0.1 x 10 <sup>6</sup> cells/mL in fresh medium. In all cases, the viability was consistently above 90 %. B cells were gated as described for cells cultured in suspension in the previous chapter. This figure is adopted from Helm et al. (2022). ....	87
Figure 39: Depiction of the encapsulation process for primary tonsillar human B cells. Also shown is the PEC, forming the capsule membrane. This figure is adopted from Helm et al. (2022). ....	88
Figure 40: Microscopic image of SCS-PDADMAC capsules with B cells inside. Representative capsules directly after encapsulation (A) and after 11 days of cultivation (with arrows pointing to aggregates) (B). All images were taken at 10x magnification. This figure is derived from Helm et al. (2022). ....	90
Figure 41: B cell subpopulation development for encapsulated cells compared to those cultivated in suspension. Day -4 refers to the day of thawing. Day 0 to Day 9 refer to the days of cultivation post-	

encapsulation or post-inoculation at  $0.1 \times 10^6$  cells/mL for the suspension culture. For each measurement, either one well of suspension culture of a 24-well plate was harvested or capsules were drawn and cells released by cellulase treatment. For flow cytometry measurements, 80,000 events were analyzed. This figure is adopted from Helm et al. (2022). ..... 91

**Figure 42:** Bar charts representing B cell subpopulations over 10 days in capsule culture with and without four days pre-culture prior to encapsulation. B cells were encapsulated at  $1 \times 10^6$  cells/mg<sub>capsules</sub> with 10 % (v/v) human serum (cells/capsules<sub>withserum</sub>) and standard GF concentrations ( $0.4 \mu\text{g}/\text{mg}_{\text{capsules}}$  and  $0.4 \mu\text{g}$  CD40L per  $10^6$  cells) in the capsules' core. The effective culturing time represents the overall duration of B cell culture after thawing. Days in capsule represents the actual time B cells were cultured inside capsules. This figure is adopted from Helm et al. (2022). ..... 97

**Figure 43:** B cell subsets development in suspension and encapsulated cultures. Grouped boxplots compare subpopulations of B cells straight after thawing (Thaw), on day 7 of encapsulated culture with (Enc D4) or without pre-culture (Enc D0) and suspension culture (Sus). Whiskers show the interquartile range. □: mean; -: Median; ◆: count for a specific donor. This figure is derived from Helm et al. (2022). ..... 98

## 7 List of Tables

Table 1: Donor list for blood derived B cells. ....	24
Table 2: Donor list for child-derived tonsillar B cells.....	26
Table 3: Donor list for adult-derived tonsillar B cells. ....	26
Table 4: Composition of media for unspecific B cell stimulation with PWM .....	27
Table 5: Composition of media for specific B cell stimulation with CD40L .....	27
Table 6: Sequences of used primer for RT-qPCR. Primers were stored at -20 °C at 100 μM and diluted with PCR water to 10 μM before use.....	32
Table 7: Percentages of divided cells in FS/SS sub-populations after 12 days of cultivation with PWM as mitogenic stimulus. Bold fonts highlight donors, proliferating best under PWM stimulation (Helm et al. 2021).....	42
Table 8: T cells and B cells distribution after 12 days of cultivation with PWM as mitogenic stimulus. Cells were cultivated for 12 days in the presence of 5 μg/mL PWM. CD19 <sup>+</sup> (B cell), CD3 <sup>+</sup> (T cell) and CD19 <sup>-</sup> CD3 <sup>-</sup> cell distribution was determined by bicolor immunostaining and flow cytometry ('Lymphocyte' gate). Bold fonts highlight donors proliferating best under PWM stimulation (Helm et al. 2021). ....	44
Table 9: Used Buffers and Solutions .....	111
Table 10: Used Cell Culture Supplements .....	112
Table 11: Used Chemicals, Reagents and Kits .....	113
Table 12: Used Accessories.....	116
Table 13: Used Devices and Equipment.....	117
Table 14: Used Software .....	119



## **8 List of Abbreviations**

<b>AB</b>	<b>Antibody</b>
<b>AID</b>	<b>Activation-induced deaminase</b>
<b>AIDS</b>	<b>Acquired Immunodeficiency Syndrome</b>
<b>ALP</b>	<b>Alkaline phosphatase</b>
<b>ANOVA</b>	<b>Analysis of variance</b>
<b>APC</b>	<b>Allophycocyanin</b>
<b>ASC</b>	<b>Antibody secreting cells</b>
<b>BAFF</b>	<b>B cell activating factor</b>
<b>BCR</b>	<b>B cell receptor</b>
<b>Blimp-1</b>	<b>B lymphocyte–induced maturation protein-1</b>
<b>BSA</b>	<b>Bovine serum albumin</b>
<b>C</b>	<b>Constant gene region of Ig</b>
<b>CAD</b>	<b>Computer-Aided Design</b>
<b>CD</b>	<b>Cluster of differentiation</b>
<b>cDNA</b>	<b>Copy DNA</b>
<b>CFSE</b>	<b>Carboxyfluorescein succinimidyl ester</b>
<b>CSA</b>	<b>Cyclosporin A</b>
<b>CSR</b>	<b>Class switch recombination</b>
<b>Ct</b>	<b>Cycle threshold</b>
<b>Cy7</b>	<b>Cyanine7</b>
<b>D</b>	<b>Diversity gene region of Ig</b>
<b>DMSO</b>	<b>Dimethyl sulfoxide</b>
<b>DNA</b>	<b>Deoxyribonucleic acid</b>
<b>DZ</b>	<b>Dark zone</b>

<b>ECM</b>	<b>Extracellular matrix</b>
<b>EDTA</b>	<b>Ethylenediaminetetraacetic acid</b>
<b>ELISA</b>	<b>Enzyme-linked Immunosorbent Assay</b>
<b>FC</b>	<b>Flow cytometry</b>
<b>FCS</b>	<b>Fetal calf serum</b>
<b>FDC</b>	<b>Follicular dendritic cells</b>
<b>FITC</b>	<b>Fluorescein-5-isothiocyanate</b>
<b>FS</b>	<b>Forward scatter</b>
<b>GAPDH</b>	<b>Glycerinaldehyd-3-phosphate-Dehydrogenase</b>
<b>GC</b>	<b>Germinal center</b>
<b>gDNA</b>	<b>Genomic DNA</b>
<b>GF</b>	<b>Growth factor</b>
<b>GOI</b>	<b>Gene of interest</b>
<b>HBSS</b>	<b>Hank's Balanced Salt Solution</b>
<b>H chain</b>	<b>Heavy chain</b>
<b>HIV</b>	<b>Human immunodeficiency virus</b>
<b>HPRT</b>	<b>Hypoxanthine-guanine-phosphoribosyltransferase</b>
<b>HS</b>	<b>Heparan sulfate</b>
<b>HSC</b>	<b>Hematopoietic stem cells</b>
<b>Ig</b>	<b>Immune globulin</b>
<b>IL</b>	<b>Interleukin</b>
<b>IMDM</b>	<b>Iscove's Modified Dulbecco Medium</b>
<b>IRF4</b>	<b>Interferon regulatory factor 4</b>
<b>ITS</b>	<b>Insulin Transferrin Selenite</b>

<b>J</b>	<b>Joining gene region of Ig</b>
<b>LZ</b>	<b>Light zone</b>
<b>MACS</b>	<b>Magnetic Activated Cell Sorting</b>
<b>MHC</b>	<b>Major histocompatibility complex</b>
<b>min</b>	<b>Minutes</b>
<b>MWCO</b>	<b>molecular weight cut-off</b>
<b>NW</b>	<b>Nylon wool</b>
<b>PAMP</b>	<b>Pathogen associated molecular pattern</b>
<b>Pax5</b>	<b>Paired box protein 5</b>
<b>PB</b>	<b>Plasmablast</b>
<b>PBS</b>	<b>Phosphate-buffered saline</b>
<b>PC</b>	<b>Plasma cell</b>
<b>PCR</b>	<b>Polymerase chain reaction</b>
<b>PDADMAC</b>	<b>poly-diallyl-dimethyl-ammonium chloride</b>
<b>PE</b>	<b>Phycoerythrin</b>
<b>PEC</b>	<b>Polyelectrolyte complexation</b>
<b>pNPP</b>	<b>para-Nitrophenylphosphate</b>
<b>PRR</b>	<b>Pattern recognition receptor</b>
<b>PWM</b>	<b>Pokeweed mitogen</b>
<b>Rev</b>	<b>Reference gene</b>
<b>RGD</b>	<b>Arginylglycylaspartic acid</b>
<b>RNA</b>	<b>Ribonucleic acid</b>
<b>RT</b>	<b>Reverse transcription</b>
<b>RT-qPCR</b>	<b>Real-time quantitative polymerase chain reaction</b>
<b>s</b>	<b>seconds</b>

<b>SAIDS</b>	<b>Space AIDS</b>
<b>SCS</b>	<b>Sodium cellulose sulfate</b>
<b>SHM</b>	<b>Somatic hypermutation</b>
<b>SiNP</b>	<b>Silicate nanoparticles</b>
<b>SS</b>	<b>Side scatter</b>
<b>StDev</b>	<b>Standard deviation</b>
<b>STL</b>	<b>Stereolithography</b>
<b>TAE</b>	<b>TRIS-Acetate-EDTA</b>
<b>Td</b>	<b>T cell-dependent</b>
<b>Th</b>	<b>T helper cell</b>
<b>TLR</b>	<b>Toll-like receptor</b>
<b>TRIS</b>	<b>Tris(hydroxymethyl)aminomethane</b>
<b>UV</b>	<b>Ultraviolet</b>
<b>V</b>	<b>Variable gene region of Ig</b>

## 9. Materials, Devices and Software

### 9.1 Buffers and Solutions

Table 9: Used Buffers and Solutions

Buffer/Solution	Constitution
Buffer 1	HBSS; 100 U/mL penicillin; 100 µg/mL Streptomycin; 2.5 µg/mL amphotericin B; 2 mM EDTA; 0.5 (w/v) BSA
Buffer 2	HBSS; 10 % (v/v) heat-inactivated FCS
CaCl <sub>2</sub> -solution for Alginate Encapsulation	90 mM CaCl <sub>2</sub> ; 154 mM NaCl; 0.02 vol% Tween 20
Cellulase solution for SCS capsule release	PBS pH 7.4; 1 % (w/v) Cellulase
Dilution Buffer for C(GF-Stock) ≤ 0.1 mg/mL	PBS; 0.1 % (w/v) BSA
Freezing solution	90 % FCS, 10 % DMSO
PBS pH 7.4 (for cell culture)	137 mM NaCl; 2.7 mM KCl; 12 mM HPO <sub>4</sub> <sup>2-</sup> ; 12 mM H <sub>2</sub> P0 <sub>4</sub> <sup>-</sup> ; pH 7.4
PBS pH 6.3 (for encapsulation and FC)	137 mM NaCl; 2.7 mM KCl; 12 mM HPO <sub>4</sub> <sup>2-</sup> ; 12 mM H <sub>2</sub> P0 <sub>4</sub> <sup>-</sup> ; pH 6.3
PDADMAC-solution for SCS Encapsulation	PBS pH 6.3; 1.8 (w/v) SCS; 0.02 vol% Tween 20
Red Blood Cell (RBC) Lysis Buffer (ery lysis-buffer)	15.5 mM NH <sub>4</sub> Cl; 1 mM KHCO <sub>3</sub> ; 0.01 mM EDTA
TAE-Buffer	40 mM TRIS; 20 mM acetic acid; 1 mM EDTA, pH 8.3

## 9.2 Cell Culture Supplements

Table 10: Used Cell Culture Supplements

Supplement	Specification	Order no.	Manufacturer	Location
<b>Amphotericin B</b>	250 µg/mL Solution	A 2612	Biochrom GmbH	Berlin, Germany
<b>Amphotericin B</b>	250 µg/mL Solution	30-003-CF	Corning Incorporated	Corning, New York, USA
<b>Cyclosporin A</b>	Ready-made solution 1 mg/mL in DMSO	SML1018	Sigma-Aldrich (Merck KGaA)	Darmstadt, Germany
<b>Cyclosporin A</b>	Powder 98.5 % (HPLC) dissolved in DMSO 1 mg/mL	30024- 25MG	Sigma-Aldrich (Merck KGaA)	Darmstadt, Germany
<b>FCS</b>	Not from USA (sterile- filtered)	F7524- 500ML	Sigma-Aldrich (Merck KGaA)	Darmstadt, Germany
<b>FCS</b>	South America, low endotoxin (sterile- filtered)	S1860-500	Biowest SAS	Nuaillé, France
<b>IMDM</b>	(sterile-filtered)	11500556	Fisher Scientific (ThermoFisher Scientific)	Waltham, Massachusetts, USA
<b>Human AB Serum</b>	Batch 1: SLCB2586 Batch 2: SLBX6357 Batch 3: SLCF0679 Batch 4: SLCF0698 Batch 5: SLCF0253	H4522	Sigma-Aldrich (Merck KGaA)	Darmstadt, Germany
<b>Human IL-4</b>	Working-Stock (0.05 µg/µL) Batch 1: 5210108306 Batch 2: 5210902857	130-093-921	Miltenyi Biotec B.V. & Co. KG	Bergisch Gladbach, Germany
<b>Human IL-10</b>	Working-Stock (0.01 µg/µL) Batch: 5200600858	130-093-947	Miltenyi Biotec B.V. & Co. KG	Bergisch Gladbach, Germany
<b>Human IL-21</b>	Working-Stock (0.01 µg/µL) Batch 1: 5200601452 Batch 2: 5201007324 Batch 3: 5210204655 Batch 4: 5210406353 Batch 5: 5210605512 Batch 6: 5210904646	130-095-768	Miltenyi Biotec B.V. & Co. KG	Bergisch Gladbach, Germany
<b>Human BAFF</b>	Working-Stock (0.001 µg/mL) Batch 1: 5200601451 Batch 2: 5201007318 Batch 3: 5210204062 Batch 4: 5210902802 Batch 5: 5210910386	130-093-806	Miltenyi Biotec B.V. & Co. KG	Bergisch Gladbach, Germany

<b>Human CD40L</b>	Working-Stock (0.1 µg/µL) Batch 1: 5200601453 Batch 2: 5201007325 Batch 3: 5210411136 Batch 4: 5210902804 Batch 5: 5210910386	130-096-713	Miltenyi Biotec B.V. & Co. KG	Bergisch Gladbach, Germany
<b>Human CD40L</b>	Batch: 148500000	34-8902-81	eBioscience	San Diego, California, USA
<b>INSULIN-TRANS-SEL-G (ITS-G)</b>	100X	41400045	Fisher Scientific (ThermoFisher Scientific)	Waltham, Massachusetts, USA
<b>Penicillin/ Streptomycin</b>	10.000 U/mL 10.1000 µg/mL	A2213	Biochrom GmbH	Berlin, Germany
<b>Penicillin/ Streptomycin</b>	10.000 U/mL 10.1000 µg/mL	DE17-602E	Lonza Group Ltd	Basel, Switzerland
<b>PWM</b>	0.5 mg/mL in PBS	L8777	Sigma-Aldrich (Merck KGaA)	Darmstadt, Germany
<b>Resveratrol</b>	2 µmol/ml in DMSO	R5010	Sigma-Aldrich (Merck KGaA)	Darmstadt, Germany
<b>RPMI-1640</b>	w/o L-Glutamine	BE12-167F	Lonza Group Ltd	Basel, Switzerland
<b>rhIL-2</b>	200 µg/mL, Batch 5090703	554603	BD Bioscience	Heidelberg, Germany
<b>Ultraglutamine<sup>TM</sup></b>	Stable Glutamine 200 mM (100x)	BE17- 60E/U1	Lonza Group Ltd	Basel, Switzerland

### 9.3 Chemicals, Reagents and Kits

Table 11: Used Chemicals, Reagents and Kits

Material	Specification	Order no.	Manufacturer	Location
<b>Acridine Orange/ Propidium Iodide Stain Cell Viability Kit</b>	-	F23001	Logos Biosystems	Gyeonggi-do, South corea
<b>Agarose</b>	-	BIO-41029	Meridian Bioscience	Memphis, Tennessee, USA
<b>Anti-human CD3-PE Antibody</b>	Mouse, Clone HIT3a	555340	BD Bioscience	Heidelberg, Germany
<b>Anti-human CD3-PE Antibody</b>	Mouse, Clone OKT3	317308	Biolegend	San Diego, California, USA
<b>Anti-human CD19- APC Antibody</b>	Mouse, Clone HIB19	302212	Biolegend	San Diego, California, USA
<b>Anti-human CD20-PE Antibody</b>	Mouse, Clone 2H7	302306	Biolegend	San Diego, California, USA
<b>Anti-human CD27- PE/Cy7 Antibody</b>	Mouse, Clone M-T271	356412	Biolegend	San Diego, California, USA

<b>Anti-human CD38-FITC Antibody</b>	Mouse, Clone HB-7	356610	Biologend	San Diego, California, USA
<b>BSA</b>	≥ 98 %, Biotinfree, Batch nr. 02892831	0163.2	Carl Roth GmbH + Co. KG	Karlsruhe, Germany
<b>Cellulase Cellulysin®</b>	Trichoderma viride	219466-50	VWR International GmbH	Darmstadt, Germany
<b>CFSE</b>	5 mM in DMSO dissolved from powder and sterile filtered	21888-25MG-F	Sigma-Aldrich (Merck KGaA)	Darmstadt, Germany
<b>Coulter Clenz</b>	-	8448222	Beckmann Coulter GmbH	Krefeld, Germany
<b>CuCl<sub>2</sub></b>	-	307-483	Sigma-Aldrich (Merck KGaA)	Darmstadt, Germany
<b>DMSO</b>	Steril-filtered	D2438-50ML	Sigma-Aldrich (Merck KGaA)	Darmstadt, Germany
<b>DNA-Primers</b>	Freeze-dried	Sequence	Microsynth	Balgach, Switzerland
<b>DPBS</b>	w/o Ca <sup>2+</sup> /Mg <sup>2+</sup>	L1825	Biochrom GmbH	Berlin, Germany
<b>DPBS</b>	w/o Ca <sup>2+</sup> /Mg <sup>2+</sup>	BE17-512Q	Lonza Group Ltd	Basel, Switzerland
<b>ELISA Wash Buffer</b>	-	421601	Biologend	San Diego, California, USA
<b>EDTA</b>	-	10305	Grüssing GmbH	Filsum, Germany
<b>Acetic acid</b>	-	A/0400/PB15	Fisher Scientific (ThermoFisher Scientific)	Waltham, Massachusetts, USA
<b>Ethanol</b>	-	20.821.310	VWR International GmbH	Darmstadt, Germany
<b>HBSS</b>	w/o Ca <sup>2+</sup> /Mg <sup>2+</sup> and Phenolred	L 2045	Biochrom GmbH	Berlin, Germany
<b>Human IgA ELISA kit (ALP)</b>	for 6 plates	MAB-3860-1AD-6	Mabtech AB	Nacka Strand, Sweden
<b>Human IgG ELISA kit (ALP)</b>	for 6 plates	MAB-3850-1AD-6	Mabtech AB	Nacka Strand, Sweden
<b>Human IgM ELISA kit (ALP)</b>	for 6 plates	MAB-3880-1AD-6	Mabtech AB	Nacka Strand, Sweden
<b>HyperLadder™</b>	1 kb	BIO-33026	Meridian Bioscience	Memphis, Tennessee, USA
<b>Isopropyl alcohol</b>	-	33539-1L-M	Sigma-Aldrich (Merck KGaA)	Darmstadt, Germany
<b>KHCO<sub>3</sub></b>	-	120291000U	Grüssing GmbH	Filsum, Germany
<b>LSM 1077 Lymphocyte Separation Medium</b>	-	J15-004	PAA Laboratories GmbH	Paschin, Austria



<b>MACSxpress Whole Blood B Cell Isolation Kit, human</b>	-	130-098-190	Miltenyi Biotec B.V. & Co. KG	Bergisch Gladbach, Germany
<b>NaCl</b>	-	27810295	VWR International GmbH	Darmstadt, Germany
<b>NaHCO<sub>3</sub></b>	-	HN01.1	Carl Roth GmbH + Co. KG	Karlsruhe, Germany
<b>NaOH</b>	-	CN30.3	Carl Roth GmbH + Co. KG	Karlsruhe, Germany
<b>NH<sub>4</sub>Cl</b>	-	1.011.451.000	Merck KGaA	Darmstadt, Germany
<b>NaCS (SCS)</b>	charge ME45	-	Sykestek GmbH	Erlangen, Germany
<b>OneComp eBeads</b>	-	01-1111-41	Fisher Scientific (ThermoFisher Scientific)	Waltham, Massachusetts, USA
<b>PCR-Water</b>	-	W4502-10X50ML	Sigma-Aldrich (Merck KGaA)	Darmstadt, Germany
<b>PDADMAC</b>	20 % (w/v)	SIAL409022-25ML	VWR International GmbH	Darmstadt, Germany
<b>peqGREEN</b>	DANN/RNA-Staining 20000 X	732-3196	Peqlab (VWR international GmbH)	Darmstadt, Germany
<b>pNPP ELISA substrate</b>	-	MAB-3652-P10	Mabtech AB	Nacka Strand, Sweden
<b>Propidiumiodide</b>	1.0 mg/mL in H <sub>2</sub> O	P4864-10ML	Sigma-Aldrich (Merck KGaA)	Darmstadt, Germany
<b>PWM</b>	-	L8777	Sigma-Aldrich (Merck KGaA)	Darmstadt, Germany
<b>Resveratrol</b>	-	R5010	Sigma-Aldrich (Merck KGaA)	Darmstadt, Germany
<b>Rneasy Mini Kit</b>	50 Isolations	74104	Qiagen	Hilden, Germany
<b>QuantiTect Rev. Transcription Kit</b>	50 Transcriptions	205311	Qiagen	Hilden, Germany
<b>SDS</b>	-	CN30.3	Carl Roth GmbH + Co. KG	Karlsruhe, Germany
<b>Supermix for PCR</b>	10 x 25 mL	733-1254	VWR International GmbH	Darmstadt, Germany
<b>Superblock Blocking-buffer</b>	in PBS	13434299	Fisher Scientific (ThermoFisher Scientific)	Waltham, Massachusetts, USA
<b>TRIS</b>	-	2449.2	Carl Roth GmbH + Co. KG	Karlsruhe, Germany
<b>TRIS-HCl</b>	-	2449.2	Carl Roth GmbH + Co. KG	Karlsruhe, Germany
<b>TWEEN® 20</b>	-	P1379-100ML	Sigma-Aldrich (Merck KGaA)	Darmstadt, Germany

## 9.4 Accessories

Table 12: Used Accessories

Material	Modell	Order no.	Manufacturer	Location
2-way valve	-	Feb 50	neoLab Migg GmbH	Heidelberg, Germany
Cell Culture Dish	100/20 mm	664970	Greiner Bio-One	Frickenhausen, Germany
Cell culture Plates	6 - Well 12-Well 24-Well 48-Well	604181 606180 607180 760180	Greiner Bio-One	Frickenhausen, Germany
Cell strainer	Easy Strainer 70 µm	542070	Greiner Bio-One	Frickenhausen, Germany
Centrifuge-Tube	15 mL 50 mL	188271 227270	Greiner Bio-One	Frickenhausen, Germany
Cryogenic Storage Vials	1.2 mL (Free-standing)	479-1254	VWR International GmbH	Darmstadt, Germany
ELISA plates	96 Well	ALEXADI-80-0144	VWR International GmbH	Darmstadt, Germany
MICROPLATE, 96 WELL	96 Well	655101	Greiner Bio-One	Frickenhausen, Germany
Micro reaction tube	1.5 mL	72.690.001	Sarstedt AG & Co. KG	Nümbrecht, Germany
Micro reaction tube	2 mL	0030 120.094	Eppendorf AG	Hamburg, Germany
Nylon Wool Fiber	-	18369-10	Polysciences, Inc.	Warrington, Pennsylvania, USA
PCR, Low Profile Reaction Plates	-	1329098	Fisher Scientific (ThermoFisher Scientific)	Waltham, Massachusetts, USA
Pipette tips	0.5 - 20 µL 2 - 20 µL 50 - 100 µL	732024 732028 732012	Brand GmbH + Co. KG	Wertheim, Germany
Pipette (Serological)	1 mL 5 mL 10 mL 25 mL	604181 606180 607180 760180	Greiner Bio-One	Frickenhausen, Germany
Silicone tubing	VMQ; 3 mm 1 mm	-	Deutsch & Neumann	Berlin, Germany
Syringe Filter	0.2 µm Celluloseacetate	514-0061	VWR International GmbH	Darmstadt, Germany
Syringe (Injekt® Solo; Luer)	20 mL	4606205V	B. Braun SE	Melsungen, Germany
Syringe (Injekt® Solo; Lock)	2 mL	4606701V	B. Braun SE	Melsungen, Germany

<b>Ultra clear cap strip for PCR</b>	-	1313638	Fisher Scientific (ThermoFisher Scientific)	Waltham, Massachusetts, USA
<b>Wipes</b>	Kimtech	115-2074	VWR International GmbH	Darmstadt, Germany

## 9.5 Devices and Equipment

**Table 13: Used Devices and Equipment**

<b>Device</b>	<b>Modell</b>	<b>Order no.</b>	<b>Manufacturer</b>	<b>Location</b>
<b>Autoclave (Table)</b>	3850 EL	-	Systec GmbH	Linden, Germany
<b>Autoclave (Standing)</b>	V150	-	Systec GmbH	Linden, Germany
<b>Automated Cell counter</b>	LUNA-FLTM Dual Fluorescence Cell Counter	-	Logos Biosystems	Gyeonggi-do, South Korea
<b>Centrifuge</b>	Sorvall LYNX6000	-	Thermo Scientific (Thermo Fisher Scientific)	Waltham, Massachusetts, USA
<b>Centrifuge</b>	Multifuge 3 S-R	-	Heraeus	Hanau, Germany
<b>Centrifuge</b>	Biofuge pico	-	Heraeus	Hanau, Germany
<b>CO2 Incubator</b>	BBD 6220	-	Thermo Scientific (Thermo Fisher Scientific)	Waltham, Massachusetts, USA
<b>CO2 Incubator</b>	Thermo Forma Direct Heat CO2 Incubator Model 311	-	Thermo Scientific (Thermo Fisher Scientific)	Waltham, Massachusetts, USA
<b>Cryogenic Cell Bank</b>	Cryo 200	-	Thermo Electron Corporation	Waltham, Massachusetts, USA
<b>Dishwasher</b>	Professional G 7883	-	Miele & Cie. KG	Güterslohe, Germany
<b>Flow cytometer</b>	Cytomics FC500	-	Beckmann Coulter GmbH	Krefeld, Germany
<b>Freezer (-20 °C)</b>	Liebherr Comfort	-	Liebherr-International AG	Bulle, Switzerland
<b>Freezing container</b>	Mr. Frosty	-	Thermo Scientific (Thermo Fisher Scientific)	Waltham, Massachusetts, USA
<b>Fridge (4 °C)</b>	Liebherr profi line	-	Liebherr-International AG	Bulle, Switzerland
<b>Form 3 SLA printer</b>	-	PKG-F3-WSVC-BASIC	Formlabs	Somerville, Massachusetts, USA
<b>Form Cure</b>	UV-Post-curing	FH-CU-01	Formlabs	Somerville, Massachusetts, USA
<b>Gel documentation imaging system</b>	Quantum CX5	-	Vilber Lourmat	Eberhardzell, Germany
<b>Gel-Electrophoresis-Chamber</b>	40-1214	-	Peqlab (VWR International GmbH)	Darmstadt, Germany
<b>Gel-Electrophoresis-Voltage-supply</b>	E835	-	Consort bvba	Turnhout, Belgium
<b>Glas-Beaker</b>	50 mL; 100 mL; 250 mL	-	Eppendorf AG	Hamburg, Germany
<b>Glas-Bottles</b>	100 mL; 250 mL; 500 mL; 1 L; 2 L	-	Eppendorf AG	Hamburg, Germany
<b>Heat-Block</b>	ThermoMixer F1.5	-	Eppendorf AG	Hamburg, Germany
<b>Laminar Flow Hood</b>	Mobilien W90 Variolab Typ SWB	-	Waldner	Wangen, Germany

<b>MACSmix Tube Rotator</b>	-	130-090-753	Miltenyi Biotec B.V. & Co. KG	Bergisch Gladbach, Germany
<b>MACSxpress Separator</b>	-	130-098-308	Miltenyi Biotec B.V. & Co. KG	Bergisch Gladbach, Germany
<b>Magnetic Stirrer</b>	RCT basic	-	IKA®-Werke GmbH & CO. KG	Staufen, Germany
<b>Membrane-Vakuum Pump</b>	AP 04	-	Hettich Benelux B.V.	Geldermalsen, Netherlands
<b>Microscope (Inverse)</b>	Primovert with Axiocam 105 color	-	Carl Zeiss Microscopy Deutschland GmbH	Oberkochen, Germany
<b>Microscope (Inverse)</b>	CKX41	-	Olympus	Hamburg, Germany
<b>Millipore water supply</b>	Synergy Water Purification System	-	Merck Millipore (Merck KGaA)	Darmstadt, Germany
<b>Minishaker</b>	MS2	-	IKA®-Werke GmbH & CO. KG	Staufen, Germany
<b>Orbital Shaker</b>	Noctua K30	-	Thermo Scientific (Thermo Fisher Scientific)	Waltham, Massachusetts, USA
<b>Pipette controller</b>	-	-	Integra Biosciences	Zizers, Switzerland
<b>Pipette</b>	Research plus 0.5 - 10 µL 2 - 20 µL 10 - 100 µL 20 - 200 µL 100 - 1000 µL	-	Eppendorf AG	Hamburg, Germany
<b>Pipette (Multichannel)</b>	Transferpette S-12 20 - 200 µL	-	Brand GmbH + Co. KG	Wertheim, Germany
<b>pH-Meter</b>	SevenCompact	-	Mettler-Toledo	Columbus, Ohio, USA
<b>Plate reader</b>	GENios Pro	-	Tecan Group AG	Männedorf, Switzerland
<b>Microvolume UV-Vis Spectrophotometer</b>	NanoDrop™	-	Thermo Scientific (Thermo Fisher Scientific)	Waltham, Massachusetts, USA
<b>Rotator</b>	SB2	-	Stuart	Stone, UK
<b>Scale (Laboratory)</b>	BP 2100 S	-	Sartorius	Göttingen, Germany
<b>Shaking flask</b>	100 mL; 250 mL; 500 mL; 1 L; 2 L	-	Schott	Mainz, Germany
<b>Standard Resin (clear resin)</b>	V4	RS-F2-GPCL-04	Formlabs	Somerville, Massachusetts, USA
<b>Storage Tank for Liquid Nitrogen</b>	CS 200 SK		Cryo Anlagenbau GmbH	Wilnsdrf, Germany
<b>Syringe Pump</b>	KDS model 100	-	KD Scientific	Holliston, Massachusetts, USA
<b>Ultra-Low Temperature Freezer</b>	HERAfreeze™ (-80 °C)	-	Thermo Scientific (Thermo Fisher Scientific)	Waltham, Massachusetts, USA
<b>UV-Lamp for sterilisation</b>	VL 215 G	-	Thermo Scientific (Thermo Fisher Scientific)	Waltham, Massachusetts, USA
<b>Waterbath</b>	WB20	-	P-D Industriegesellschaft GmbH	Wilsdruff, Germany

## 9.6 Software

**Table 14: Used Software**

<b>Software</b>	<b>Function</b>	<b>Producer</b>	<b>Location</b>
<b>BioVision</b>	Gel-Imaging	Vilber Lourmat	Eberhardzell, Germany
<b>Citavi</b>	Writing	Swiss Academic Software	Wädenswil, Switzerland
<b>FlowJo</b>	FC-Data-Analyses	Tree Star, Inc.	Ashland, Oregon, USA
<b>Fusion 360</b>	CAD	Autodesk	Santa Clara, California, USA
<b>Inkscape</b>	Rendering	open-source	
<b>Microsoft Office</b>	Writing, Data curation	Microsoft	Redmond, Washington, USA
<b>MxPro</b>	qPCR-cycling	Agilent	Santa Clara, California, USA
<b>Origin</b>	Data curation, Plotting	OriginLab Corporation	Northampton, Massachusetts, USA
<b>PreForm</b>	Slicer	Formlabs	Somerville, Massachusetts, USA
<b>Xfluor</b>	Plate-Reading	Tecan	Männedorf, Switzerland
<b>Zenlite</b>	Microscope-Imaging	Carl Zeiss AG	Oberkochen, Germany

## 10 References

- Aggarwal, Bharat B.; Bhardwaj, Anjana; Aggarwal, Rishi S.; Seeram, Navindra P.; Shishodia, Shishir; Takada, Yasunori (2004): Role of Resveratrol in Prevention and Therapy of Cancer: Preclinical and Clinical Studies. In *Anticancer Res* 24 (5A), pp. 2783–2840. Available online at <http://ar.iiajournals.org/content/24/5A/2783.full.pdf>.
- Alonso-Guallart, P.; Llore, N.; Lopes, E.; Kofman, S-B; Ho, S-H; Stern, J. et al. (2021): CD40L-stimulated B cells for ex-vivo expansion of polyspecific non-human primate regulatory T cells for translational studies. In *Clinical and experimental immunology* 203 (3), pp. 480–492. DOI: 10.1111/cei.13537.
- Amino, N.; Tanizawa, O.; Miyai, K.; Tanaka, F.; Hayashi, C.; Kawashima, M.; Ichihara, K. (1978): Changes of serum immunoglobulins IgG, IgA, IgM, and IgE during pregnancy. In *Obstetrics and gynecology* 52 (4), pp. 415–420.
- Armitage, R. J.; Macduff, B. M.; Spriggs, M. K.; Fanslow, W. C. (1993): Human B cell proliferation and Ig secretion induced by recombinant CD40 ligand are modulated by soluble cytokines. In *The Journal of Immunology* 150 (9), pp. 3671–3680. Available online at <https://www.jimmunol.org/content/jimmunol/150/9/3671.full.pdf>.
- Auner, Holger W.; Beham-Schmid, Christine; Dillon, Niall; Sabbattini, Pierangela (2010): The life span of short-lived plasma cells is partly determined by a block on activation of apoptotic caspases acting in combination with endoplasmic reticulum stress. In *Blood* 116 (18), pp. 3445–3455. DOI: 10.1182/blood-2009-10-250423.
- Avery, Danielle T.; Kalled, Susan L.; Ellyard, Julia I.; Ambrose, Christine; Bixler, Sarah A.; Thien, Marilyn et al. (2003): BAFF selectively enhances the survival of plasmablasts generated from human memory B cells. In *J Clin Invest* 112 (2), pp. 286–297. DOI: 10.1172/JCI18025.
- Banchereau, J.; Bazan, F.; Blanchard, D.; Brière, F.; Galizzi, J. P.; van Kooten, C. et al. (1994): The CD40 antigen and its ligand. In *Annual review of immunology* 12, pp. 881–922. DOI: 10.1146/annurev.iy.12.040194.004313.
- Banchereau, Jacques; Rousset, Françoise (1992): Human B Lymphocytes: Phenotype, Proliferation, and Differentiation. In Frank J. Dixon (Ed.): *Advances in Immunology*, vol. 52: Academic Press, pp. 125–262. Available online at <http://www.sciencedirect.com/science/article/pii/S0065277608608767>.
- Bannard, Oliver; Horton, Robert M.; Allen, Christopher D.C.; An, Jinping; Nagasawa, Takashi; Cyster, Jason G. (2013): Germinal Center Centroblasts Transition to a Centrocyte Phenotype According to a Timed Program and Depend on the Dark Zone for Effective Selection. In *Immunity* 39 (5), pp. 912–924. DOI: 10.1016/j.immuni.2013.08.038.
- Barr, T. A.; Heath, A. W. (2001): Functional activity of CD40 antibodies correlates to the position of binding relative to CD154. In *Immunology* 102 (1), pp. 39–43. DOI: 10.1046/j.1365-2567.2001.01148.x.
- Bekeredjian-Ding, Isabelle; Foermer, Sandra; Kirschning, Carsten J.; Parcina, Marijo; Heeg, Klaus (2012): Poke weed mitogen requires Toll-like receptor ligands for proliferative activity in human and murine B lymphocytes. In *PLoS one* 7 (1), e29806. DOI: 10.1371/journal.pone.0029806.
- Bergwelt-Baildon, Michael S. von; Vonderheide, Robert H.; Maecker, Britta; Hirano, Naoto; Anderson, Karen S.; Butler, Marcus O. et al. (2002): Human primary and memory cytotoxic T lymphocyte responses are efficiently induced by means of CD40-activated B cells as antigen-presenting cells: potential for clinical application. In *0006-4971* 99 (9), pp. 3319–3325. DOI: 10.1182/blood.V99.9.3319.
- Boyaka, P. N.; Wright, P. F.; Marinaro, M.; Kiyono, H.; Johnson, J. E.; Gonzales, R. A. et al. (2000): Human nasopharyngeal-associated lymphoreticular tissues. Functional analysis of subepithelial and intraepithelial B and T cells from adenoids and tonsils. In *The American journal of pathology* 157 (6), pp. 2023–2035. DOI: 10.1016/S0002-9440(10)64841-9.
- Bryant, Vanessa L.; Ma, Cindy S.; Avery, Danielle T.; Li, Ying; Good, Kim L.; Corcoran, Lynn M. et al. (2007): Cytokine-Mediated Regulation of Human B Cell Differentiation into Ig-Secreting Cells: Predominant Role of IL-21 Produced by CXCR5+ T Follicular Helper Cells. In *The Journal of Immunology* 179 (12), pp. 8180–8190. DOI: 10.4049/jimmunol.179.12.8180.
- Carpenter, Erica L.; Mick, Rosemarie; Rüter, Jens; Vonderheide, Robert H. (2009): Activation of human B cells by the agonist CD40 antibody CP-870,893 and augmentation with simultaneous toll-like receptor 9 stimulation. In *Journal of translational medicine* 7, p. 93. DOI: 10.1186/1479-5876-7-93.
- Carsetti, R.; Köhler, G.; Lamers, M. C. (1995): Transitional B cells are the target of negative selection in the B cell compartment. In *J Exp Med* 181 (6), pp. 2129–2140. DOI: 10.1084/jem.181.6.2129.
- Castigli, E.; Alt, F. W.; Davidson, L.; Bottaro, A.; Mizoguchi, E.; Bhan, A. K.; Geha, R. S. (1994): CD40-deficient mice generated by recombination-activating gene-2-deficient blastocyst complementation. In *Proceedings of the National Academy of Sciences of the United States of America* 91 (25), pp. 12135–12139. DOI: 10.1073/pnas.91.25.12135.
- Chan, Tyani D.; Gatto, Dominique; Wood, Katherine; Camidge, Tahra; Basten, Antony; Brink, Robert (2009): Antigen affinity controls rapid T-dependent antibody production by driving the expansion rather than the differentiation or extrafollicular migration of early plasmablasts. In *Journal of immunology (Baltimore, Md. : 1950)* 183 (5), pp. 3139–3149. DOI: 10.4049/jimmunol.0901690.
- Cobleigh, M. A.; Braun, D. P.; Harris, J. E. (1980): Age-dependent changes in human peripheral blood B cells and T-cell subsets: correlation with mitogen responsiveness. In *Clinical immunology and immunopathology* 15 (2), pp. 162–174. DOI: 10.1016/0090-1229(80)90028-8.
- Crotty, Shane; Aubert, Rachael D.; Glidewell, John; Ahmed, Rafi (2004): Tracking human antigen-specific memory B cells: a sensitive and generalized ELISPOT system. In *Journal of Immunological Methods* 286 (1), pp. 111–122. DOI: 10.1016/j.jim.2003.12.015.
- Defrance, T.; Vanbervliet, B.; Aubry, J. P.; Takebe, Y.; Arai, N.; Miyajima, A. et al. (1987): B cell growth-promoting activity of recombinant human interleukin 4. In *Journal of immunology (Baltimore, Md. : 1950)* 139 (4), pp. 1135–1141.

- Ding, B. Belinda; Bi, Enguang; Chen, Hongshan; Yu, J. Jessica; Ye, B. Hilda (2013): IL-21 and CD40L Synergistically Promote Plasma Cell Differentiation through Upregulation of Blimp-1 in Human B Cells. In *The Journal of Immunology* 190 (4), pp. 1827–1836. DOI: 10.4049/jimmunol.1201678.
- Do, R. K.; Hatada, E.; Lee, H.; Tourigny, M. R.; Hilbert, D.; Chen-Kiang, S. (2000): Attenuation of apoptosis underlies B lymphocyte stimulator enhancement of humoral immune response. In *J Exp Med* 192 (7), pp. 953–964. DOI: 10.1084/jem.192.7.953.
- Duarte, João H. (2016): Functional switching. In *Nature immunology* 17 (S1), S12-S12. DOI: 10.1038/ni.3607.
- Durandy, Anne (2003): Activation-induced cytidine deaminase: a dual role in class-switch recombination and somatic hypermutation. In *Eur. J. Immunol.* 33 (8), pp. 2069–2073. DOI: 10.1002/eji.200324133.
- Eales, Lesley-Jane (2003): Immunology for Life Scientists. Chichester, UK: John Wiley & Sons, Ltd.
- Edry, Efrat; Melamed, Doron (2004): Receptor editing in positive and negative selection of B lymphopoiesis. In *Journal of immunology (Baltimore, Md. : 1950)* 173 (7), pp. 4265–4271. DOI: 10.4049/jimmunol.173.7.4265.
- Elgueta, Raul; Benson, Micah J.; Vries, Victor C. de; Wasiuk, Anna; Guo, Yanxia; Noelle, Randolph J. (2009): Molecular mechanism and function of CD40/CD40L engagement in the immune system. In *Immunological reviews* 229 (1), pp. 152–172. DOI: 10.1111/j.1600-065X.2009.00782.x.
- Ettinger, Rachel; Kuchen, Stefan; Lipsky, Peter E. (2008): The role of IL-21 in regulating B-cell function in health and disease. In *Immunological reviews* 223, pp. 60–86. DOI: 10.1111/j.1600-065X.2008.00631.x.
- Ettinger, Rachel; Sims, Gary P.; Fairhurst, Anna-Marie; Robbins, Rachel; Silva, Yong Sing da; Spolski, Rosanne et al. (2005): IL-21 Induces Differentiation of Human Naive and Memory B Cells into Antibody-Secreting Plasma Cells. In *The Journal of Immunology* 175 (12), pp. 7867–7879. DOI: 10.4049/jimmunol.175.12.7867.
- Ettinger, Rachel; Sims, Gary P.; Robbins, Rachel; Withers, David; Fischer, Randy T.; Grammer, Amrie C. et al. (2007): IL-21 and BAFF/BLyS synergize in stimulating plasma cell differentiation from a unique population of human splenic memory B cells. In *Journal of immunology (Baltimore, Md. : 1950)* 178 (5), pp. 2872–2882. DOI: 10.4049/jimmunol.178.5.2872.
- Fanslow, W. C.; Srinivasan, S.; Paxton, R.; Gibson, M. G.; Spriggs, M. K.; Armitage, R. J. (1994a): Structural characteristics of CD40 ligand that determine biological function. In *Seminars in immunology* 6 (5), pp. 267–278. DOI: 10.1006/smim.1994.1035.
- Fanslow, William C.; Srinivasan, Subhashini; Paxton, Ray; Gibson, Marylou G.; Spriggs, Melanie K.; Armitage, Richard J. (1994b): Structural characteristics of CD40 ligand that determine biological function. In *Seminars in immunology* 6 (5), pp. 267–278. DOI: 10.1006/smim.1994.1035.
- Farnes, P.; Barker, B. E.; Brownhill, L. E.; Fanger, H. (1964): MITOGENIC ACTIVITY IN. In *The Lancet* 284 (7369), pp. 1100–1101. DOI: 10.1016/S0140-6736(64)92616-9.
- Flores, Camila; Fouquet, Guillemette; Moura, Ivan Cruz; Maciel, Thiago Trovati; Hermine, Olivier (2019): Lessons to Learn From Low-Dose Cyclosporin-A: A New Approach for Unexpected Clinical Applications. In *Frontiers in immunology* 10, p. 588. DOI: 10.3389/fimmu.2019.00588.
- Fluckiger, A. C.; Garrone, P.; Durand, I.; Galizzi, J. P.; Banchereau, J. (1993): Interleukin 10 (IL-10) upregulates functional high affinity IL-2 receptors on normal and leukemic B lymphocytes. In *Journal of Experimental Medicine* 178 (5), pp. 1473–1481. DOI: 10.1084/jem.178.5.1473.
- Fournel, Sylvie; Wieckowski, Sébastien; Sun, Weimin; Trouche, Nathalie; Dumortier, Hélène; Bianco, Alberto et al. (2005): C3-symmetric peptide scaffolds are functional mimetics of trimeric CD40L. In *Nat Chem Biol* 1 (7), pp. 377–382. DOI: 10.1038/nchembio746.
- Fuxa, Martin; Busslinger, Meinrad (2007): Reporter gene insertions reveal a strictly B lymphoid-specific expression pattern of Pax5 in support of its B cell identity function. In *Journal of immunology (Baltimore, Md. : 1950)* 178 (12), pp. 8222–8228. DOI: 10.4049/jimmunol.178.12.8221-a.
- Garcia-Marquez, Maria A.; Shimabukuro-Vornhagen, Alexander; Theurich, Sebastian; Kochanek, Matthias; Weber, Tanja; Wennhold, Kerstin et al. (2014): A multimerized form of recombinant human CD40 ligand supports long-term activation and proliferation of B cells. In *Cytotherapy* 16 (11), pp. 1537–1544. DOI: 10.1016/j.jcyt.2014.05.011.
- Gardell, Jennifer L.; Parker, David C. (2017): CD40L is transferred to antigen-presenting B cells during delivery of T-cell help. In *European journal of immunology* 47 (1), pp. 41–50. DOI: 10.1002/eji.201646504.
- Gehrcke, Jan-Philip; Pisabarro, M. Teresa (2015): Identification and characterization of a glycosaminoglycan binding site on interleukin-10 via molecular simulation methods. In *Journal of Molecular Graphics and Modelling* 62, pp. 97–104. DOI: 10.1016/j.jmkgm.2015.09.003.
- Giese, Christoph; Lubitz, Annika; Demmler, Christian D.; Reuschel, Jana; Bergner, Konstanze; Marx, Uwe (2010): Immunological substance testing on human lymphatic micro-organoids in vitro. In *Journal of Biotechnology* 148 (1), pp. 38–45. DOI: 10.1016/j.jbiotec.2010.03.001.
- Goetghebeur, S.; Hu, W. S. (1991): Cultivation of anchorage-dependent animal cells in microsphere-induced aggregate culture. In *Applied microbiology and biotechnology* 34 (6), pp. 735–741. DOI: 10.1007/BF00169343.
- Goldstein, I. J.; Hayes, C. E. (1978): The lectins: carbohydrate-binding proteins of plants and animals. In *Advances in carbohydrate chemistry and biochemistry* 35, pp. 127–340. DOI: 10.1016/S0065-2318(08)60220-6.
- Good, Kim L.; Bryant, Vanessa L.; Tangye, Stuart G. (2006): Kinetics of human B cell behavior and amplification of proliferative responses following stimulation with IL-21. In *Journal of immunology (Baltimore, Md. : 1950)* 177 (8), pp. 5236–5247. DOI: 10.4049/jimmunol.177.8.5236.

- Gordon, J.; Pound, J. D. (2000): Fortifying B cells with CD154: an engaging tale of many hues. In *Immunology* 100 (3), pp. 269–280. DOI: 10.1046/j.1365-2567.2000.00074.x.
- Gross, J. A.; Johnston, J.; Mudri, S.; Enselman, R.; Dillon, S. R.; Madden, K. et al. (2000): TACI and BCMA are receptors for a TNF homologue implicated in B-cell autoimmune disease. In *Nature* 404 (6781), pp. 995–999. DOI: 10.1038/35010115.
- Harada, Michishige; Magara-Koyanagi, Kumiko; Watarai, Hiroshi; Nagata, Yuko; Ishii, Yasuyuki; Kojo, Satoshi et al. (2006): IL-21-induced Bepsilon cell apoptosis mediated by natural killer T cells suppresses IgE responses. In *J Exp Med* 203 (13), pp. 2929–2937. DOI: 10.1084/jem.20062206.
- Hardy, R. R.; Carmack, C. E.; Shinton, S. A.; Kemp, J. D.; Hayakawa, K. (1991): Resolution and characterization of pro-B and pre-pro-B cell stages in normal mouse bone marrow. In *J Exp Med* 173 (5), pp. 1213–1225. DOI: 10.1084/jem.173.5.1213.
- Hartmann, Gunther; Krieg, Arthur M. (2000): Mechanism and Function of a Newly Identified CpG DNA Motif in Human Primary B Cells. In *The Journal of Immunology* 164 (2), pp. 944–953. DOI: 10.4049/jimmunol.164.2.944.
- Harwood, Naomi E.; Batista, Facundo D. (2011): The Cytoskeleton Coordinates the Early Events of B-cell Activation. In *Cold Spring Harbor Perspectives in Biology* 3 (2). DOI: 10.1101/cshperspect.a002360.
- Haswell, Linsey E.; Glennie, Martin J.; Al-Shamkhani, Aymen (2001): Analysis of the oligomeric requirement for signaling by CD40 using soluble multimeric forms of its ligand, CD154. In *Eur. J. Immunol.* 31 (10), pp. 3094–3100. DOI: 10.1002/1521-4141(200110)31:10<3094::AID-IMMU3094>3.0.CO;2-F.
- Helm, M.; A. B. Riedl, S.; Gollner, K.; Gollner, U.; Jérôme, V.; Freitag, R. (2021): Isolation of primary human B lymphocytes from tonsils compared to blood as alternative source for ex vivo application. In *Journal of Chromatography B*, p. 122853. DOI: 10.1016/j.jchromb.2021.122853.
- Helm, Moritz; Huang, Songyan B.; Gollner, Katrin; Gollner, Ulrich; Jérôme, Valérie; Freitag, Ruth (2022): Cultivation of Encapsulated Primary Human B Lymphocytes: A First Step towards a Bioartificial Germinal Center. In *Macromolecular bioscience*, e2200256. DOI: 10.1002/mabi.202200256.
- Hermansen, Johanne U.; Tjønnfjord, Geir E.; Munthe, Ludvig A.; Taskén, Kjetil; Skånland, Sigrid S. (2018): Cryopreservation of primary B cells minimally influences their signaling responses. In *Sci Rep* 8 (1), pp. 1–7. DOI: 10.1038/s41598-018-36121-9.
- Hernández, Rosa M. A.; Orive, Gorka; Murua, Ainhoa; Pedraz, José Luis (2010): Microcapsules and microcarriers for in situ cell delivery. In *Advanced Drug Delivery Reviews* 62 (7-8), pp. 711–730. DOI: 10.1016/j.addr.2010.02.004.
- Hivrale, A. U.; Ingale, A. G. (2013): Plant as a plenteous reserve of lectin. In *Plant Signaling & Behavior* 8 (12). DOI: 10.4161/psb.26595.
- Howard, M.; Farrar, J.; Hilfiker, M.; Johnson, B.; Takatsu, K.; Hamaoka, T.; Paul, W. E. (1982): Identification of a T cell-derived b cell growth factor distinct from interleukin 2. In *J Exp Med* 155 (3), pp. 914–923. DOI: 10.1084/jem.155.3.914.
- Huang, Jinghe; Kang, Byong H.; Ishida, Elise; Zhou, Tongqing; Griesman, Trevor; Sheng, Zizhang et al. (2016): Identification of a CD4-Binding-Site Antibody to HIV that Evolved Near-Pan Neutralization Breadth. In *Immunity* 45 (5), pp. 1108–1121. DOI: 10.1016/j.immuni.2016.10.027.
- Ivanov, R.; Aarts, T.; Hagenbeek, A.; Hol, S.; Ebeling, S. (2005): B-cell expansion in the presence of the novel 293-CD40L-sCD40L cell line allows the generation of large numbers of efficient xenoantigen-free APC. In *Cytotherapy* 7 (1), pp. 62–73. DOI: 10.1016/S1465-3249(05)70790-8.
- Jain, Nitin; Vergish, Satyam; Khurana, Jitendra P. (2018): Validation of house-keeping genes for normalization of gene expression data during diurnal/circadian studies in rice by RT-qPCR. In *Sci Rep* 8. DOI: 10.1038/s41598-018-21374-1.
- Jazayeri, Mir Hadi; Pourfathollah, Ali Akbar; Rasaei, Mohammad Javad; Porpak, Zahra; Jafari, Mohammad Ebrahim (2013): The concentration of total serum IgG and IgM in sera of healthy individuals varies at different age intervals. In *Biomedicine & Aging Pathology* 3 (4), pp. 241–245. DOI: 10.1016/j.biomag.2013.09.002.
- Jérôme, Valérie; Werner, Melanie; Kaiser, Patrick; Freitag, Ruth (2017): Creating a Biomimetic Microenvironment for the Ex Vivo Expansion of Primary Human T Lymphocytes. In *Macromolecular bioscience* 17 (9). DOI: 10.1002/mabi.201700091.
- Jourdan, Michel; Robert, Nicolas; Cren, Maïlys; Thibaut, Coraline; Duperray, Christophe; Kassambara, Alboukadel et al. (2017): Characterization of human FCRL4-positive B cells. In *PLoS one* 12 (6), e0179793. DOI: 10.1371/journal.pone.0179793.
- Kallies, Axel; Hasbold, Jhagvaral; Tarlinton, David M.; Dietrich, Wendy; Corcoran, Lynn M.; Hodgkin, Philip D.; Nutt, Stephen L. (2004): Plasma cell ontogeny defined by quantitative changes in blimp-1 expression. In *J Exp Med* 200 (8), pp. 967–977. DOI: 10.1084/jem.20040973.
- Kaminski, Denise A.; Wei, Chungwen; Qian, Yu; Rosenberg, Alexander F.; Sanz, Ignacio (2012): Advances in human B cell phenotypic profiling. In *Frontiers in immunology* 3, p. 302. DOI: 10.3389/fimmu.2012.00302.
- Kanutte Huse; Cara E. Wogslund; Hannah G. Polikowsky; Kirsten E. Diggins; Erlend B. Smeland; June H. Myklebust; Jonathan M. Irish (2019): Human Germinal Center B Cells Differ from Naïve and Memory B Cells in CD40 Expression and CD40L-Induced Signaling Response. In *Cytometry Part A* 95 (4), pp. 442–449. DOI: 10.1002/cyto.a.23737.
- Kardar, G. A.; Shams, S. H.; Pourpak, Z.; Moin, M. (2003): Normal value of immunoglobulins IgA, IgG, and IgM in Iranian healthy adults, measured by nephelometry. In *Journal of immunoassay & immunochemistry* 24 (4), pp. 359–367. DOI: 10.1081/IAS-120025774.
- Keightley, R. G.; Cooper, M. D.; Lawton, A. R. (1976): The T cell dependence of B cell differentiation induced by pokeweed mitogen. In *Journal of immunology (Baltimore, Md. : 1950)* 117 (5 Pt 1), pp. 1538–1544.
- Kerfoot, Steven M.; Yaari, Gur; Patel, Jaymin R.; Johnson, Kody L.; Gonzalez, David G.; Kleinstein, Steven H.; Haberman, Ann M. (2011): Germinal center B cell and T follicular helper cell development initiates in the interfollicular zone. In *Immunity* 34 (6), pp. 947–960. DOI: 10.1016/j.immuni.2011.03.024.



- Kindler, V.; Zubler, R. H. (1997): Memory, but not naive, peripheral blood B lymphocytes differentiate into Ig-secreting cells after CD40 ligation and costimulation with IL-4 and the differentiation factors IL-2, IL-10, and IL-3. In *Journal of immunology* (Baltimore, Md. : 1950) 159 (5), pp. 2085–2090.
- Kjeldsen, M. K.; Perez-Andres, M.; Schmitz, A.; Johansen, P.; Boegsted, M.; Nyegaard, M. et al. (2011): Multiparametric flow cytometry for identification and fluorescence activated cell sorting of five distinct B-cell subpopulations in normal tonsil tissue. In *American journal of clinical pathology* 136 (6). DOI: 10.1309/AJCPDQNP2U5DZHVV.
- Klein, U.; Rajewsky, K.; Küppers, R. (1998): Human immunoglobulin (Ig)M+IgD+ peripheral blood B cells expressing the CD27 cell surface antigen carry somatically mutated variable region genes: CD27 as a general marker for somatically mutated (memory) B cells. In *J Exp Med* 188 (9), pp. 1679–1689. DOI: 10.1084/jem.188.9.1679.
- Krieg, Arthur M.; Yi, Ae-Kyung; Matson, Sara; Waldschmidt, Thomas J.; Bishop, Gail A.; Teasdale, Rebecca et al. (1995): CpG motifs in bacterial DNA trigger direct B-cell activation. In *Nature* 374 (6522), p. 546. DOI: 10.1038/374546a0.
- Kuo, Tracy C.; Shaffer, Arthur L.; Haddad, Joseph; Choi, Yong Sung; Staudt, Louis M.; Calame, Kathryn (2007): Repression of BCL-6 is required for the formation of human memory B cells in vitro. In *J Exp Med* 204 (4), pp. 819–830. DOI: 10.1084/jem.20062104.
- Kuraoka, M.; McWilliams, L.; Kelsoe, G. (2011): AID expression during B-cell development: searching for answers. In *Immunologic research* 49 (1-3). DOI: 10.1007/s12026-010-8185-7.
- Kwak, Kihyuck; Akkaya, Munir; Pierce, Susan K. (2019): B cell signaling in context. In *Nature immunology* 20 (8), pp. 963–969. DOI: 10.1038/s41590-019-0427-9.
- Kwong, Peter D.; Mascola, John R.; Nabel, Gary J. (2011): Rational Design of Vaccines to Elicit Broadly Neutralizing Antibodies to HIV-1. In *Cold Spring Harb Perspect Med* 1 (1), a007278. DOI: 10.1101/cshperspect.a007278.
- Lacerda, Ana L. M.; Fonseca, Leonardo N.; Blawid, Rosana; Boiteux, Leonardo S.; Ribeiro, Simone G.; Brasileiro, Ana C. M. (2015): Reference Gene Selection for qPCR Analysis in Tomato-Bipartite Begomovirus Interaction and Validation in Additional Tomato-Virus Pathosystems. In *PLoS one* 10 (8), e0136820. DOI: 10.1371/journal.pone.0136820.
- Lancaster, Madeline A.; Knoblich, Juergen A. (2014): Organogenesis in a dish: modeling development and disease using organoid technologies. In *Science (New York, N.Y.)* 345 (6194), p. 1247125. DOI: 10.1126/science.1247125.
- Lanza, R. P.; Hayes, J. L.; Chick, W. L. (1996): Encapsulated cell technology. In *Nature biotechnology* 14 (9), pp. 1107–1111. DOI: 10.1038/nbt0996-1107.
- Laura E. Collins; Linda Troeberg (2019): Heparan sulfate as a regulator of inflammation and immunity. In *Journal of leukocyte biology* 105 (1), pp. 81–92. DOI: 10.1002/JLB.3RU0618-246R.
- Leitner, Judith; Drobits, Karin; Pickl, Winfried F.; Majdic, Otto; Zlabinger, Gerhard; Steinberger, Peter (2011): The effects of Cyclosporine A and azathioprine on human T cells activated by different costimulatory signals. In *Immunology letters* 140 (1-2), pp. 74–80. DOI: 10.1016/j.imlet.2011.06.010.
- Letvin, Norman L. (2006): Progress and obstacles in the development of an AIDS vaccine. In *Nature Reviews Immunology* 6 (12), p. 930. DOI: 10.1038/nri1959.
- Liu, Grace J.; Jaritz, Markus; Wöhner, Miriam; Agerer, Benedikt; Bergthaler, Andreas; Malin, Stephen G.; Busslinger, Meinrad (2020): Repression of the B cell identity factor Pax5 is not required for plasma cell development. In *The Journal of experimental medicine* 217 (11). DOI: 10.1084/jem.20200147.
- Llames, Sara; García-Pérez, Eva; Meana, Álvaro; Larcher, Fernando; del Río, Marcela (2015): Feeder Layer Cell Actions and Applications. In *Tissue Engineering. Part B, Reviews* 21 (4), pp. 345–353. DOI: 10.1089/ten.teb.2014.0547.
- Lohr, Jens G.; Stojanov, Petar; Lawrence, Michael S.; Auclair, Daniel; Chapuy, Bjoern; Sougnez, Carrie et al. (2012): Discovery and prioritization of somatic mutations in diffuse large B-cell lymphoma (DLBCL) by whole-exome sequencing. In *Proceedings of the National Academy of Sciences of the United States of America* 109 (10), pp. 3879–3884. DOI: 10.1073/pnas.1121343109.
- Lortat-Jacob, Hugues; Garrone, Pierre; Banchereau, Jaques; Grimaud, Jean-Alexis (1997): HUMAN INTERLEUKIN 4 IS A GLYCOSAMINOGLYCAN-BINDING PROTEIN. In *Cytokine* 9 (2), pp. 101–105. DOI: 10.1006/cyto.1996.0142.
- Luo, Xin M.; Maarschalk, Emily; O'Connell, Ryan M.; Wang, Pin; Yang, Lili; Baltimore, David (2009): Engineering human hematopoietic stem/progenitor cells to produce a broadly neutralizing anti-HIV antibody after in vitro maturation to human B lymphocytes. In *Blood* 113 (7), pp. 1422–1431. DOI: 10.1182/blood-2008-09-177139.
- Maciel, Elva V. M.; Araújo-Filho, Vanduir S.; Nakazawa, Mineo; Gomes, Yara M.; Coelho, Luana C. B. B.; Correia, Maria T. S. (2004): Mitogenic activity of Cratylia mollis lectin on human lymphocytes. In *Biologicals : journal of the International Association of Biological Standardization* 32 (1), pp. 57–60. DOI: 10.1016/j.biologicals.2003.12.001.
- Mackey, M. F.; Barth, R. J.; Noelle, R. J. (1998): The role of CD40/CD154 interactions in the priming, differentiation, and effector function of helper and cytotoxic T cells. In *Journal of leukocyte biology* 63 (4), pp. 418–428. DOI: 10.1002/jlb.63.4.418.
- MacLennan, Ian C. M. (1994): Germinal Centers. DOI: 10.1146/annurev.iy.12.040194.001001.
- Mandel, T. E.; Phipps, R. P.; Abbot, A.; Tew, J. G. (1980): The follicular dendritic cell: long term antigen retention during immunity. In *Immunological reviews* 53, pp. 29–59. DOI: 10.1111/j.1600-065x.1980.tb01039.x.
- Medvedovic, Jasna; Ebert, Anja; Tagoh, Hiromi; Busslinger, Meinrad (2011): Pax5: a master regulator of B cell development and leukemogenesis. In *Advances in immunology* 111, pp. 179–206. DOI: 10.1016/B978-0-12-385991-4.00005-2.
- Mellstedt, H. (1975): In vitro activation of human T and B lymphocytes by pokeweed mitogen. In *Clinical and experimental immunology* 19 (1), pp. 75–82.

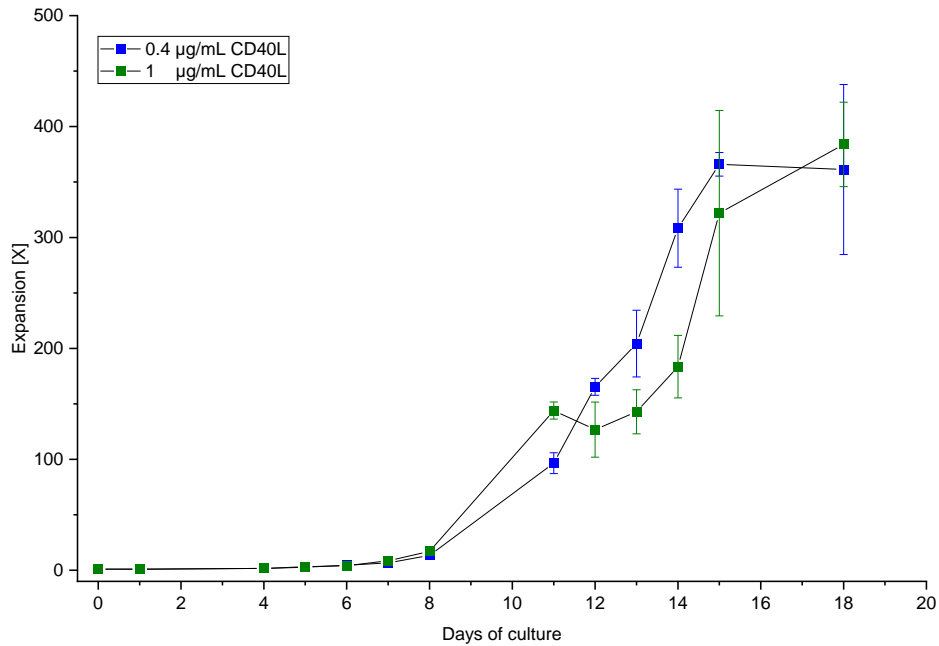
- Mickoleit, Frank; Jérôme, Valérie; Freitag, Ruth; Schüler, Dirk (2020): Bacterial Magnetosomes as Novel Platform for the Presentation of Immunostimulatory, Membrane-Bound Ligands in Cellular Biotechnology. In *Advanced biosystems* 4 (3), e1900231. DOI: 10.1002/adbi.201900231.
- Mond, J. J.; Lees, A.; Snapper, C. M. (1995): T cell-independent antigens type 2. In *Annual review of immunology* 13, pp. 655–692. DOI: 10.1146/annurev.iy.13.040195.003255.
- Moore, P. A.; Belvedere, O.; Orr, A.; Pieri, K.; LaFleur, D. W.; Feng, P. et al. (1999): BLYS: member of the tumor necrosis factor family and B lymphocyte stimulator. In *Science* 285 (5425), pp. 260–263. DOI: 10.1126/science.285.5425.260.
- Morris, A. E.; Remmele, R. L.; Klinke, R.; Macduff, B. M.; Fanslow, W. C.; Armitage, R. J. (1999): Incorporation of an isoleucine zipper motif enhances the biological activity of soluble CD40L (CD154). In *The Journal of biological chemistry* 274 (1), pp. 418–423. DOI: 10.1074/jbc.274.1.418.
- Mukhopadhyay, A.; Ni, J.; Zhai, Y.; Yu, G. L.; Aggarwal, B. B. (1999): Identification and characterization of a novel cytokine, THANK, a TNF homologue that activates apoptosis, nuclear factor-kappaB, and c-Jun NH2-terminal kinase. In *The Journal of biological chemistry* 274 (23), pp. 15978–15981. DOI: 10.1074/jbc.274.23.15978.
- Muramatsu, Masamichi; Kinoshita, Kazuo; Fagarasan, Sidonia; Yamada, Shuichi; Shinkai, Yoichi; Honjo, Tasuku (2000): Class Switch Recombination and Hypermutation Require Activation-Induced Cytidine Deaminase (AID), a Potential RNA Editing Enzyme. In *Cell* 102 (5), pp. 553–563. DOI: 10.1016/S0092-8674(00)00078-7.
- Naito, Masayasu; Hainz, Ursula; Burkhardt, Ute E.; Fu, Buyin; Aho, Deborah; Stevenson, Kristen E. et al. (2013): CD40L-Tri, a novel formulation of recombinant human CD40L that effectively activates B cells. In *Cancer immunology, immunotherapy : CII* 62 (2), pp. 347–357. DOI: 10.1007/s00262-012-1331-4.
- Najjam, Saloua; Gibbs, Roslyn V.; Gordon, Myrtle Y.; Rider, Christopher C. (1997): CHARACTERIZATION OF HUMAN RECOMBINANT INTERLEUKIN 2 BINDING TO HEPARIN AND HEPARAN SULFATE USING AN ELISA APPROACH. In *Cytokine* 9 (12), pp. 1013–1022. DOI: 10.1006/cyto.1997.0246.
- Néron, Sonia; Nadeau, Philippe J.; Darveau, André; Leblanc, Jean-François (2011a): Tuning of CD40-CD154 interactions in human B-lymphocyte activation: a broad array of in vitro models for a complex in vivo situation. In *Archivum immunologiae et therapeuticae experimentalis* 59 (1), pp. 25–40. DOI: 10.1007/s00005-010-0108-8.
- Néron, Sonia; Racine, Claudia; Roy, Annie; Guérin, Matthieu (2005): Differential responses of human B-lymphocyte subpopulations to graded levels of CD40-CD154 interaction. In *Immunology* 116 (4), pp. 454–463. DOI: 10.1111/j.1365-2567.2005.02244.x.
- Néron, Sonia; Roy, Annie; Dumont, Nellie (2012): Large-scale in vitro expansion of polyclonal human switched-memory B lymphocytes. In *PLoS one* 7 (12), e51946. DOI: 10.1371/journal.pone.0051946.
- Néron, Sonia; Roy, Annie; Dumont, Nellie; Dussault, Nathalie (2011b): Effective in vitro expansion of CD40-activated human B lymphocytes in a defined bovine protein-free medium. In *Journal of Immunological Methods* 371 (1-2), pp. 61–69. DOI: 10.1016/j.jim.2011.06.013.
- Nieuwenhuis, P.; Ford, W. L. (1976): Comparative migration of B- and T-lymphocytes in the rat spleen and lymph nodes. In *Cellular Immunology* 23 (2), pp. 254–267. DOI: 10.1016/0008-8749(76)90191-X.
- Nojima, Takuya; Haniuda, Kei; Moutai, Tatsuya; Matsudaira, Moeko; Mizokawa, Sho; Shiratori, Ikuo et al. (2011): In-vitro derived germinal centre B cells differentially generate memory B or plasma cells in vivo. In *Nature communications* 2, p. 465. DOI: 10.1038/ncomms1475.
- Noviski, Mark; Mueller, James L.; Satterthwaite, Anne; Garrett-Sinha, Lee Ann; Brombacher, Frank; Zikherman, Julie (2018): IgM and IgD B cell receptors differentially respond to endogenous antigens and control B cell fate. In *eLife* 7. DOI: 10.7554/eLife.35074.
- Nutt, S. L.; Taubenheim, N.; Hasbold, J.; Corcoran, L. M.; Hodgkin, P. D. (2011): The genetic network controlling plasma cell differentiation. In *Seminars in immunology* 23 (5). DOI: 10.1016/j.smim.2011.08.010.
- Nutt, Stephen L.; Kee, Barbara L. (2007): The transcriptional regulation of B cell lineage commitment. In *Immunity* 26 (6), pp. 715–725. DOI: 10.1016/j.immuni.2007.05.010.
- O'Leary, Karen A.; Pascual-Tereasa, Sonia de; Needs, Paul W.; Bao, Yong-Ping; O'Brien, Nora M.; Williamson, Gary (2004): Effect of flavonoids and Vitamin E on cyclooxygenase-2 (COX-2) transcription. Nutrition and Carcinogenesis. In *Mutation Research/Fundamental and Molecular Mechanisms of Mutagenesis* 551 (1), pp. 245–254. DOI: 10.1016/j.mrfmmm.2004.01.015.
- Okada, Takaharu; Miller, Mark J.; Parker, Ian; Krummel, Matthew F.; Neighbors, Margaret; Hartley, Suzanne B. et al. (2005): Antigen-engaged B cells undergo chemotaxis toward the T zone and form motile conjugates with helper T cells. In *PLoS biology* 3 (6), e150. DOI: 10.1371/journal.pbio.0030150.
- Orive, Gorka; Hernández, Rose Maria; Rodríguez Gascón, Alicia; Calafiore, Riccardo; Chang, Thomas Ming Swi; Vos, Paul de et al. (2004): History, challenges and perspectives of cell microencapsulation. In *Trends in biotechnology* 22 (2), pp. 87–92. DOI: 10.1016/j.tibtech.2003.11.004.
- Osmond, Dennis G. (1991): Proliferation kinetics and the lifespan of B cells in central and peripheral lymphoid organs. In *Current Opinion in Immunology* 3 (2), pp. 179–185. DOI: 10.1016/0952-7915(91)90047-5.
- Pape, Kathryn A.; Catron, Drew M.; Itano, Andrea A.; Jenkins, Marc K. (2007): The humoral immune response is initiated in lymph nodes by B cells that acquire soluble antigen directly in the follicles. In *Immunity* 26 (4), pp. 491–502. DOI: 10.1016/j.immuni.2007.02.011.
- Parish, Christopher R.; Glidden, Megan H.; Quah, Ben J. C.; Warren, Hilary S. (2009): Use of the Intracellular Fluorescent Dye CFSE to Monitor Lymphocyte Migration and Proliferation. In *Current Protocols in Immunology* 84 (1), 4.9.1-4.9.13. DOI: 10.1002/0471142735.im0409s84.

- Parrish-Novak, J.; Dillon, S. R.; Nelson, A.; Hammond, A.; Sprecher, C.; Gross, J. A. et al. (2000): Interleukin 21 and its receptor are involved in NK cell expansion and regulation of lymphocyte function. In *Nature* 408 (6808), pp. 57–63. DOI: 10.1038/35040504.
- Pavri, Rushad; Nussenzweig, Michel C. (2011): AID targeting in antibody diversity. In *Advances in immunology* 110, pp. 1–26. DOI: 10.1016/B978-0-12-387663-8.00005-3.
- Pérez, M. Eugenia; Billordo, Luis Ariel; Baz, Plácida; Fainboim, Leonardo; Arana, Eloisa (2014): Human memory B cells isolated from blood and tonsils are functionally distinctive. In *Immunology and cell biology* 92 (10), pp. 882–887. DOI: 10.1038/icb.2014.59.
- Pers, Jacques-Olivier; Daridon, Capucine; Devauchelle, Valérie; Jousse, Sandrine; Saraux, Alain; Jamin, Christophe; Youinou, Pierre (2005): BAFF overexpression is associated with autoantibody production in autoimmune diseases. In *Annals of the New York Academy of Sciences* 1050, pp. 34–39. DOI: 10.1196/annals.1313.004.
- Pitisuttithum, Punnee; Gilbert, Peter; Gurwith, Marc; Heyward, William; Martin, Michael; van Griensven, Fritz et al. (2006): Randomized, Double-Blind, Placebo-Controlled Efficacy Trial of a Bivalent Recombinant Glycoprotein 120 HIV-1 Vaccine among Injection Drug Users in Bangkok, Thailand. In *J Infect Dis* 194 (12), pp. 1661–1671. DOI: 10.1086/508748.
- Purwada, Alberto; Jaiswal, Manish K.; Ahn, Haelee; Nojima, Takuya; Kitamura, Daisuke; Gaharwar, Akhilesh K. et al. (2015): Ex vivo engineered immune organoids for controlled germinal center reactions. In *Biomaterials* 63, pp. 24–34. DOI: 10.1016/j.biomaterials.2015.06.002.
- Purwada, Alberto; Singh, Ankur (2017): Immuno-engineered organoids for regulating the kinetics of B-cell development and antibody production. In *Nature Protocols* 12 (1), pp. 168–182. DOI: 10.1038/nprot.2016.157.
- Quah, Ben J. C.; Warren, Hilary S.; Parish, Christopher R. (2007): Monitoring lymphocyte proliferation *in vitro* and *in vivo* with the intracellular fluorescent dye carboxyfluorescein diacetate succinimidyl ester. In *Nature Protocols* 2 (9), p. 2049. DOI: 10.1038/nprot.2007.296.
- Quah, Benjamin J. C.; Parish, Christopher R. (2010): The Use of Carboxyfluorescein Diacetate Succinimidyl Ester (CFSE) to Monitor Lymphocyte Proliferation. In *JoVE (Journal of Visualized Experiments)* (44), e2259. DOI: 10.3791/2259.
- Radonić, Aleksandar; Thulke, Stefanie; Mackay, Ian M.; Landt, Olfert; Siegert, Wolfgang; Nitsche, Andreas (2004): Guideline to reference gene selection for quantitative real-time PCR. In *Biochemical and biophysical research communications* 313 (4), pp. 856–862. DOI: 10.1016/j.bbrc.2003.11.177.
- Rebecca Caeser; Jie Gao; Miriam Di Re; Chun Gong; Daniel J. Hodson (2021): Genetic manipulation and immortalized culture of ex vivo primary human germinal center B cells. In *Nat Protoc* 16 (5), pp. 2499–2519. DOI: 10.1038/s41596-021-00506-4.
- Reed, Jim; Reichelt, Madison; Wetzel, Scott A. (2021): Lymphocytes and Trogocytosis-Mediated Signaling. In *Cells* 10 (6). DOI: 10.3390/cells10061478.
- Reijmers, Rogier M.; Spaargaren, Marcel; Pals, Steven T. (2013): Heparan sulfate proteoglycans in the control of B cell development and the pathogenesis of multiple myeloma. In *The FEBS journal* 280 (10), pp. 2180–2193. DOI: 10.1111/febs.12180.
- Reimer, Dorothea; Meyer-Hermann, Michael; Rakhymzhan, Asylkhan; Steinmetz, Tobit; Tripal, Philipp; Thomas, Jana et al. (2020): B Cell Speed and B-FDC Contacts in Germinal Centers Determine Plasma Cell Output via Swiprosin-1/EFhd2. In *Cell reports* 32 (6), p. 108030. DOI: 10.1016/j.celrep.2020.108030.
- Reisfeld, R. A.; Börjeson, J.; Chessin, L. N.; Small, P. A. (1967): Isolation and characterization of a mitogen from pokeweed (*Phytolacca americana*). In *Proceedings of the National Academy of Sciences of the United States of America* 58 (5), pp. 2020–2027.
- Robinson, Marcus J.; Pitt, Catherine; Brodie, Erica J.; Valk, Anika M.; O'Donnell, Kristy; Nitschke, Lars et al. (2019): BAFF, IL-4 and IL-21 separably program germinal center-like phenotype acquisition, BCL6 expression, proliferation and survival of CD40L-activated B cells *in vitro*. In *Immunology and cell biology* 97 (9), pp. 826–839. DOI: 10.1111/imcb.12283.
- Röhlich, K. (1930): Beitrag zur Cytologie der Keimzentren der Lymphknoten.
- Rolink, Antonius G.; Schaniel, Christoph; Andersson, Jan; Melchers, Fritz (2001): Selection events operating at various stages in B cell development. In *Current Opinion in Immunology* 13 (2), pp. 202–207. DOI: 10.1016/S0952-7915(00)00205-3.
- Roy, A.; Krzykwa, E.; Lemieux, R.; Néron, S. (2001): Increased efficiency of gamma-irradiated versus mitomycin C-treated feeder cells for the expansion of normal human cells in long-term cultures. In *Journal of hematotherapy & stem cell research* 10 (6), pp. 873–880. DOI: 10.1089/152581601317210962.
- Sanderson, R. D.; Lalor, P.; Bernfield, M. (1989): B lymphocytes express and lose syndecan at specific stages of differentiation. In *Cell Regulation* 1 (1), pp. 27–35. DOI: 10.1091/mbc.1.1.27.
- Sanz, Ignacio; Wei, Chungwen; Jenks, Scott A.; Cashman, Kevin S.; Tipton, Christopher; Woodruff, Matthew C. et al. (2019): Challenges and Opportunities for Consistent Classification of Human B Cell and Plasma Cell Populations. In *Frontiers in immunology* 10, p. 2458. DOI: 10.3389/fimmu.2019.02458.
- Schneider, P.; MacKay, F.; Steiner, V.; Hofmann, K.; Bodmer, J. L.; Holler, N. et al. (1999): BAFF, a novel ligand of the tumor necrosis factor family, stimulates B cell growth. In *J Exp Med* 189 (11), pp. 1747–1756. DOI: 10.1084/jem.189.11.1747.
- Seifert, M.; Küppers, R. (2016): Human memory B cells. In *Leukemia* 30 (12), pp. 2283–2292. DOI: 10.1038/leu.2016.226.
- Shaffer, Arthur L.; Emre, N. C. Tolga; Romesser, Paul B.; Staudt, Louis M. (2009): IRF4: Immunity. Malignancy! Therapy? In *Clinical cancer research : an official journal of the American Association for Cancer Research* 15 (9), pp. 2954–2961. DOI: 10.1158/1078-0432.CCR-08-1845.

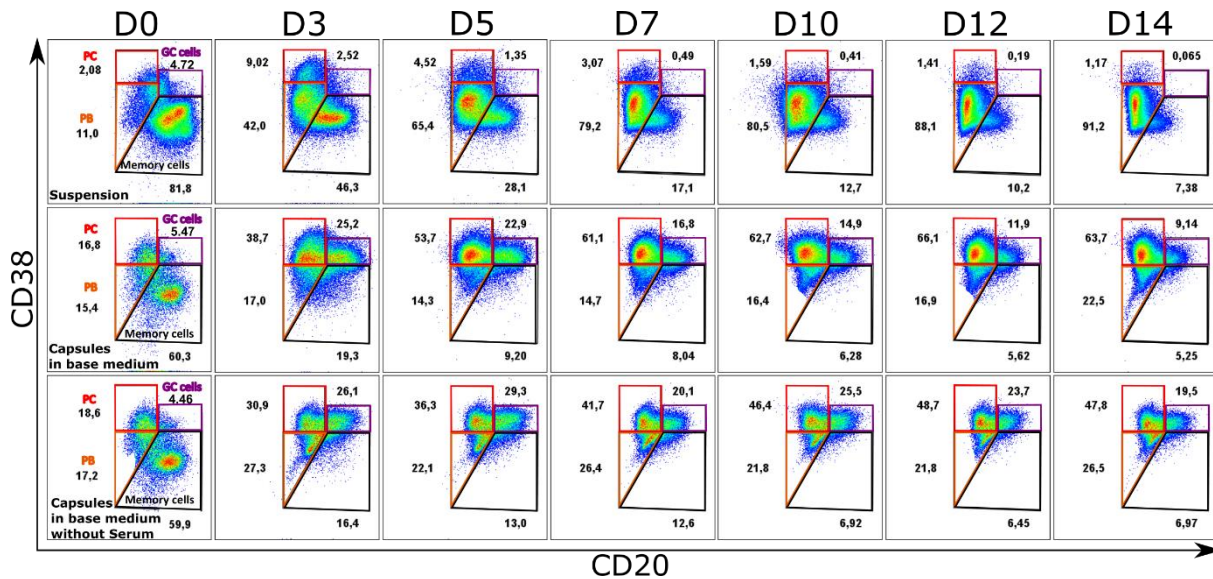
- Shahaf, Gitit; Zisman-Rozen, Simona; Benhamou, David; Melamed, Doron; Mehr, Ramit (2016): B Cell Development in the Bone Marrow Is Regulated by Homeostatic Feedback Exerted by Mature B Cells. In *Front. Immunol.* 7, p. 77. DOI: 10.3389/fimmu.2016.00077.
- Shapiro-Shelef, M.; Lin, K. I.; McHeyzer-Williams, L. J.; Liao, J.; McHeyzer-Williams, M. G.; Calame, K. (2003): Blimp-1 is required for the formation of immunoglobulin secreting plasma cells and pre-plasma memory B cells. In *Immunity* 19 (4). DOI: 10.1016/s1074-7613(03)00267-x.
- Shinnakasu, Ryo; Kurosaki, Tomohiro (2017): Regulation of memory B and plasma cell differentiation. In *Current Opinion in Immunology* 45, pp. 126–131. DOI: 10.1016/j.coi.2017.03.003.
- Shu, Hong-Bing; Hu, Wen-Hui; Johnson, Holly (1999): TALL-1 is a novel member of the TNF family that is down-regulated by mitogens. In *J Leukoc Biol* 65 (5), pp. 680–683. DOI: 10.1002/jlb.65.5.680.
- Simon Davis, David Anak; Parish, Christopher R. (2013): Heparan sulfate: a ubiquitous glycosaminoglycan with multiple roles in immunity. In *Front. Immunol.* 4, p. 470. DOI: 10.3389/fimmu.2013.00470.
- Spolski, Rosanne; Leonard, Warren J. (2008): Interleukin-21: basic biology and implications for cancer and autoimmunity. In *Annual review of immunology* 26, pp. 57–79. DOI: 10.1146/annurev.immunol.26.021607.090316.
- Spriggs, M. K.; Armitage, R. J.; Strockbine, L.; Clifford, K. N.; Macduff, B. M.; Sato, T. A. et al. (1992): Recombinant human CD40 ligand stimulates B cell proliferation and immunoglobulin E secretion. In *The Journal of experimental medicine* 176 (6), pp. 1543–1550. DOI: 10.1084/jem.176.6.1543.
- STEMCELL Technologies (2021): ImmunoCult™ Human B Cell Expansion Kit. Product Information Sheet #1000001049. Available online at <https://www.stemcell.com/products/immunocult-human-b-cell-expansion-kit.html>, checked on 9/30/2022.
- Straitsresearch (2022): Serum-Free Media Market: Information by Type (CHO Cell Media, Protein Expression Media), End-user (Biopharma Industry, Clinical Research Organizations), and Region — Forecast till 2030. Available online at <https://straitsresearch.com/reports>, checked on 11/17/2022.
- Su, Kuei-Ying; Watanabe, Akiko; Yeh, Chen-Hao; Kelsoe, Garnett; Kuraoka, Masayuki (2016): Efficient Culture of Human Naive and Memory B Cells for Use as APCs. In *The Journal of Immunology* 197 (10), pp. 4163–4176. DOI: 10.4049/jimmunol.1502193.
- Suzuki, Kazuhiro; Grigorova, Irina; Phan, Tri Giang; Kelly, Lisa M.; Cyster, Jason G. (2009): Visualizing B cell capture of cognate antigen from follicular dendritic cells. In *The Journal of experimental medicine* 206 (7), pp. 1485–1493. DOI: 10.1084/jem.20090209.
- Tadmori, W.; Lee, H. K.; Clark, S. C.; Choi, Y. S. (1989): Human B cell proliferation in response to IL-4 is associated with enhanced production of B cell-derived growth factors. In *The Journal of Immunology* 142 (3), pp. 826–832. Available online at <https://www.jimmunol.org/content/jimmunol/142/3/826.full.pdf>.
- Tangye, Stuart G.; Avery, Danielle T.; Hodgkin, Philip D. (2003): A division-linked mechanism for the rapid generation of Ig-secreting cells from human memory B cells. In *Journal of immunology (Baltimore, Md. : 1950)* 170 (1), pp. 261–269. DOI: 10.4049/jimmunol.170.1.261.
- Tepljakov, Alexey; Obmolova, Galina; Malia, Thomas J.; Gilliland, Gary L. (2017): Crystal structure of CD27 in complex with a neutralizing noncompeting antibody. In *Acta Crystallogr F Struct Biol Commun* 73 (5), pp. 294–299. DOI: 10.1107/S2053230X17005957.
- Thomas Groth; Christian Willems; Kai Zhang; Steffen Fischer (2020): Development of bioactive cellulose sulfates for biomedical applications. In *1* 59 (3). Available online at <https://aseestant.ceon.rs/index.php/amm/article/view/24232>.
- Tolbert, W. R.; Hitt, M. M.; Feder, J. (1980): Cell aggregate suspension culture for large-scale production of biomolecules. In *In vitro* 16 (6), pp. 486–490. DOI: 10.1007/BF02626461.
- Tu, Wenwei; Lau, Yu-Lung; Zheng, Jian; Liu, Yinping; Chan, Ping-Lung; Mao, Huawei et al. (2008): Efficient generation of human alloantigen-specific CD4+ regulatory T cells from naive precursors by CD40-activated B cells. In *Blood* 112 (6), pp. 2554–2562. DOI: 10.1182/blood-2008-04-152041.
- Turner, C.Alexander; Mack, David H.; Davis, Mark M. (1994): Blimp-1, a novel zinc finger-containing protein that can drive the maturation of B lymphocytes into immunoglobulin-secreting cells. In *Cell* 77 (2), pp. 297–306. DOI: 10.1016/0092-8674(94)90321-2.
- Uludag, Hasan; Vos, Paul de; Tresco, Patrick A. (2000): Technology of mammalian cell encapsulation. In *Advanced Drug Delivery Reviews* 42 (1-2), pp. 29–64. DOI: 10.1016/S0169-409X(00)00053-3.
- van Belle, Kristien; Herman, Jean; Boon, Louis; Waer, Mark; Sprangers, Ben; Louat, Thierry (2016): Comparative In Vitro Immune Stimulation Analysis of Primary Human B Cells and B Cell Lines. In *Journal of immunology research* 2016, p. 5281823. DOI: 10.1155/2016/5281823.
- van Kooten, Cees; Banchereau, Jacques (2000): CD40-CD40 ligand. In *Journal of leukocyte biology* 67 (1), pp. 2–17. DOI: 10.1002/jlb.67.1.2.
- van Steirteghem, A. C.; Robertson, E. A.; Young, D. S. (1978): Variance components of serum constituents in healthy individuals. In *Clinical chemistry* 24 (2), pp. 212–222.
- Vandesompele, Jo; Preter, Kathleen de; Pattyn, Filip; Poppe, Bruce; van Roy, Nadine; Paepe, Anne de; Speleman, Frank (2002): Accurate normalization of real-time quantitative RT-PCR data by geometric averaging of multiple internal control genes. In *Genome Biol* 3 (7), pp. 1–12. DOI: 10.1186/gb-2002-3-7-research0034.
- Vos, Paul de; Marchetti, Piero (2002): Encapsulation of pancreatic islets for transplantation in diabetes: the untouchable islets. In *Trends in Molecular Medicine* 8 (8), pp. 363–366. DOI: 10.1016/S1471-4914(02)02381-X.

- Wagar, Lisa E.; Salahudeen, Ameen; Constantz, Christian M.; Wendel, Ben S.; Lyons, Michael M.; Mallajosyula, Vamsee et al. (2021): Modeling human adaptive immune responses with tonsil organoids. In *Nature Medicine* 27 (1), pp. 125–135. DOI: 10.1038/s41591-020-01145-0.
- Watkins, David I.; Burton, Dennis R.; Kallas, Esper G.; Moore, John P.; Koff, Wayne C. (2008): Nonhuman primate models and the failure of the Merck HIV-1 vaccine in humans. In *Nature Medicine* 14 (6), p. 617. DOI: 10.1038/nm.f.1759.
- Werner, Melanie (2013): Charakterisierung von Polyelektrolytkapseln hinsichtlich materialtechnischer und zellbiologischer Eigenschaften und Anwendung dieser für die Analyse der Mikroumgebung verkapselter T-Lymphozyten. Zugl.: Bayreuth, Univ., Diss., 2012. 1. Aufl. Berlin: Köster (Wissenschaftliche Schriftenreihe Bioprozesstechnik, 4).
- Werner, Melanie; Schmoltd, Daria; Hilbrig, Frank; Jérôme, Valérie; Raup, Alexander; Zambrano, Kenny et al. (2015): High cell density cultivation of human leukemia T cells (Jurkat cells) in semipermeable polyelectrolyte microcapsules. In *Eng. Life Sci.* 15 (4), pp. 357–367. DOI: 10.1002/elsc.201400186.
- Williams, Andrew E.; Hussell, Tracy (2012): Immunology. Mucosal and body surface defences. Chichester, West Sussex: Wiley-Blackwell.
- Wilson, Jenna L.; McDevitt, Todd C. (2013): Stem cell microencapsulation for phenotypic control, bioprocessing, and transplantation. In *Biotechnology and bioengineering* 110 (3), pp. 667–682. DOI: 10.1002/bit.24802.
- Xu, Jianchao; Foy, Teresa M.; Laman, Jon D.; Elliott, Eileen A.; Dunn, Jonathan J.; Waldschmidt, Thomas J. et al. (1994): Mice deficient for the CD40 ligand. In *Immunity* 1 (5), pp. 423–431. DOI: 10.1016/1074-7613(94)90073-6.
- Xu, Zhenming; Zan, Hong; Pone, Egest J.; Mai, Thach; Casali, Paolo (2012): Immunoglobulin class-switch DNA recombination: induction, targeting and beyond. In *Nature reviews. Immunology* 12 (7), pp. 517–531. DOI: 10.1038/nri3216.
- Yoon, Sung Hee; Cho, Hyun Il; Kim, Tai Gyu (2005): Activation of B cells using Schneider 2 cells expressing CD40 ligand for the enhancement of antigen presentation in vitro. In *Experimental & molecular medicine* 37 (6), pp. 567–574. DOI: 10.1038/emm.2005.70.
- Zhang, Rong; Mjoseng, Heidi K.; Hoeve, Marieke A.; Bauer, Nina G.; Pells, Steve; Besseling, Rut et al. (2013): A thermoresponsive and chemically defined hydrogel for long-term culture of human embryonic stem cells. In *Nature communications* 4, p. 1335. DOI: 10.1038/ncomms2341.
- Zhang, Wujie; He, Xiaoming (2011): Microencapsulating and Banking Living Cells for Cell-Based Medicine. In *Journal of healthcare engineering* 2 (4), pp. 427–446. DOI: 10.1260/2040-2295.2.4.427.
- Zunino, Susan J.; Storms, David H. (2009): Resveratrol Alters Proliferative Responses and Apoptosis in Human Activated B Lymphocytes in Vitro. In *J Nutr* 139 (8), pp. 1603–1608. DOI: 10.3945/jn.109.105064.

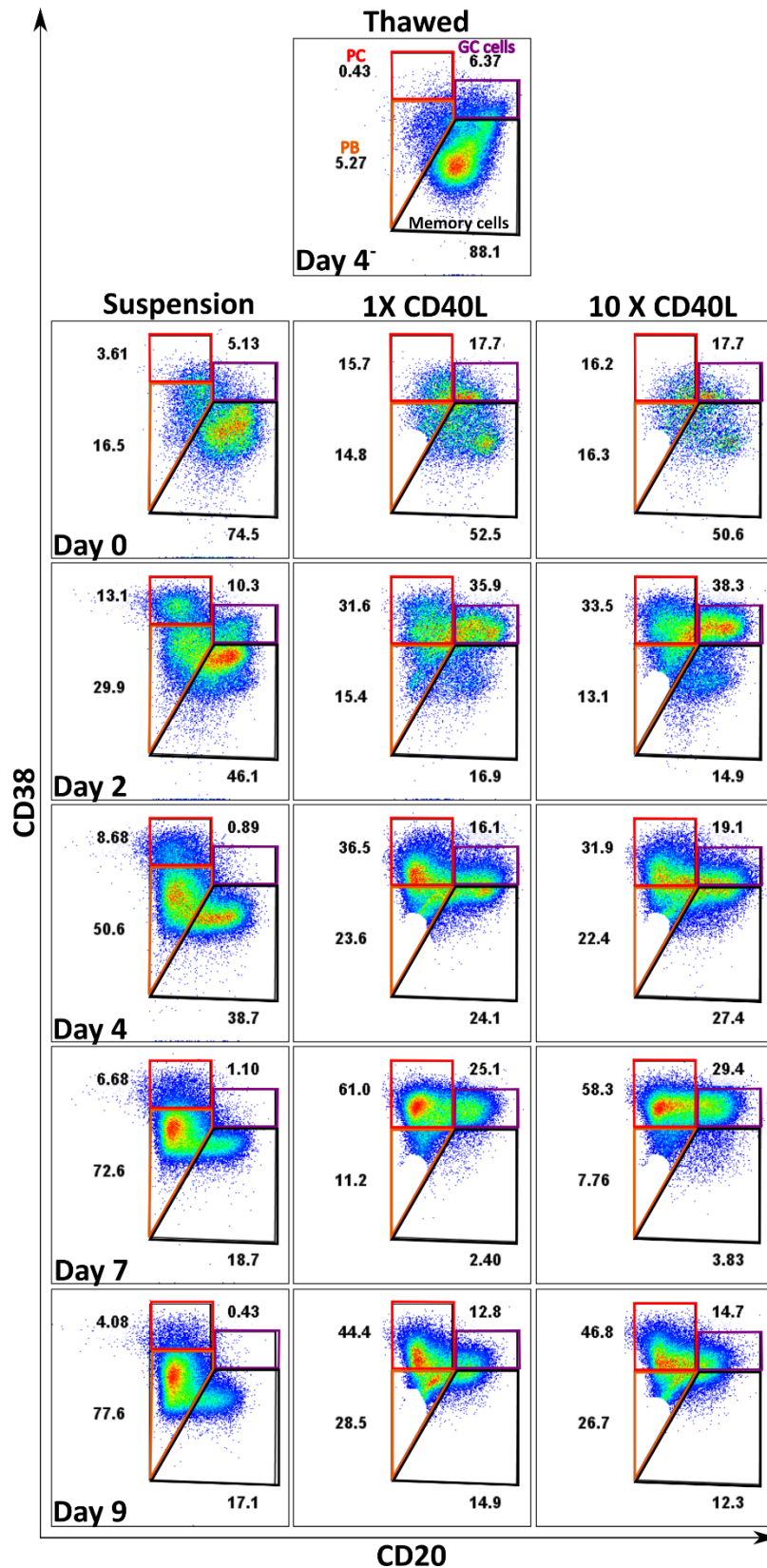
# 11 Appendix



Appendix 1: Memory pre-cultured B cells with 0.4 and 1 µg/mL CD40L.  $0.1 \times 10^6$  B cells of donor C3 were reseeded every 3 – 4 days.



Appendix 2: Comparison of B cell subpopulation development in suspension and encapsulated culture. B cells were precultured for 4 days and then reseeded ( $0.1 \times 10^6$  cells/mL) in standard medium for suspension culture or encapsulated ( $1 \times 10^6$  cells/mL<sub>capsule</sub>) under standard conditions. Capsules were cultured in base medium with or without human AB serum.



Appendix 3: Comparison of B cell subpopulation development in suspension and encapsulated culture for varying CD40L concentrations inside capsules. CD40L concentrations in the capsules was 0.4  $\mu\text{g}/\text{mg}_{\text{capsules}}$  (corresponding to 0.4  $\text{pg}/\text{cell}$ , (1X CD40L)) and 4  $\mu\text{g}/\text{mg}_{\text{capsules}}$  (corresponding to 4  $\text{pg}/\text{cell}$ , (10X CD40L)). Day -4 refers to the day of thawing. Day 0 to Day 9 refer to the days of cultivation post-encapsulation. The suspension culture was reseeded after 4 days pre-culture at  $0.1 \times 10^6$  cells/mL in ASC medium supplemented containing 0.4  $\mu\text{g}/\text{mL}$  CD40L concentration (corresponding to 4  $\text{pg}/\text{cell}$ , (Suspension)). This figure is adopted from Helm & Huang et al. (Helm et al. 2022).

	Donor variation																			
	Donor 1				Donor 2				Donor 3				Donor 4				Donor 5			
	HPRT	B2Microglobuline	GAPDH	Bactin	HPRT	B2Microglobuline	GAPDH	Bactin	HPRT	B2Microglobuline	GAPDH	Bactin	HPRT	B2Microglobuline	GAPDH	Bactin	HPRT	B2Microglobuline	GAPDH	Bactin
	Ct (HPRT)	Ct (B2Micro)	Ct (GAPDH)	Ct (Bactin)	Ct (HPRT)	Ct (B2Micro)	Ct (GAPDH)	Ct (Bactin)	Ct (HPRT)	Ct (B2Micro)	Ct (GAPDH)	Ct (Bactin)	Ct (HPRT)	Ct (B2Micro)	Ct (GAPDH)	Ct (Bactin)	Ct (HPRT)	Ct (B2Micro)	Ct (GAPDH)	Ct (Bactin)
/Bactin	HPRT/Bactin	B2Microgl/Bactin	GAPDH/Bactin	1			1				1				1					1
/GAPDH	HPRT/GAPDH	B2Microgl/GAPDH	1	Bactin/GAPDH			1				1				1					1
/B2Microgl	HPRT/B2Microgl	1	GAPDH/B2Microgl	Bactin/B2Microgl			1				1				1					1
/HPRT	1	B2Microgl/HPRT	GAPDH/HPRT	Bactin/HPRT			1				1				1					1
StDev across donors	StDev(D1,2,3,4,5)	StDev(D1,2,3,4,5)	StDev(D1,2,3,4,5)	0																
	StDev(D1,2,3,4,5)	StDev(D1,2,3,4,5)	0	StDev(D1,2,3,4,5)																
	StDev(D1,2,3,4,5)	0	StDev(D1,2,3,4,5)	StDev(D1,2,3,4,5)																
	0	StDev(D1,2,3,4,5)	StDev(D1,2,3,4,5)	StDev(D1,2,3,4,5)																
Mvalue	Avg (HPRT/X/HPRT)																			
Stability	Ln(1/M value (HPRT))																			
	HPRT	B2Microglobuline	GAPDH	Bactin																

Appendix 4: Example for the calculation of gene stability for HPRT and 5 donors.



**Bayreuth 23.06.2022**

---